Function of STAMBPL1 in *Helicobacter pylori*-associated cell death

Thesis

for the degree of

doctor rerum naturalium (Dr. rer. nat.)

approved by the Faculty of Natural Sciences of Otto von Guericke University Magdeburg

by   M.Sc. Supattra Chaithongyot

born on   15.01.1992 in Nakhon Phanom, Thailand

Examiner: Prof. Dr. Michael Naumann
               Prof. Dr. Gerhard Braus

submitted on: 29.03.2022

defended on: 05.07.2022

Summary (English)

M.Sc. Chaithongyot Supattra. Function of STAMBPL1 in *Helicobacter pylori*-associated cell death, 84 pages, 27 figures.

Deubiquitinylases (DUBs) are central regulators of the ubiquitin system involved in protein regulation and cell signalling and are important for a variety of physiological processes. Most DUBs are cysteine proteases, and few other proteases are metalloproteases of the JAB1/MPN+/MOV34 protease family (JAMM). STAM-binding protein like 1 (STAMBPL1), a member of the JAMM family, cleaves ubiquitin bonds and has a function in regulating cell survival, Tax-mediated nuclear factor kappa-light-chain-enhancer of activated B cells (NF-κB) activation and epithelial-mesenchymal transition. However, the molecular mechanism by which STAMBPL1 influences cell survival is not well defined, especially with regard to its deubiquitinylation function. Here, we show that reactive oxygen species (ROS) induced by chemotherapeutic agents or the human microbial pathogen *Helicobacter pylori* can induce cullin 1-RING ubiquitin ligase (CRL1) and 26S proteasome-dependent degradation of STAMBPL1. Interestingly, STAMBPL1 has a direct interaction with the COP9 signalosome subunits (CSN) CSN5 and CSN6. The interaction with the CSN is required for the stabilisation and function of the STAMBPL1 protein. In addition, STAMBPL1 deubiquitinylates the anti-apoptotic protein Survivin and thus ameliorates cell survival. In summary, our data reveal a previously unknown mechanism by which the deubiquitinylase STAMBPL1 and the E3 ligase CRL1 balance the level of Survivin degradation and thereby determine apoptotic cell death. In response to genotoxic stress, the degradation of STAMBPL1 augments apoptotic cell death. This new mechanism may be useful to develop therapeutic strategies targeting STAMBPL1 in tumours that have high STAMBPL1 and Survivin protein levels.

Summary (German)

M.Sc. Chaithongyot Supattra. Funktion von STAMBPL1 beim *Helicobacter pylori-*assoziierten Zelltod, 84 Seiten, 27 Abbildungen.

Deubiquitinylasen (DUBs) sind wichtige Regulatoren des Ubiquitinsystems, die an der Proteinregulierung und der Signaltransduktion beteiligt und für eine Vielzahl physiologischer Prozesse von Bedeutung sind. Die meisten DUBs sind Cysteinproteasen und andere Proteasen sind Metalloproteasen der JAB1/MPN+/MOV34-Proteasefamilie (JAMM). STAM-binding protein like 1 (STAMBPL1), ein Mitglied der JAMM-Familie, spaltet Ubiquitin-Bindungen und hat eine Funktion bei der Regulation des Zellüberlebens, bei der Tax-vermittelten Aktivierung von Nuclear Factor Kappa-Light-Chain-Enhancer von aktivierten B-Zellen (NF-κB) und bei der epithelialen-mesenchymalen Transition. Der molekulare Mechanismus, durch den STAMBPL1 das Zellüberleben beeinflusst, ist jedoch nicht genau bekannt, insbesondere im Hinblick auf seine Deubiquitinylierungsfunktion. Hier zeigen wir, dass reaktive Sauerstoffspezies (ROS), die durch Chemotherapeutika oder den humanen Keim Helicobacter pylori induziert werden, die Cullin-1-RING-Ubiquitin-Ligase (CRL1) und den 26S-Proteasom-abhängigen Abbau von STAMBPL1 induzieren können. Interessanterweise besteht eine direkte Interaktion zwischen STAMBPL1 und den COP9-Signalosom-Untereinheiten (CSN) CSN5 und CSN6. Die Interaktion mit dem CSN ist für die Stabilisierung und Funktion des STAMBPL1-Proteins erforderlich. Darüber hinaus deubiquitinyliert STAMBPL1 das anti-apoptotische Protein Survivin und erhöht so das Überleben der Zellen. Zusammenfassend zeigen unsere Daten einen bisher unbekannten Mechanismus, durch den die Deubiquitinylase STAMBPL1 und die E3-Ligase CRL1 das Ausmaß des Abbaus von Survivin regulieren und dadurch den apoptotischen Zelltod bestimmen. Als Reaktion auf genotoxischen Stress verstärkt der Abbau von STAMBPL1 den apoptotischen Zelltod. Dieser neue Mechanismus kann von Bedeutung sein, um therapeutische Strategien zu entwickeln, die auf STAMBPL1 in Tumoren mit hohen STAMBPL1- und Survivin-Proteinspiegeln abzielen.

Table of contents

1. Introduction

1.1 The ubiquitin system

Protein modifications (PMs) are a dynamic strategy to affect e.g., function, localisation, protein-protein interaction, and turnover of proteins, influencing various signalling cascades [Chen et al., 2021]. More than 200 PMs have been identified [Venne et al., 2014]. Ubiquitin and ubiquitin like modifications represent an important group of PMs which control cellular fate [Swatek & Kommander, 2016; Pérez Berrocal et al., 2020]. Ubiquitinylation is regulated by a highly dynamic and sequential multi-enzymatic cascade that covalently attaches ubiquitin to substrate proteins and thereby influences the stability, activity, interaction, or localisation of the target protein. The 76 amino acid polypeptide ubiquitin (Ub) is highly conserved among all eukaryotes, which indicates a conserved function [Swatek & Komander, 2016].
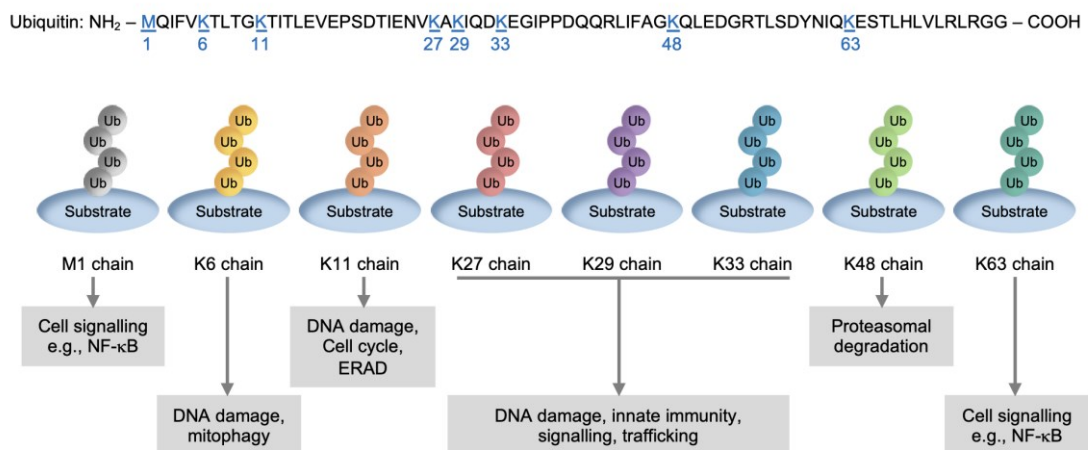
Figure 1   Schematic representation of ubiquitin linkage types and putative functions. The sequence of ubiquitin has seven internal lysine (K) residues. Within polyubiquitin chains, ubiquitin can form eight different linkage types, linked through the internal lysine residues or through M1. In addition, mixed chains are possible. Abbreviations: ERAD, endoplasmatic reticulum-associated protein degradation; NF-κB, nuclear factor kappa-light-chain-enhancer of activated B cells.

Ubiquitin-like proteins (UBLs) are related in sequence and exert a similar 3D structure to ubiquitin, such as small ubiquitin-like modifier (SUMO), neural precursor cell expressed, developmentally down-regulated 8 (NEDD8), interferon-stimulated gene product 15 (ISG15) and autophagy-related protein 8 (Atg8). Similar to ubiquitin, UBLs are covalently conjugated to a target protein via an enzymatic cascade utilising an assembly mechanism similar to those seen in ubiquitinylation [Cappadocia et al., 2018].

Proteomic investigations have revealed that thousands of proteins are targeted by ubiquitinylation, and several ubiquitin linkage types are present in cells [Tracz et al., 2021]. Different ubiquitinylation patterns adopt different structural conformations and biological roles [Deol et al., 2019; Khago et al., 2020]. Ubiquitin can be covalently linked to protein substrates as a monomer (monoubiquitinylation) or in the form of polymeric chains (polyubiquitinylation) to form variable length, linkage type and configuration of the ubiquitin chains (Figure 1). Linkage types are possible via the seven lysine (K) residues (K6, K11, K27, K29, K33, K48 and K63) and the N-terminal methionine (M1) [Swatek & Komander, 2016].

Modification by a K48-linked polyubiquitin is the most abundant linkage that serves as recognition signal for the 26S proteasome to target proteins for degradation [Swatek & Komander, 2016]. Proteasomal degradation is not restricted to K48 linkages. Substrates marked with K11 and linear ubiquitin chains linked through the initial methionine have also been reported as substrates for 26S proteasomal degradation [Xu et al., 2009]. K11 linked chains were implicated in cell cycle regulation and endoplasmatic reticulum-associated protein degradation (ERAD) [Bremm & Komander, 2011]. Furthermore, K6 linkages are involved in DNA damage response and mitophagy [Morris et al., 2004; Ordureau et al., 2014]. The K63-polyubiquitin chain is involved in the active regulation of signalling processes, e.g., NF-κB signalling [Cohen et al., 2017]. While K27-linked chains are known to play a role in innate immunity and DNA damage response [Peng et al., 2011; Gatti et al., 2015], K29-linked chains play a role in the AMPK-related kinases and Wnt/β-catenin signalling pathway [Al-Hakim et al., 2008; Hay-Koren et al., 2011], and K33 linkages were attributed to post-Golgi protein trafficking [Yuan et al., 2014] (Figure 1).

1.1.1 The ubiquitinylation cascade

Ubiquitin is covalently attached to the ε-amino group of lysines or (less frequently) to the N-terminal amino group of the substrate proteins through its C-terminal carboxyl group via an isopeptide bond formation. This process is achieved by a three-step enzymatic cascade: an initial activation step catalysed by ubiquitin-activating enzymes (E1s), an intermediate conjugation step catalysed by ubiquitin-conjugating enzymes (E2s) and a final ligation step catalysed by ubiquitin ligases (E3s) [Oh et al., 2018] (Figure 2).

The initial step requires the activation of the ubiquitin molecule in an adenosine 5′-triphosphate (ATP)-dependent reaction (Figure 2). E1 activates ubiquitin molecules by forming a thioester linkage between its catalytic cysteine residue and the di-glycine motif at the C-terminus of ubiquitin. The activated ubiquitin molecule is subsequently transferred to the active-site cysteine of an E2 enzyme by the formation of another thioester bond. E3 ligases mediate the final step by bringing the E2 enzymes conjugated to ubiquitin and the substrate for ubiquitinylation into proximity, resulting in the transfer of ubiquitin to the substrate through isopeptide bond formation [Ye & Rape, 2009]. All E3s harbour an E2-ubiquitin binding domain and can be mechanistically divided into four main classes: RING (Really Interesting New Gene), U-box, HECT (Homologous to E6AP C-terminus) and RBR (RING-Between-RING) type ligases. Additionally, the four major classes can be further categorised with distinct structure and substrate recognition [Yang et al., 2021]. The RING and U-box E3 ligases interact simultaneously with the ubiquitin loaded E2 intermediate and catalysed a direct transfer of ubiquitin from the E2 to the substrate [Metzger et al., 2014]. In contrast, HECT and RBR E3 ligases require a two-step reaction by forming an intermediate thioester of ubiquitin intermediate with a catalytic cysteine residue before transferring ubiquitin onto a target protein [Rotin & Kumar, 2009; Walden & Rittinger, 2018; Reiter et al., 2018] (Figure 2).

In the human genome, there are two E1s and a limited number of E2s (~40) but a number of E3 ligases (>600). Within this cascade, E3s play an essential role in determining substrate specificity and the architecture within polyubiquitin linkage modifications [Yang et al., 2021].

Cullin-RING ligases (CRLs) are the largest family of E3 ubiquitin ligases [Harper & Schulman, 2021]. CRLs consist of a cullin protein (Cul1, Cul2, Cul3, Cul4A/4B, Cul5, Cul7, or Cul9), which acts as a scaffold protein that binds to an adaptor protein and a substrate recognition protein at the N-terminus and a RING protein (RBX1 or RBX2) at the C-terminus [Lydeard et al., 2013]. The availability of hundreds of substrate receptors enables the formation of a variety of CRLs that, in turn, ubiquitinylate a broad range of targets. A well-studied example of CRLs is the S-phase kinase-associated protein 1-cullin-1/F-box (SCF) ubiquitin ligase complex. It consists of the Cul1 scaffold protein, the RING domain protein Rbx1/Roc1/Het1, the adapter protein Skp1, and F-box domain containing receptor proteins [Reitsma et al., 2017]. In addition, other CRLs

are assembled using other cullin and many substrate-recognition subunits, which enables ubiquitin-mediated degradation of different target proteins.
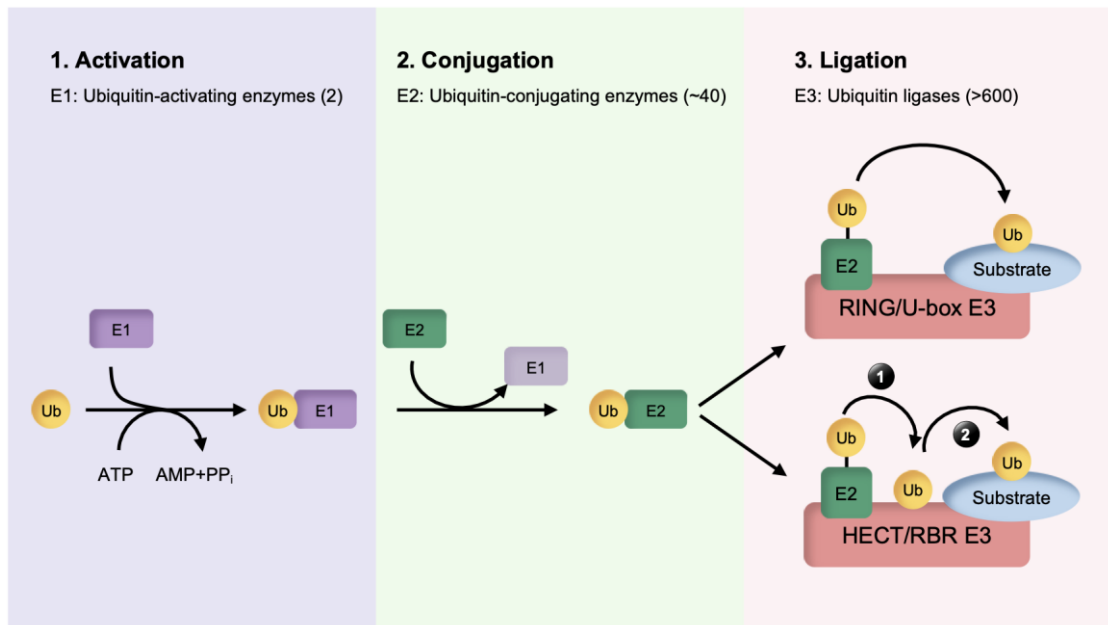
Figure 2   The ubiquitinylation reactions. Coordinated activity of Ub-activating (E1), Ub-conjugating (E2), and Ub-ligating enzyme (E3) is required for Ub attachment to substrate proteins. First, Ub is attached to the E1 in an ATP-dependent manner and subsequently transfer to an E2. Finally, the activated Ub is covalently attached to the substrate lysine residue, mediated by an E3. The RING type E3 ligases are characterised by the presence of a RING domain while U-box E3s contain U-box domain at the N-terminal. RING and U-box E3s mediate a direct transfer of ubiquitin from E2 ligase to the substrate. HECT type E3 ligases contains HECT domain whereas RBR type E3 ligases consist of two predicted RING domains (RING1 and RING2) separated by an in-between RING (IBR) domain. HECT and RBR E3 ligases catalysed ubiquitinylation process involve a two-step reaction where ubiquitin is first transferred to a catalytic cysteine on the E3 ligase and then to the substrate protein. Abbreviations: ATP, adenosine 5′-triphosphate; HECT, Homologous to E6AP C-terminus; RBR, RING-Between-RING; RING, Really Interesting New Gene.

The activity of CRLs requires protein modifications with the ubiquitin-like protein NEDD8 at a conserved lysine residue of cullin [Duda et al., 2008]. Neddylation of cullins activates CRLs by inducing a conformational change in the cullin C-terminus, which enables the transfer of the ubiquitin from the E2 enzyme to the protein substrate. Consequently, removal of the NEDD8 from cullin (deneddylation) leads to inhibition of CRL activity which is mediated by the constitutive photomorphogenesis 9 (COP9) signalosome (CSN) [Enchev et al., 2015] (Figure 3). CSN is an evolutionarily conserved protein complex with a composition of eight subunits (CSN1-8) with similarity to the lid of the 26S proteasome regulatory particle [Dubiel et al., 2020]. Five subunits (CSN1,2,3,4,7 and 8) contain a PCI (proteasome, COP9 signalosome, initiation factor 3) domain and the other two subunits (CSN5 and 6) contain an MPN (Mpr1-Pad1-N-

terminal) domain (Figure 3). While the PCI domains are thought to facilitate protein-protein interactions, the CSN5 MPN domain contains a JAMM (Jab1/MPN/Mov34) motif, which is the catalytic center of the CSN's deneddylase activity [Cope et al., 2002]. Apart from regulating the CRLs through its deneddylase activity, CSN promotes cullin-associated Nedd8-dissociated protein 1 (CAND1) binding and consequently facilitate the exchange of substrate-receptor complexes [Helmstaedt et al., 2011]. Hence, the functional CSN, through the mediation of the CRLs, is critical for the regulation of protein stability in the ubiquitin-proteasome pathway.
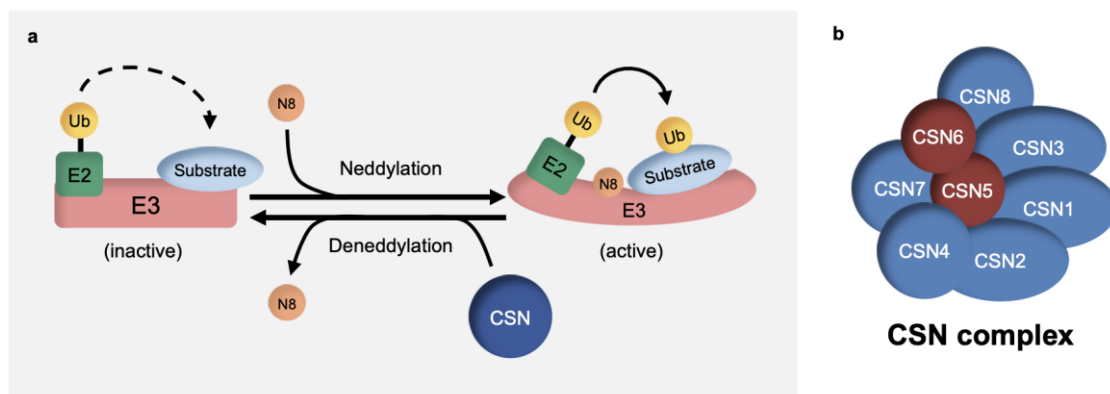
Figure 3   Regulation of cullin-RING ubiquitin ligases (CRLs). (a) Schematic illustration showing the mechanism of CRL activation by neddylation. After ubiquitinylation, the deneddylase CSN removes NEDD8 from cullin, leading to the disassembly of CRL. (b) The CSN complex consists of eight subunits, six of which possess PCI domains (blue) and two subunits possess MPN domains (red). Abbreviation: CSN, constitutive photomorphogenesis 9 (COP9) signalosome, E1, ubiquitin-activating enzyme; E2, ubiquitin-conjugating enzyme; E3, ubiquitin-ligating enzyme; N8, ubiquitin-like protein NEDD8; Ub, ubiquitin.

1.1.2 Ubiquitin-mediated protein degradation by the 26S proteasome

The 26S proteasome is a 2.5 MDa multisubunit protease highly conserved in evolution composed of two components, a barrel-shaped 20S core particle and a 19S regulatory particle [Finley, 2012; Kleiger et al., 2014]. The 26S proteasome degrades ubiquitinylated proteins into small peptides in an ATP-dependent manner involving two main steps. First, the protein substrate must be covalently tagged with ubiquitin to generate the polyubiquitin chain (at least tetramer) linked via the K48, which serves as a recognition signal for the 26S proteasome [Thrower et al., 2000]. Such polyubiquitinylated proteins are recognised by the 19S regulatory particle, then are deubiquitinylated, unfolded, and translocated into the 20S core particle, which is mediated by ubiquitin-specific proteases (UBPs) and DUBs such as RPN11, USP14 and UCH37 [Worden et al., 2017]. Once the targeted protein is in the interior of the 20S

core particle catalytic sites, peptide bonds that link amino acids are hydrolysed by different enzymatic activities, e.g., trypsin-like (β2 subunit), chymotrypsin-like (β5 subunit), and post-glutamyl peptide hydrolysing, or caspase-like (β1 subunit) activities, and free amino acids are released [Collins et al., 2017] (Figure 4). Within this process, ubiquitin is not degraded but is reused in another substrate modification cycle [Komander et al., 2009].
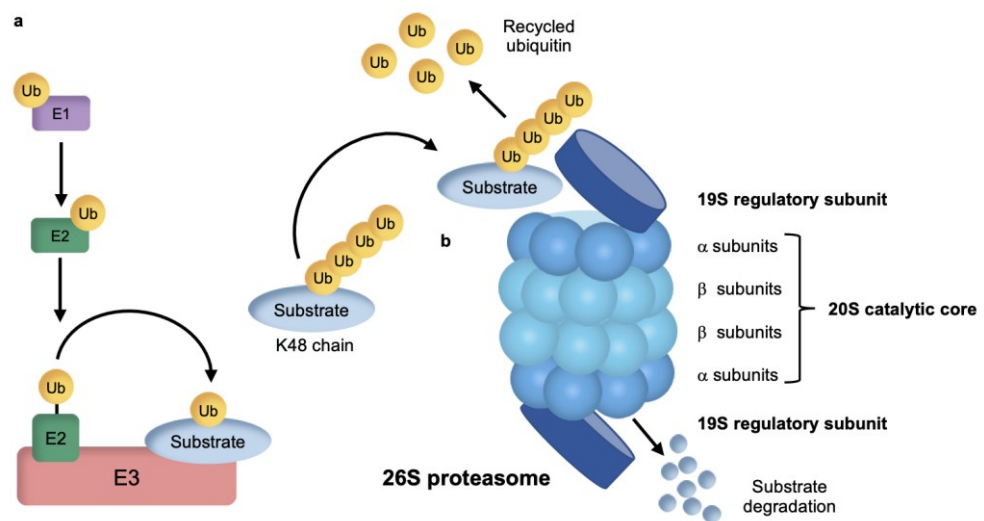
Figure 4   Protein degradation mediated by the UPS. (a) E3 ubiquitin ligases determine the substrate specificity of UPS-dependent proteolysis. (b) Schematic structure of the 26S proteasome. Once the protein has been tagged with K48-linked, it is recognised for degradation by the 26S proteasome. Abbreviation: E1, ubiquitin-activating enzyme; E2, ubiquitin-conjugating enzyme; E3, ubiquitin-ligating enzyme; Ub, ubiquitin.

It was reported that several specific degradation signals of the ubiquitin-proteasome system (UPS) substrates mediate the recognition by E3 ligases [Varshavsky, 2019; Gierisch et al., 2020]. For example, recognition via the NH$_2$-terminal residue so-called the N-end rule pathway. The alteration of the peptide sequences within the N-terminus of the substrate is sufficient for the recognition by E3 ligases and promoting ubiquitin-dependent turnover [Tasaki et al., 2012]. Phosphorylation of protein substrates frequently enables access to recognition by E3 ligases, which are typically recognised by the SCF complexes [Hayes et al., 2015]. Proteins that have been mutated or misfolded often have more hydrophobic amino acids on their surface than correctly folded proteins. These serve as recognition regions for subsequent polyubiquitinylation reactions. In addition to the examples of recognition via the NH$_2$-terminal residue, phosphorylation and hydrophobic amino acids discussed above, other degradation signals e.g., recognition in trans, recognition by UBLs [Perry et al., 2008], recognition

by chaperones [Rosser et al., 2007], and recognition by specificity factors have been shown to aid in selection of the proteins for E3 ligases [Ravid & Hochstrasser, 2008].

1.1.3 Deubiquitinylation

Like other types of PMs, ubiquitinylation is a reversible process, which is carried out by a family of proteases known as deubiquitinylases (DUBs). There are approximately 100 putative DUBs encoded in the human genome, which are classified into six subclasses based on the structure of their catalytic domains and likely mechanisms of action. These include five families of cysteine proteases: ubiquitin carboxy-terminal hydrolases (UCHs), ubiquitin-specific proteases (USPs), ovarian tumor proteases (OTUs), Machado-Joseph disease protein domain proteases, and the most recently discovered motif interacting with ubiquitin containing novel DUB family (MINDY), and a family of zinc metalloproteases: Jab1/Pad1/MPN domain-associated metallopeptidases (JAMMs) [Mevissen & Komander, 2017]. Similar to the effects of ubiquitinylation, the removal of the ubiquitin can change the conformation, function, stability, activity, or localisation of the target protein. DUBs control diverse cellular processes [Clague et al., 2019], and their dysfunction contributes to the pathogenesis of many human diseases [Popovic et al., 2014].

Mechanistically, DUBs remove ubiquitin from protein substrates by specific cleavage of the isopeptide bond at the C-terminus of ubiquitin (Figure 5). The isopeptide bond is cleaved by a nucleophilic attack to the carbonyl group of the isopeptide bond, resulting in hydrolysis [Li & Reverter, 2021]. Apart from substrate protein specificity, DUBs are able to distinguish between different ubiquitin linkage types [Li et al., 2020; de Cesare et al., 2021], adding an additional regulatory level to their activity.
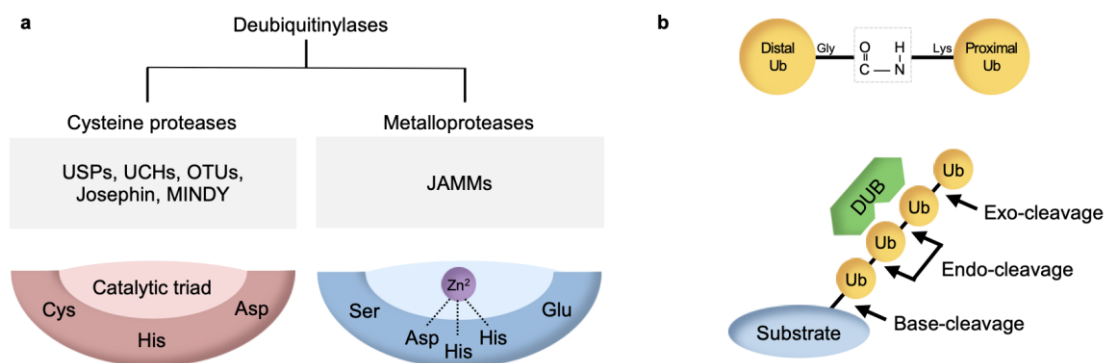
Figure 5 Mechanism of ubiquitin cleavage by DUBs. (a) Schematic illustration showing the active sites of DUBs. The catalytic triad of cysteine protease DUBs consists of Cys-His-Asp/Asn residues whereas metalloproteases active site contains Glu-His-His-Asp. (b) Cleavage modes of DUBs. Abbreviation: DUB,

deubiquitinylases; JAMMs, Jab1/Pad1/MPN domain-associated metallopeptidases; Josephin, Machado-Joseph disease protein domain proteases; MINDY, motif interacting with ubiquitin containing novel DUB family; OTUs, ovarian tumor proteases; Ub, ubiquitin; UCHs, ubiquitin carboxy-terminal hydrolases; USPs, ubiquitin-specific proteases.

1.1.4 The JAMM deubiquitinylase STAMBPL1

DUBs are isopeptidases capable of binding ubiquitinylated substrates and then hydrolysing the amide bond between ubiquitin and a lysine side chain, thus, removing the covalently linked ubiquitin molecule from the substrates. In contrast to cysteine proteases, the JAMM family members are zinc metalloproteases. Of the 14 JAMM proteins in the human genome, only 7 contain a complete set of conserved residues needed for Zn^{2+} coordination in the active site, which includes AMSH, STAMBPL1, CSN5, RPN11, MYSM1, and BRCC36 [Nijman et al., 2005].

STAM-binding protein like 1 (STAMBPL1 also known as AMSH-LP), a member of the JAMM family of DUBs, is closely related to an associated molecule with the SRC Homology 3 (SH3) domain of STAM (AMSH) by sharing 56% identity and 75% sequence similarity (Figure 6). Both STAMBPL1 and AMSH possess an N-terminal microtubule-interacting and transport (MIT) domain, a putative nuclear localisation sequence (NLS), a clathrin binding site (CBS), and a C-terminal MPN domain containing a JAMM motif. Although their amino acid sequences are divergent, the JAMM motif is conserved. While AMSH contains a functional SH3 binding motif, it is lost in STAMBPL1. Structural studies revealed that the catalytic domains of STAMBPL1 and AMSH are nearly identical; however, STAMBPL1 is thermodynamically more stable than AMSH [Davies et al., 2011]. AMSH is known as an endosome-associated DUB playing a critical role in the endosomal sorting complexes required for transport (ESCRT) machinery to facilitate the recycling of receptors by removing K63-linked polyubiquitin on the substrates [Ribeiro-Rodrigues et al., 2014]. However, STAMBPL1 is unable to bind to the members of the ESCRT machinery because it has Thr^{250} instead of Lys^{250}, which is a crucial amino acid for binding to the SH3 domain [Kikuchi et al., 2003].

```
a
                              1                                              436
   STAMBPL1          ┌────┬────┬──┬───────┬──────────────┬───────┬──────┐
   (AMSH-LP)         │ MIT│NLS │  │  CBS  │              │ JAMM  │      │
                     └────┴────┴──┴───────┴──────────────┴───────┴──────┘

                              1                                    424
   AMSH              ┌────┬───┬──┬────┬──────┬─────┬──────┬───────┬───┐
                     │ MIT│NLS│  │CBS │      │ SBM │      │ JAMM  │   │
                     └────┴───┴──┴────┴──────┴─────┴──────┴───────┴───┘

                     56% Identity
                     75% Similarity of MPN domain containing JAMM motif
```

```
b

AMSH          1 MSDHGDVSLPPEDRVRALSQLGSAVEVNEDIPPRRYFRSGVEIIRMASIYSEEGNIEHAF
STAMBPL1     16 MPDHTDVSLSPEERVRALSKLGCNITISEDITPRRYFRSGVEMERMASVYLEEGNLENAF
                * ** **** ** ****** **       *** **********  **** * **** * **

AMSH         61 ILYNKYITLFIEKLPKHRDYKSAVIPEKKDTVKKLKEIAFPKAEELKAELLKRYTKEYTE
STAMBPL1     76 VLYNKFITLFVEKLPNHRDYQQCAVPEKQDIMKKLKEIAFPRTDELKNDLLKKYNVEYQE
                 **** **** **** ****    *** *  ********  ***  *** *  ** *

AMSH        121 YNEEKKKEAEELARNMAIQQELEKEKQRVAQQKQQQLEQEQFHAFEEMIRNQELEKERLK
STAMBPL1    136 YLQSKNKYKAEILKKLEHQRLIEAERKRIAQMRQQQLESEQFLFFEDQLKKQELARGQMR
                *   *  *     *       *  * *  *   **** *** **    ***

AMSH        181 IVQEFGKVDPGLGGPLVPDLEKPSLDVFPTLTVSSIQPSDCHTTVRPAKPPVVDRSLKPG
STAMBPL1    196 SQQTSGLSEQIDGSALSCFSTHQNNSL---LNVFADQPNKSDATNYASHSPPVNRALTPA
                 *  *     *  *       * *    **  **     *      * * * * *

AMSH        241 ALSNSESIPTIDGLRHVVVPGRLCPQFLQLASANTARGVETCGILCGKLMRNEFTITHVL
STAMBPL1    253 ATLSAVQNLVVEGLRCVVLPEDLCHKFLQLAESNTVRGIETCGILCGKLTHNEFTITHVI
                *         *** *** *  **  ***** ** ** **********  ********

AMSH        301 IPKQSAGSDYCNTENEEELFLIQDQQGLITLGWIHTHPTQTAFLSSVDLHTHCSYQMMLP
STAMBPL1    313 VPKQSAGPDYCDMENVEELFNVQDQHDLLTLGWIHTHPTQTAFLSSVDLHTHCSYQLMLP
                ****** ***  ** ****  ***   * ************************** ***

AMSH        361 ESVAIVCSPKFQETGFFKLTDHGLEEISSCRQKGFHPHSKDPPLFCSCSHVTVVDRAVTI
STAMBPL1    373 EAIAIVCSPKHKDTGIFRLTNAGMLEVSACKKKGFHPHTKEPRLFSICKHVLVKDIKIIV
                * *******  ** * **  *  * *   ****** * * **  * ** * *

AMSH        421 TDLR
STAMBPL1    433 LDLR
                ***
```

Figure 6   Domain structure and sequence alignment of STAMBPL1 and AMSH. (a) Schematic representation of the domain structure of STAMBPL1 and AMSH. (b) Sequence alignment of amino acid of AMSH and STAMBPL1. Alignment was performed with Clustal X. The underline shows the MPN domain. Identical amino acids are marked with asterisks. Abbreviations: AMSH, associated molecule with the SRC Homology 3 (SH3) domain of STAM; AMSH-LP, AMSH-like protein; CBS, clathrin binding site; JAMM, JAB1/MPN+/MOV34 domain; MIT, microtubule-interacting and transport domain; NLS, nuclear localisation sequence; SBM, SH3-binding motif.

The DUB domain, a region containing residues 264-436 of human STAMBPL1, is sufficient for the K63-linkage-specific DUB activity [Sato et al., 2008]. The crystal structure of the STAMBPL1 reveals that the DUB domain consists of a Zn^{2+}-coordinating catalytic core and two AMSH-family-specific insertions, Ins-1 (residues 314-339) and Ins-2 (residues 393-415), which are important and conserved among AMSH family members. The single domain containing two characteristic insertions is required for linkage-specific recognition of STAMBPL1 [Sato et al., 2008]. In addition, STAMBPL1 has been shown to recognise both proximal and distal ubiquitins.

Generally, the catalytic sites of the DUB metalloproteases contain an aspartate, a serine, and two histidine residues [Shrestha & Das, 2021] (Figure 5). The catalytic site also requires a zinc ion, which is coordinated by two histidine residues, an aspartate (or a glutamate) as well as a water molecule. A zinc ion is then bound to a polarized molecule of water generating a hydroxide ion from water to hydrolyse the isopeptide bond between ubiquitin and substrate [Komander, 2010].

In the crystal structure of STAMBPL1 DUB-Zn^{2+} complex, Zn^{2+} is stabilised in the active site by forming coordinate bonds with residues His347, His349, Asp360 and a water molecule which is hydrogen bonded to Glu292. The quantum mechanical/molecular mechanical (QM/MM) method shows that Zn^{2+} plays an essential role in the catalytic reaction of STAMBPL1 by coordinating to the water and Gly76. The catalytic reaction of STAMBPL1 requires the activation of the water molecule. The Zn^{2+}-coordinated water molecule is first activated by Glu292, and the resulting hydroxyl attacks the carbonyl group of Gly76 in the distal ubiquitin, leading to the isopeptide bond cleavage. Thus, Glu292 acts as the proton donor/acceptor during the catalytic reaction whereas Ser357 serves to stabilise the negative charge in Gly76 [Zhu et al., 2015].

1.1.5 STAMBPL1 function

Two decades ago, STAMBPL1 was originally identified as an AMSH paralogue [Kikuchi et al., 2003], functioning as an inducer of the interleukin-2-mediated c-myc expression; however, its cellular substrates and functions are not fully characterised. STAMBPL1 has 56% amino acid sequence identity with AMSH, but it does not play a role in the endosomal-lysosomal sorting of cell-surface receptors [Ribeiro-Rodrigues et al., 2014]. Instead, it has been implicated as positive regulator in the TGF-β signalling through their interaction with inhibitory I-SMADs [Ibarrola et al., 2004] and has been shown to be an indirect activator of NF-κB signalling by exporting Tax from the nucleus to the cytoplasm, where it triggers NF-κB activation [Lavorgna et al., 2011]. Studies have further shown that methylation of STAMBPL1 results in cell proliferation and anti-apoptosis via NF-κB, TGF-β and PI3K signalling pathways [Li & Chen, 2016]. In addition, STAMBPL1 has been described as a mediator in epithelial-mesenchymal transition (EMT) by stabilising a transcription factor Signal transducer and activator of transcription 3 (STAT3) down-regulates SNAI-1 (Snail-1) [Ambroise et al., 2020], indicating that STAMBPL1 is linked to tumour development [Lee, 2017]. STAMBPL1 also has a fundamental function in regulating apoptotic cell death in renal and prostate cancer cells [Shahriyar et al., 2018; Chen et al., 2019; Woo et al., 2019; Yu et al., 2019].

More recently, STAMBPL1 has been shown to function co-ordinately with ring finger protein 167 (RNF167) ubiquitin ligase controlling Sestrin2 ubiquitinylation in response to leucine availability [Wang et al., 2022], and play a role in stabilisation of a dual-specificity mitogen-activated protein kinase phosphatase-1 (MKP-1) in breast cancer cells [Liu et al., 2022]. STAMBPL1 expression is ubiquitous among a variety of human tissues [Kikuchi et al., 2003] and shows overexpression in human cancer [Chen et al., 2019; Ambroise et al., 2020].

1.2 Helicobacter pylori

1.2.1 *H. pylori* associated diseases

H. pylori, an extracellular spiral-shaped gram-negative bacterium that specifically colonises the human gastric epithelium, is the main risk factor for gastric cancer and has been linked to gastrointestinal diseases such as gastritis and peptic ulcers [Alipour, 2021]. Infection with *H. pylori* is estimated to persist in approximately 50% of the world's population [Zamani et al., 2018]. However, the prevalence of *H. pylori* infection is highly variable across different countries; for example, the overall prevalence in developed countries is lower than in developing countries [Hooi et al., 2017]. Acquisition of *H. pylori* infection is predominantly in childhood and can persist for decades or even a whole lifetime. This pathogen is transmitted vertically via direct human to human contact by faecal-oral or oral-oral routes [De Falco et al., 2015].

The *H. pylori* infection initially induces an inflammation (gastritis) of the gastric mucosa, often asymptomatic. It also has the potential to induce other severe illnesses such as duodenal and gastric ulcers [Burkitt et al., 2017; de Brito et al., 2019]. However, only a minor fraction of the *H. pylori*-infected individuals develops gastric cancer, while most of the infections remain benign indicating involvement of multiple factors [De Falco et al., 2015]. The disease outcome depends on the interplay between the host-bacterial responses, gastritis phenotype and environmental factors (Figure 7).
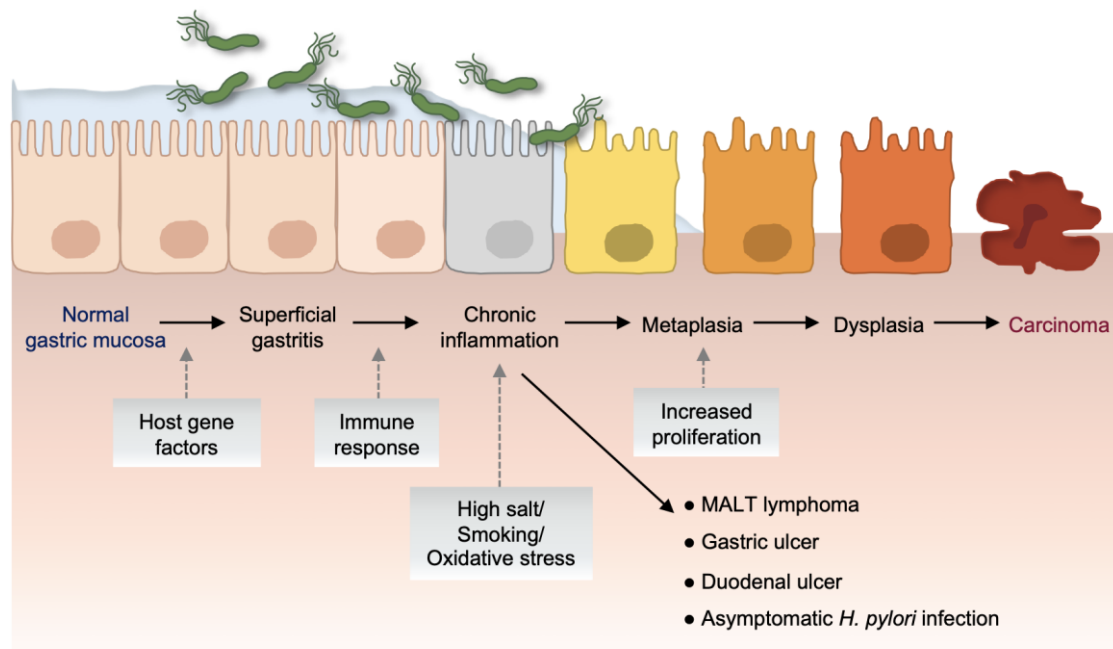
Figure 7   Changes in gastric mucosa during *H. pylori* infection. A combination of several host responses, bacterial and environmental factors contribute to gastric diseases. Chronic inflammation develops in almost all persistently colonised patients, of which, 90% remains asymptomatic. Abbreviation: MALT, mucosa-associated lymphoid tissue.

1.2.2 *H. pylori* virulence factors

The human stomach has a pH of 1-2, thus, lethal to most other microbes and limiting bacterial colonisation. By utilising the urease-catalysed ammonium production, *H. pylori* effectively tolerate the low-pH environment of the gastric lumen. Urease-mediated conversion of urea to ammonia and carbon dioxide, resulting in increased pH in the microenvironment around the bacteria [Miller et al., 2014]. The helical shape and flagella-mediated motility of the bacteria are supposed to function as a corkscrew to move toward host gastric epithelium cells through viscous media [Salama et al., 2013]. After reaching the gastric epithelium, *H. pylori* interacts with host cell receptors through bacterial adhesins to protect the bacteria clearance by liquid flow or peristaltic movement [De Falco et al., 2015], which leads to successful colonisation and persistent infection. Finally, *H. pylori* release several effector proteins/toxins, including cytotoxin-associated gene A (CagA), vacuolating cytotoxin A (VacA), and gamma-glutamyl transferase (GGT) causing host tissue damage. In addition, the gastric epithelial layer, which serves as the primary interface between *H. pylori* and the host, secretes chemokines that trigger innate immunity and activate neutrophils, resulting in the development of clinical diseases such as gastritis and ulcer [Gravina et al., 2018].

Several bacterial components contribute to gastric inflammation, either by interfering with host-signalling pathways or by interacting with host immune cells [Ansari et al., 2019]. The cag pathogenicity island (cagPAI) is located in the 40 kb DNA insertion element region containing about 31 genes, which are responsible for encoding the type IV secreted system (T4SS) and the virulence protein factor CagA [Backert et al., 2015]. T4SS is a multiprotein complex syringe-like structure that translocates CagA into the epithelial host cells [Naumann et al., 2017]. After delivery via T4SS, CagA becomes phosphorylated at the Glu-Pro-Ile-Tyr-Ala (EPIYA) motif present at its C-terminus by host Src and Abl kinases [Backert et al., 2010]. Phosphorylated CagA forms complexes with eukaryotic tyrosine phosphatase (SHP-2), leading to the activation of ERK 1/2, Crk adaptor or C-terminal Src kinase, which are involved in the regulation of cellular processes [Higashi et al., 2002]. The EPIYA motifs can be classified into EPIYA-A, EPIYA-B, EPIYA-C, and EPIYA-D that vary in amino-acid sequence. EPIYA-A and EPIYA-B motifs presents in almost all CagA, followed by either EPIYA-C or EPIYA-D. Studies have shown that EPIYA-C motif is characteristic of Western strains, whereas the EPIYA-D motif is observed in East-Asian strains [Takahashi-Kanemitsu et al., 2020]. Interestingly, the East-Asian CagA is supposed to be more virulent when compared to the Western subtype due to its ability to bind to SHP-2, resulting in aggressive diseases [Jones et al., 2009]. Translocated CagA interacts with diverse host proteins, thereby activating downstream signalling pathways, such as RAS/mitogen-activated protein kinase (MEK)/extracellular signal-regulated kinase (ERK), nuclear factor kappa-light-chain-enhancer of activated B cells (NF-κB), and β-catenin. These affect the host cell e.g., abnormal cytoskeletal changes, chronic inflammation, modulation of apoptosis, and genetic instability [Hatakeyama, 2014].

The vacuolating cytotoxin A (VacA) is a pore-forming secreted toxin expressed by the majority of all *H. pylori* strains. The secreted VacA, 88-kDa in size constituting N-terminal (p33) and C-terminal (p55) [Pyburn et al., 2016], inserts itself into the host cell membrane. VacA is known to bind several receptors on gastric epithelium cells [Isomoto et al., 2010] e.g., sphingomyelin [Gupta et al., 2008], fibronectin [Hennig et al., 2005], receptor protein-tyrosine phosphatase α (RPTPα) [Yahiro et al., 2003], RPTPβ [de Guzman et al., 2005], and low-density lipoprotein receptor-related protein 1 (LRP1) [Yahiro et al., 2012] and subsequently internalised through a cell division cycle 42 (Cdc42)-dependent pinocytic pathway to late endosomes, where it induces

the formation of large vacuoles [Gauthier et al., 2005]. Besides induction of vacuolation, the p33 subunit of VacA can induce mitochondrial damage and promotes apoptotic cell death [Cover et al., 2005; Yamasaki et al., 2006; Rassow et al., 2012]. On the other hand, it was also proposed that VacA causing death of gastric epithelial cells via programmed necrosis [Radin et al., 2011]. VacA also activates the p38/activating transcription factor 2-mediated signalling pathway resulting in impairment of the cell cycle in gastric epithelial cells [Palframan et al., 2012].

The gamma-glutamyl transpeptidase (GGT) is first synthesized as a 60 kDa pro-enzyme, which will be processed to get a large (37 kDa) and a small (20 kDa) subunit. The active enzyme is subsequently formed as heterodimer by the association of the large and small subunits. GGT has been shown to be implicated in the colonisation of *H. pylori* in the gastric mucosa [Wüstner et al., 2017], inhibit T-cell proliferation [Schmees et al., 2007], and mediate cell apoptosis [Handa et al., 2010]. GGT also play a role in the regulation of cyclooxygenase 2 (COX-2) expression in human gastric cells [Busiello et al., 2004]. In addition, GGT emerged as virulence factor that contributes to increase H_2O_2 levels and DNA damage in gastric cells [Flahou et al., 2011].

1.2.3 *H. pylori* induced ROS and apoptosis

The presence of *H. pylori* results in reactive oxygen species (ROS) and reactive nitrogen species (RNS) produced by the host in the gastric mucosa [Ma et al., 2013]. Excessive ROS production has been reported in *H. pylori*-infected human gastric mucosa and correlates with bacterial load [Jain et al., 2021]. Although neutrophils primarily contribute the most remarkable amount of ROS [Naito et al., 2002], gastric epithelial cells are another source of ROS in the *H. pylori*-infected stomach. Upon infection, *H. pylori* lipopolysaccharide (LPS) not only activate neutrophils to produce superoxide anions ($O^{2\bullet-}$), but also activates the small GTPase, Ras-related C3 botulinum toxin substrate 1 (Rac1), leading to nicotinamide adenine dinucleotide phosphate (NADPH) oxidase 1 (Nox1) activation and production of ROS on gastric epithelial cells [Lambeth et al., 2004; Kawahara et al., 2005; Cheng et al., 2006]. In addition to LPS, bacterial factors of *H. pylori* such as VacA and GGT also contribute to the host's production of oxidative stress resulted in cell apoptosis.

Apoptosis, a form of programmed cell death, is a sequential process of caspases cascade to destroy cells, within the extrinsic and intrinsic pathways (Figure 8). *H. pylori* is capable of triggering apoptosis through both the extrinsic (death receptor-mediated) [Domhan et al., 2004] and intrinsic (mitochondrial) pathways [Ashktorab et al., 2004;

Zhang et al., 2007]. The extrinsic pathway involves death receptors which are members of the tumor necrosis factor (TNF) receptor gene superfamily. The interaction of death receptors with their ligands at the plasma membrane, in turn, recruit adaptor proteins and pro-caspase, leading to the assembly of the death-inducing signalling complex (DISC) and the activation of initiator caspase-8. *H. pylori* has been shown to induce the extrinsic pathway by e.g., increasing the expression of CD95 in gastric epithelial cells [Domhan et al., 2004]. In addition, it has been shown that *H. pylori*-directed ROS also trigger apoptosis by inducing ubiquitin-proteasomal degradation of cellular FLICE (FADD-like IL-1β-converting enzyme)-inhibitory protein (c-FLIP), thus enhancing the extrinsic pathway [Lin et al., 2014].

The intrinsic pathway, on the other hand, is triggered by cellular stresses including oxidative stress [Ghavami et al., 2004; Kim et al., 2007]. VacA is translocated into the inner mitochondrial membrane [Domańska et al., 2010] and the pro-apoptotic factor Bcl-2-associated X protein (Bax) is recruited to mitochondria via VacA-containing endosomes where it forms channels [Calore et al., 2010]. This disruption in mitochondrial dynamics leads to an influx of Cl^- ion into the mitochondrial matrix, loss of the mitochondrial membrane potential [Willhite & Blanke, 2004], and the release of cytochrome c [Yamasaki et al., 2006]. The release of cytochrome c from mitochondria binds to apoptosis-activating factor 1 (Apaf-1) to form a complex called apoptosome for the activation of procaspase-9, resulting in apoptotic cell death [Cover et al., 2005; Shalini et al., 2015]. Another source of ROS within the epithelial cells during *H. pylori* infection is GGT, a virulence factor that contributes to the production of H_2O_2 [Gong et al. 2004]. *H. pylori* GGT hydrolysed glutamine into glutamate and ammonia and converts glutathione into glutamate and cysteinylglycine [Shibayama et al., 2007; Flahou et al., 2011]. The glutathione is an essential antioxidant which detoxify ROS, hence depletion of glutathione by GGT contributes to an impaired redox balance and ROS generation. ROS-related GGT-induced apoptosis has been shown to occur via a mitochondria-mediated pathway with the release of cytochrome c and the activation of caspase-9 and -3 [Kim et al., 2007; Flahou et al., 2011]. However, another study revealed that GGT induced apoptosis by inducing cell cycle arrest in the G1 phase [Kim et al., 2010]. *H. pylori* lacking GGT was no longer able to cause epithelial cells death [Kim et al., 2007; Flahou et al., 2011; Valenzuela et al., 2013].
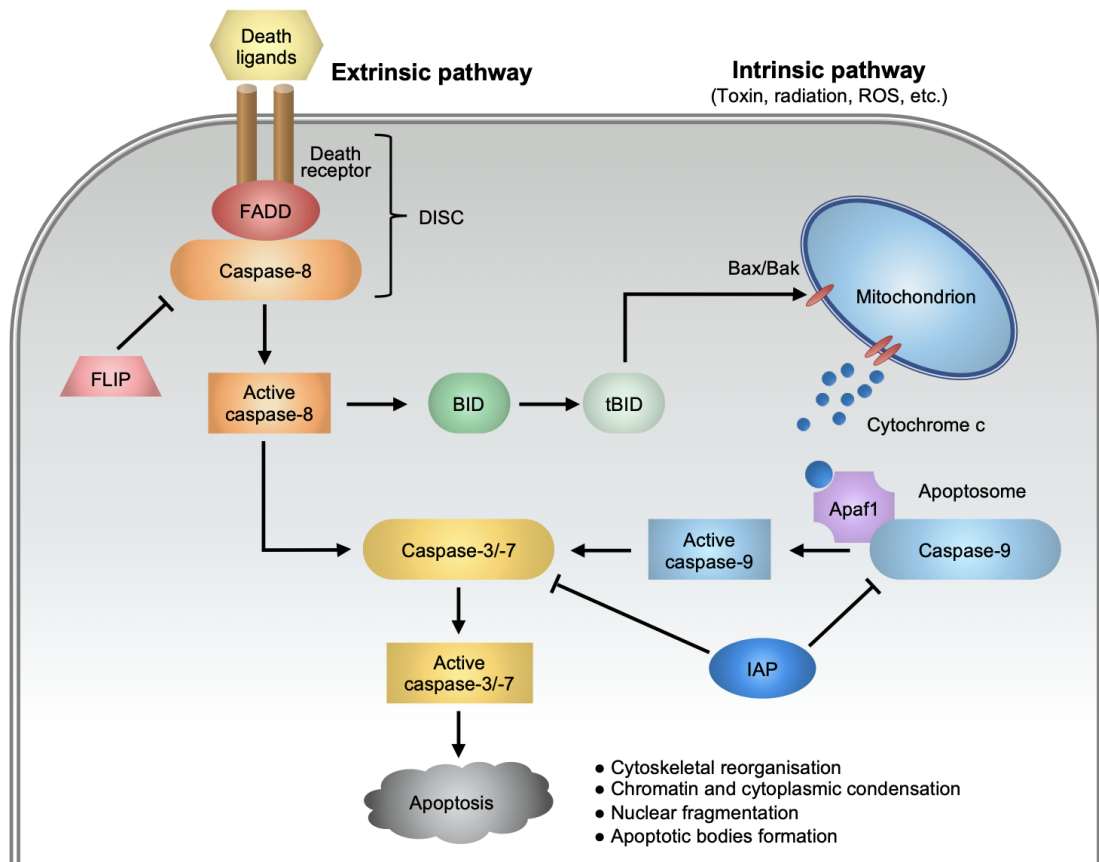
Figure 8   Schematic representation of apoptotic pathways. The extrinsic pathway (left) involves the binding of extracellular ligands to death-promoting receptors, resulting in the formation of DISC. The intrinsic pathway (right) is regulated by a series of specific death-promoting molecules released from the mitochondrion. Each pathway activates its own initiator caspase-8 or -9, which in turn activate the executioner caspase-3. Abbreviations: Apaf-1, apoptotic protease activating factor 1; Bak, Bcl2 antagonist/killer 1; Bax, Bcl-2-associated X protein; Bid, BH3-interacting domain death agonist; DISC, death-inducing signalling complex; FADD, Fas-associated death domain; FLIP, FLICE (FADD-like IL-1β-converting enzyme)-inhibitory protein; IAP, inhibitor of apoptosis protein; ROS, reactive oxygen species; tBID, truncated Bid.

Further, *H. pylori* regulates a number of pro- and anti-apoptotic proteins such as Bax [Ashktorab et al., 2004], B-cell lymphoma 2 (Bcl-2) [Lei et al., 2021], Induced myeloid leukemia cell differentiation protein (Mcl-1) [Mimuro et al., 2007], TNF receptor-associated factor 1 (TRAF1) [Wan et al., 2016], TNF receptor-associated factor 2 (TRAF2) [He et al., 2020], cellular inhibitor of apoptosis protein 1 (cIAP1), and cellular inhibitor of apoptosis protein 1 (cIAP2) [Maubach et al., 2021].

The anti-apoptotic proteins cIAP1 and cIAP2 are members of the inhibitor of apoptosis protein (IAP) family, a group of eight structurally related proteins that share the baculovirus IAP repeat (BIR) domain (XIAP, cIAP1, cIAP2, ILP-2, ML-IAP, NAIP, Apollon, and Survivin) (Figure 9), which can block apoptosis by either directly inhibiting

caspase activity or by controlling signalling through the death receptors [Valenzuela et al., 2013; Lalaoui et al., 2018]. In addition, the expression of IAPs have been implicated in apoptosis resistance, for instance, *H. pylori* induced the upregulation of cIAP2 expression in gastric epithelial cells and the gastric mucosa of *H. pylori* infected mice [Li et al., 2011], indicating an important role of IAPs in *H. pylori*-mediated gastric disease.

1.2.4 Apoptotic cell death and Survivin

Survivin (also known as BIRC5) is a member of the IAP family that has been implicated in regulation of cell division and inhibition of apoptotic cell death. Survivin is the smallest mammalian IAP with 142 amino acids, 16.5 kDa. Structurally, Survivin contains a single BIR domain and an extended carboxyl-terminus α-helical coiled-coil domain (Figure 9). Moreover, it does not contain a RING-finger domain, found in other IAPs. It has been demonstrated that Survivin localises in both nuclear and cytosolic compartments. Localisation within the cytoplasm is crucial to the anti-apoptotic activity of Survivin [Knauer et al., 2007; Connell, et al., 2008].
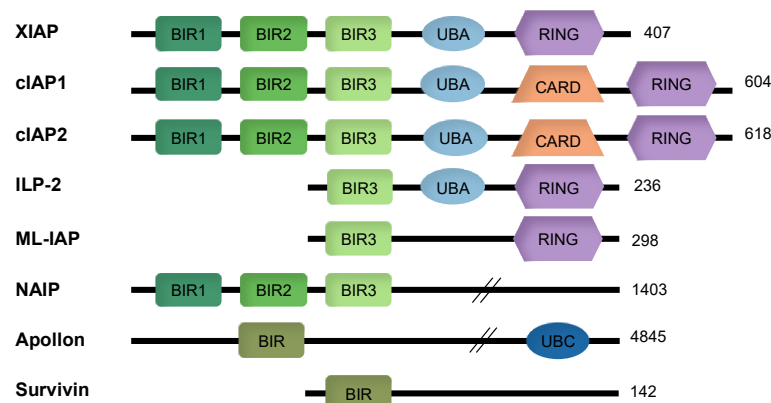
Figure 9   Domain structure of inhibitor of apoptosis protein (IAP) family. Abbreviations: BIR, baculoviral IAP repeat domain; CARD, caspase recruitment domain; cIAP1, cellular inhibitor of apoptosis protein 1; cIAP2, cellular inhibitor of apoptosis protein 2; ILP-2, inhibitor of apoptosis protein-like protein-2; ML-IAP, melanoma inhibitor of apoptosis protein; NAIP, neuronal apoptosis inhibitory protein; RING, really interesting new gene; UBA, ubiquitin-associated domain; UBC, ubiquitin conjugating domain.

Survivin is only expressed in actively proliferating cells but is upregulated in most cancers. The gastric epithelium represents an exception in which Survivin is essential to ensure survival of epithelial cells in the stomach environment [Valenzuela et al., 2010]. Survivin level is controlled by both transcriptional regulation [Hoffman et al., 2002; Torres et al., 2006] and degradation via the proteasome [Lladser et al., 2011]. At the transcriptional level, expression is favoured by activation of the β-catenin pathway

[Torres et al., 2006] or by direct binding of p53 to the Survivin promoter [Hoffman et al., 2002]. Further, regulation of Survivin is achieved by proteasome-mediated degradation, in which, binding to X-linked inhibitor of apoptosis protein (XIAP) increases Survivin turnover [Arora et al., 2007]. In addition, oxidative stress promotes Survivin loss in various cells [Jeong et al., 2009].

Functionally, Survivin cooperates with XIAP and hepatitis B virus X-interacting protein (HBXIP) in a complex with XIAP-associated factor 1 (XAF1) to affect the interaction of XIAP with caspases or to augment the effect of other IAP family members [Marusawa et al., 2003]. Survivin may also prevent the release of Apaf-1 from the mitochondria or sequester the IAP inhibitor second mitochondrial-derived activator of caspases (Smac; also known as Diablo), away from other IAPs [Song et al., 2004].

While Survivin mRNA levels are unchanged in the presence of *H. pylori*, the *H. pylori* virulence factor GGT enhanced loss of Survivin via the proteasome by a Fe^{3+}-dependent pathway in gastric epithelial cells [Valenzuela et al., 2013]. However, another study provides an alternative mechanism that *H. pylori*-induced changes in the ER stress sensor, protein kinase R-like endoplasmic reticulum kinase (PERK), contributed to the loss of Survivin [Díaz et al., 2021]. Thus, Survivin down-regulation upon *H. pylori* infection coincides with reduced cell viability and augmented apoptotic cell death in gastric epithelial cells.

2. Materials and methods

2.1 Materials

2.1.1 Cell lines

Cell line	Origin	Catalogue number
AGS	Human gastric carcinoma	ATCC, CRL-1739
NCI-N87	Human gastric carcinoma	ATCC, CRL-5822
HeLa	Human cervical carcinoma	ATCC, CCL-2

2.1.2 Bacteria

Strain	Mutation	Resistance
P1 wt	wildtype	Vancomycin
P1 *cagA*	*cagA*	Vancomycin, Chloramphenicol
P1 *virB7*	*virB7*	Vancomycin, Chloramphenicol
P12 wt	wildtype	Vancomycin
NEB 5-alpha competent *E. coli*	wildtype	-

2.1.3 siRNAs

Target	siRNA sequence (5'→3')	Supplier	Order number
AMSH	UUACAAAUCUGCUGUCAUUUU	Eurofins Genomics	Custom synthesized
CSN2	AssayID: 140004	Thermo Scientific	AM16708
CSN5	AssayID: 108110	Thermo Scientific	AM16708
Cullin1	CAACGAAGAGUUCAGGUUU	Dharmacon	J-004086-06-0005
Cullin3	GAGAUCAAGUUGUACGUUA	Eurofins Genomics	Custom synthesized
Scramble	Non-targeting pool	Dharmacon	D-001810-10
STAMBPL1	CGUAGAAUACCAAGAAUAU	Eurofins Genomics	Custom synthesized

2.1.4 Antibodies

Secondary antibodies	Supplier	Catalogue number
Anti-mouse IgG-HRP	Santa Cruz Biotechnology	sc-2005
Anti-rabbit IgG-HRP	Santa Cruz Biotechnology	sc-2004
Anti-mouse IgG (Light chain)	Jackson ImmunoResearch	115-035-174
Anti-rabbit IgG (Light chain)	Jackson ImmunoResearch	211-032-171

Primary antibodies	Supplier	Catalogue number
AMSH	Santa Cruz Biotechnology	sc-271641
c-Myc	Santa Cruz Biotechnology	sc-40
c-Myc	Santa Cruz Biotechnology	sc-789
CagA	Austral Biologicals	#HPM-5001-5
Cleaved caspase3	Cell Signaling Technology	#9661
CSN2	Abcam	ab155774
CSN5	GeneTex	GTX70207
CSN6	Santa Cruz Biotechnology	sc-137153
CSN7A	Santa Cruz Biotechnology	sc-398882
Cullin1	Abcam	ab2964-500
Cullin3	Novus	NB100-58787
DDDDK Tag	Abcam	ab1162
FLAG	Sigma-Aldrich	#F3165
Flagellin	Acris	AM00865PU-N
GAPDH	Millipore	#MAB374
GST	Santa Cruz Biotechnology	sc-53909
His	Santa Cruz Biotechnology	sc-53073
His	Proteintech	66005-1
Lamin B2	Santa Cruz Biotechnology	sc-377379
Nucleolin	Santa Cruz Biotechnology	sc-13057
STAMBPL1	Santa Cruz Biotechnology	sc-376526
STAMBPL1	Abcam	ab99172
Survivin	Santa Cruz Biotechnology	sc-17779
Ub (PAN)	Santa Cruz Biotechnology	sc-8017
Ubiquitin K48 linkage	Millipore	05-1307
USP15	Abnova	H00009958-M01
USP7	Bethyl	A300-033A

2.1.5 Plasmid

Plasmid	Supplier	Order number
STAMBPL1 Myc-DDK-pCMV	OriGene	RC201884

2.1.6 Gene-specific RT-qPCR primers

RT-qPCR primers	Supplier	Order number
STAMBPL1 (Hs00697415_m1)	Thermo Fisher Scientific	4331182
GAPDH (Hs99999905_m1)	Thermo Fisher Scientific	4331182

2.1.7 Kits

Kits	Supplier	Order number
Annexin V-FITC/PI Kit	MabTag GmbH	AnxF100PI
DCFDA/H2DCFDA-cellular ROS assay kit	Abcam	ab113851
HiSpeed® Plasmid Midi Kit	Qiagen	12663
IncuCyte® Caspase-3/7 green apoptosis reagent	Essen Bioscience	4440
METAFECTENE® PRO	Biontex	T040-1.0
NucleoSpin® RNA plus kit	Macherey-Nagel	740984-50x
Pierce™ BCA protein assay kit	Thermo Scientific	23225
PURExpress® In vitro protein synthesis kit	New England Biolabs	E6800S
RT² First strand kit	Qiagen	330411
TaqMan® Fast universal PCR master mix	Thermo Scientific	4352042

2.1.8 Recombinant proteins

Recombinant proteins	Supplier	Order number
Human GST	Abcam	ab81793
Human GST-STAMBPL1	R&D System	E-551
Human His6-USP15	Enzo Life Sciences	BML-UW9845
Human His6-USP7	R&D System	E-519
Interleukin-1β (IL-1β)	PeproTech	12242S
Tumor necrosis factor (TNF)	PeproTech	300-01A-50ug

2.1.9 Buffers and solutions

Protein extraction buffer	Compositions
RIPA	50 mM Tris/HCl, pH 7.5
	150 mM NaCl
	2 mM EDTA
	10 mM K_2HPO_4
	10 % glycerol
	1 % Triton X-100
	0.05 % SDS
	0.5 mM AEBSF
	1 mM Sodium orthovanadate
	1 mM Sodium molybdate
	10 mM Sodium fluoride
	20 mM Glycerol-2-phosphate
	7.5 mM NEM
	1 x Protease Inhibitor Cocktail

SDS-PAGE and blotting buffers	Compositions
Bovine serum albumin (BSA) (5%)	5 g BSA powder 100 ml TBST
Laemmli buffer (4X)	0.5 M Tris base, pH 6.8 8% (w/v) SDS 40% (v/v) Glycerin 0.04% Bromophenol blue 5% β-Mercaptoethanol
Milk blocking solution (5%)	5 g milk powder 100 ml TBST
SDS gel buffer	0.5 M Tris, pH 6.8 1.5 M Tris, pH 8.8
SDS-PAGE running buffer	25 mM Tris 0.2 M Glycine 0.1 % SDS
Stripping buffer	62.5 mM Tris, pH 6.7 2% SDS
TBS (10 X)	100 mM Tris, pH 7.6 1.5 M NaCl
TBS-T	1 X TBS 0.1 % (v/v) Tween-20
Western blotting running buffer	25 mM Tris 0.2 M Glycine 10 % methanol

Survivin elution buffer	Compositions
Elution buffer	0.1 M glycine, pH 2.5
Neutralization buffer	1 M Tris-HCl, pH 8.5

In vitro DUB assay buffer	Compositions
Ubiquitinylation assay buffer	50 mM HEPES, pH 8.0 100 mM NaCl 1 mM DTT

IP buffers	Compositions
Co-IP	50 mM Tris/HCl, pH 7.5 150 mM NaCl 2 mM EDTA 10 mM K_2HPO_4 10 % glycerol 1 % Triton X-100 0.05 % SDS
Denaturation IP	50 mM Tris/HCl, pH 7.5 150 mM NaCl 2 mM EDTA 10 mM K_2HPO_4 10 % glycerol 1 % Triton X-100 0.1 % SDS
In vitro binding assay IP	20 mM Tris/HCl, pH 7.4 150 mM NaCl 2 mM EDTA 1 % Triton X-100 0.1 % SDS
Mono-detergent IP buffer	50 mM Tris/HCl, pH 7.4 150 mM NaCl 1 mM EDTA 1 % Triton X-100

Subcellular fractionation buffers	Compositions
Buffer A	20 mM Tris base, pH 7.9 10 mM NaCl 1.5 mM $MgCl_2$ 10 % Glycerin 0.5 mM AEBSF 1 mM Sodium orthovanadate 1 mM Sodium molybdate 10 mM Sodium fluoride 10 mM K_2HPO_4 20 mM Glycerol-2-phosphate 7.5 mM NEM 1 x Protease Inhibitor Cocktail

Buffer C	20 mM Tris base, pH 7.9
	420 mM NaCl
	1.5 mM $MgCl_2$
	10 % Glycerin
	0.2 mM EDTA
	0.5 mM AEBSF
	1 mM Sodium orthovanadate
	1 mM Sodium molybdate
	10 mM Sodium fluoride
	10 mM K_2HPO_4
	20 mM Glycerol-2-phosphate
	7.5 mM NEM
	1 x Protease Inhibitor Cocktail
Buffer E	20 mM Tris base, pH 7.9
	150 mM NaCl
	1.5 mM $MgCl_2$
	5 mM $CaCl_2$
	10 % Glycerin
	2 % SDS
	0.5 mM AEBSF
	1 mM Sodium orthovanadate
	1 mM Sodium molybdate
	10 mM Sodium fluoride
	20 mM Glycerol-2-phosphate
	7.5 mM NEM
	1 x Protease Inhibitor Cocktail

2.1.10 Chemicals and reagents

Antibiotics	Supplier	Order number
Chloramphenicol	Sigma	C0378-5g
Kanamycin	Sigma	K4000-1g
Vancomycin	Applichem	A1839-1g

Media	Supplier	Order number
LB Medium	Carl Roth	X968.2
RPMI 1640 medium	Thermo Scientific	21875034

Chemicals and reagents	Supplier	Order number
Acrylamide	Applichem	A0951-1L
Agarose	Invitrogen	16500-100g
Ammonium persulfate	Applichem	A2941-100g
Benzonase	Sigma	70746-3
Beta-mercaptoethanol	Sigma	63689-100ml
Bovine serum albumin (Fraction V) (BSA)	Applichem	A1391-250g

Bromophenol blue	Waldech GmbH	441619-25g
Calcium chloride	Sigma	102382-250g
Chemiluminescent HRP Substrate	Millipore	WBKLS0500
Color Prestained Protein Standard, Broad range (11-245 kDa)	New England Biolabs	P7712L
Dimethyl sulfoxide (DMSO)	Sigma	34869-1L
Dithiothreitol (DTT)	Applichem	A2948-25g
Dulbecco's PBS	Thermo Scientific	14190094
Dulbecco's PBS (Ca^{2+}, Mg^{2+})	Thermo Scientific	14040091
Ethanol	Fischer	8025-1L
Ethanol	ChemSolute	22.461.000-1L
Ethylenediaminetetraacetic acid (EDTA)	Sigma	E1644-250g
Fetal bovine serum (FBS)	Capricorn Scientitic	FBS-12A
GeneRuler 1 kb Plus DNA ladder	Thermo Scientific	SM1331
Glucose	Merck	143856
Glycerol	Sigma	G7893-500ml
Glycine	Applichem	A1067-5kg
HDGreen® Plus Safe DNA Dye	Intas	ISII-HDGreen Plus
HEPES	Applichem	A1069-500g
Horse serum	Th.Geyer	S0900-500
Hydrogen chloride	Chemsolute	836-1L
Hydrogen peroxide solution	Sigma	H1009-100ml
Magnesium chloride	Merk	A537.1-100g
Magnesium sulfate	Sigma	M7506-1kg
Methanol	J.T.Baker	8045-1L
Milk powder	Roth	T145.3-1kg
NP40	Calbiochem	492016
Nystatin	Sigma	N4014-50mg
Pierce™ protein A/G magnetic beads	Thermo Scientific	88803
Potassium chloride	Roth	6781.1
Protein G sepharose beads	GE Healthcare	17-0780-01
PVDF membranes	Millipore	T831.1
Sodium chloride	Roth	3957.1-1kg
Sodium dodecyl sulfate (SDS)	Applichem	A1112-1kg
Sodium hydroxide	Roth	6771.1-1kg
Tetramethylethylenediamine (TEMED)	Roth	2367.1-100ml
Trimethoprim	Applichem	T7883-5g
Tris	Applichem	A1086-5kg
Triton X-100	Sigma	X100-500ml
Trypan blue	Invitrogen	T8154-100ml
Trypsin 0.25 % EDTA	Thermo Scientific	25200072
Tryptone	Roth	8952.1-250g
Tween 20	Roth	9127.2-1kg
Yeast extract	Roth	2363.3-500g

Inhibitors	Supplier	Order number
AEBSF	Applichem	A1421-1g
Camptothecin (CPT)	Sigma	C9911-100mg
Cycloheximide (CHX)	Sigma	2112S-1g
Doxorubicin (DOX)	Sigma	15007-50mg
Glycerol-2-phosphate	Sigma	G9422-100g
Lactacystin	Sigma	426100-400ug
MG132	Selleckchem	S2619
MLN4924	Active Biochem	A1139-M010
N-ethylmaleimide (NEM)	Sigma	04259-5g
Phenanthroline (OPT)	Sigma	S4014-5g
Potassium hydrogen phosphate	Roth	P749.2
Protease inhibitor cocktail	Roche	0000000050564 89001
Pyrrolidine dithiocarbamate (PDTC)	Selleckchem	S3633
RNase inhibitor	New England Biolabs	M0314S
Sodium fluoride	Sigma	S1504-100g
Sodium molybdate	Sigma	331058-100g
Sodium orthovanadate	Sigma	S6508-50g
Staurosporine (STS)	Enzo Life Sciences GmbH	380-014-M001

2.1.11 Instruments

Instruments	Supplier
C1000 Touch™ Thermal cycler	Bio-Rad
Centrifuge (5415R)	Eppendorf
Centrifuge (5810R)	Eppendorf
ChemoCam Imager	Intas
Countess	Invitrogen
CyFlow™ Space	PARTEC
Heidolph 3001 magnetic stirring hotplate	Merck
Heracell CO_2 Incubators	Thermo Fisher Scientific
HERAfreeze™ upright ultra-low temperature freezers	Thermo Fisher Scientific
Herasafe™ Class II Biological Safety Cabinet	Thermo Fisher Scientific
IncuCyte® S3 Live Cell Analysis System	Sartorius, Essen Biosciences
Microscope	Windaus-Labortechnik GmbH
Mixing Block MB-102	Biozym Scientific GmbH
Multifuge 3 S-R	Heraeus
Nanodrop 2000c	Thermo Fisher Scientific
PowerPac™	Bio-Rad
Rotator for IP	Windaus-Labortechnik GmbH
See-saw rocker SSL4	Stuart

Spectramax M5 plate reader	Molecular Devices GmbH
StepOnePlus™ real time qPCR platform	Applied Biosystems
Triple Stack Incubator Shakers AG CH-4103	Infors HT
Ultrospec 3100 pro	GE Healthcare
Vortex-Genie™ 2	Thermo Fisher Scientific
Water bath	GFL

2.2 Methods

2.2.1 Cell culture and bacteria

Human gastric carcinoma AGS and NCI-N87 cells and human cervical carcinoma HeLa cells were cultured in RPMI 1640 medium supplemented with 10 % heat-in-activated fetal bovine serum (FBS) in a humidified incubator at 37 °C with 5 % CO_2 and passaged once every 2-3 days.

H. pylori strain P1wt (wildtype) and isogenic mutants P1*cagA* (CagA-deficient) and P1*virB7* (T4SS-deficient) [Backert et al., 2000] as well as strain P12 [Königer et al., 2016] were grown on agar plates containing 10 % horse serum, 5 µg/ml trimethoprim, 1 µg/ml nystatin, and 10 µg/ml vancomycin under microaerophilic conditions at 37 °C for three days. For the P1*cagA* and P1*virB7* strains, the agar plates were supplemented with chloramphenicol. Bacteria were replated and cultured for another two days before use.

2.2.2 Bacterial transformation and plasmid preparation

The NEB 5-alpha competent *E. coli* bacteria were thawed on ice. 50 µl of competent cells were incubated with 10 ng of plasmid DNA (STAMBPL1 Myc-DDK-pCMV) and incubated on ice for 30 min followed by a heat shock at 42 °C for 30 s. Samples were immediately put back on ice for additional 2 min. Then, bacteria were incubated in 500 µl of SOC media without antibiotics in 37 °C shaking incubator for 1 h. Transformed bacteria (100 µl) were plated on selective LB agar plates and incubated overnight at 37 °C with shaking. The next day, a single colony was inoculated in 3-5 ml of LB medium with 25 ug/ml Kanamycin and grown overnight at 37 °C with shaking. The starter culture was inoculated in 150 ml medium and grown overnight with vigorous shaking. Cells were harvested by centrifugation at 4000 rpm for 15 min at 4 °C. Plasmid DNA was isolated using HiSpeed® Plasmid Midi Kit according to the manufacturer's protocol. Nanodrop2000c was used to measure the DNA concentration.

2.2.3 Transfection of siRNAs and plasmids

Cells (0.4×10^6 per 60 mm or 0.8×10^6 per 100 mm culture dish) were transfected with siRNAs against STAMBPL1, AMSH, Cul1, Cul3, CSN2, and CSN5 using METAFECTENE® PRO transfection reagent according to the manufacturer's protocol. The siRNAs were used at a final concentration of 50 nM for STAMBPL1 and AMSH, and 40 nM for Cullin1, Cullin3, CSN2, and CSN5. A scrambled siRNA was used as a negative control. Cells were harvested 24 h after siRNA transfection or at times as indicated. All siRNA sequences used in this study are shown in 3.1.3.

For overexpression of STAMBPL1 protein, AGS cells were transfected with 1 µg of pCMV-STAMBPL1 containing Myc-DDK tagged by using METAFECTENE® PRO transfection reagent. Six h after transfection, the medium was changed to fresh RPMI 1640 containing 10 % FBS.

2.2.4 Cell treatments and *H. pylori* infection

The cell culture medium was changed to fresh RPMI-1640 containing 10 % FBS 4 h prior to the treatment of the cells. For infection, the *H. pylori* bacteria were suspended in PBS and eukaryotic cells were infected at a multiplicity of infection (MOI) of 50, 100 or 200 as indicated or stimulated with 10 ng/ml TNF or 10 ng/ml IL-1β. Camptothecin (CPT), doxorubicin (DOX) and staurosporine (STS) were used at the final concentration of 5 µM, 1 µM, and 1 µM, respectively. For cycloheximide (CHX) chase experiments, cells were pretreated with CHX (50 µg/ml) for 30 min prior to *H. pylori* infection. For protein degradation analysis, MG132 (20 µM) and lactacystin (10 µM) was added at times indicated. For inhibition of NEDD8-activating enzyme (NAE), MLN4924 was used at the concentration of 1 µM.

2.2.5 Preparation of whole cell lysates and subcellular fractionation

Cells were lysed for 30 min on ice in RIPA buffer and lysates were cleared by centrifugation (13000 x g, 10 min, 4 °C). Nuclear and cytoplasmic cell fractions were generated by subcellular fractionation as described previously [Schweitzer and Naumann, 2015]. Protein concentration was determined using the Pierce™ BCA protein assay kit according to the manufacturer's instructions.

2.2.6 SDS-PAGE and immunoblotting

Samples were mixed with Laemmli's loading buffer [Laemmli, 1970], boiled for 5 min at 95 °C, separated by SDS-PAGE and electrotransferred onto PVDF membranes at 100 V constant. Membranes were blocked for 1 h at room temperature using 5 % skim milk in TBS containing 0.1 % Tween (TBS-T) and incubated with primary antibodies

overnight in either 5 % BSA or 5 % skim milk in TBS-T at 4 °C on a rocking platform. The membranes were washed three times in TBS-T and incubated with the appropriate HRP-conjugated secondary antibody for 1 h at room temperature, followed by three washes in TBS-T. Immunoblots were developed using a chemiluminescent substrate and visualized using the ChemoCam Imager. All antibodies used in this study are shown in 3.1.4.

2.2.7 Immunoprecipitation (IP)

Equal amounts of protein (0.5-1 mg in a volume of 700 μl) were incubated with 1 μg of specific antibodies or with isotype IgG of the same species as a negative control overnight on a permanent rotator (7 rpm, 4 °C). Afterwards, pre-washed Pierce™ protein A/G magnetic beads were added to the reaction and rotated for 2 h at 4 °C. The beads were washed four times with RIPA buffer containing all inhibitors and eluted in 2 x Laemmli sample buffer (30 ul) for 20 min at room temperature. The eluate was transferred to a clean tube and heated for 5 min at 95 °C. Further, the IP buffer was additionally supplemented with 7.5 mM NEM and 5 mM OPT.

For immunoprecipitation of the CSN complex, 0.5 mg of protein were incubated with 1 μg of CSN2 antibody in a volume of 700 μl mono-detergent buffer. After overnight on a permanent rotator, pre-washed protein G sepharose beads were added to the reaction and incubated for 2 h at 4 °C. After centrifugation (500 x g, 2 min, 4 °C), supernatants were discarded, and beads were washed four times in 700 μl of IP mono-detergent buffer. After complete removal of the supernatants, beads were suspended and boiled in 30 μl 2 x Laemmli sample buffer.

2.2.8 RNA isolation, reverse transcription, and quantitative PCR

Total RNA from AGS cells was extracted using the NucleoSpin® RNA Plus kit according to the manufacturer's protocol. 1 μg of RNA was reverse transcribed into cDNA using RT^2 First Strand Kit according to the manual on the C1000 Thermal cycler. The quantitative PCR was performed on a StepOnePlus™ real time qPCR platform using the TaqMan® Fast Universal PCR Master Mix and TaqMan® assays specific for STAMBPL1 and GAPDH. Relative quantification of gene expression was performed with the comparative CT method ($\Delta\Delta C_t$). RT-qPCR specificity was controlled by no-template and no-RT samples. The PCR cycle used is as follows:

Temperature (°C)	Time (mm:ss)	Cycle
95	0:20	1
95	0:01	40
60	0:20	
4	∞	

2.2.9 Measurement of cellular ROS

The cellular ROS level was detected using H2DCF-DA, which can be oxidized to a highly fluorescent 2′,7′-dichlorofluorescein (DCF). AGS cells grown to confluence on 60 mm culture dish were treated with *H. pylori* (MOI 100 wt, *cagA*, *virB7*), chemotherapeutics (5 µM CPT, 1 µM DOX, 1 µM STS) or cytokines (10 ng/ml IL-1β, 10 ng/ml TNF) for 4 h. For the analysis of intracellular ROS levels, cells were stained with 20 µM H2DCF-DA for 30 min at 37 °C according to the manufacturer's protocol and DCF fluorescence was measured by CyFlow™ Space. H_2O_2-treated cells served as positive control. Where indicated, AGS cells were treated with 20 or 40 µM of ROS inhibitor pyrrolidine dithiocarbamate (PDTC). For DCF imaging, images were captured with a 20 x objective in green channel by the IncuCyte® S3 Live Cell Analysis System.

2.2.10 *In vitro* translation and *in vitro* binding assay

CSN plasmid constructs as described previously were used [Lee et al., 2013]. Protein expression of CSN subunits was performed with the PURExpress® *In Vitro* Protein Synthesis kit according to the manufacturer's protocol for 3 h at 37 °C. Final reaction volumes were 25 µl and contained 300 ng plasmid. Afterwards, equal molar amounts of recombinant human GST-STAMBPL1 were mixed and coincubated for 1 h at 37 °C, followed by IP using the respective anti-GST antibody. IP buffer for *in vitro* binding assay and pre-washed Pierce™ protein A/G magnetic beads were used (see 3.2.7). The IPs were separated by SDS-PAGE and analysed by immunoblots. Recombinant human GST protein was used as a negative control.

2.2.11 *In vitro* DUB assay

AGS cells were transfected with siRNA against STAMBPL1 for 24 h to allow Survivin ubiquitinylation, followed by MG132 treatment for 4 h before harvesting the cells. Survivin was immunoprecipitated and eluted by elution buffer for 10 min at room temperature. The eluted Survivin sample was neutralized immediately after recovery by addition of 1/10th volume of neutralization buffer. *In vitro* DUB assay was carried out in 10 µl containing 500 ng of ubiquitinylated immunoprecipitated Survivin and 100 nM of GST-tagged STAMBPL1 in 1 x ubiquitinylation assay buffer. The reactions were

performed in the presence or absence of phenanthroline (5 mM) at 30 °C for 2 h and stopped by addition of 4 x Laemmli sample buffer. Samples were then separated by SDS-PAGE and analysed by immunoblots.

2.2.12 Apoptotic cell death analysis by flow cytometry

Apoptotic cell death was determined by Annexin V/PI staining. Briefly, 24 h after siRNA/cDNA transfection, cells were infected with *H. pylori* for 24 h. The cells were harvested using trypsin and stained with an Annexin V-FITC/PI Kit according to the manufacturer's instructions. The detection of apoptotic cell death was carried out on a CyFlow™ Space. Data were processed using Flowing Software 2 (Turku Bioscience) and the percentage of apoptotic cells were calculated.

2.2.13 Caspase 3/7 Assay

The IncuCyte® Caspase-3/7 reagents are a membrane-permeable substrate, which can release a fluorescent DNA-intercalating dye when cleaved by executioner caspases. After 24 h of siRNA/cDNA transfection, cells were re-seeded at a density of 50 000 cells/well in a 24-well plate and allowed to adhere overnight. Cell culture media were changed to media containing *H. pylori* (MOI 100) and IncuCyte® Caspase-3/7 Green reagent diluted to the manufacturer's recommended concentration. Plates were pre-warmed to 37 °C for 30 min before data acquisition to avoid condensation and expansion of the plate. Caspase-3/7 cleavage was measured every 2 h in an IncuCyte® S3 Live Cell Analysis System and four image sets from distinct regions per well were captured with phase contrast and green channel at a magnification of 20 x. Analyses were performed by IncuCyte® S3 Live Cell Analysis System integrated software and the percentages of apoptotic cells were calculated.

2.2.14 Statistical analysis

All quantitative data were repeated at least two times and presented as mean ± S.D (standard deviation). Statistical analysis was performed using Student's t-test (SPSS Statistics 18.0). Values of $p \leq 0.05$ and $p \leq 0.01$ were considered as significant (*, **). N.S. stands for not statistically significant.

3. Results

3.1 *H. pylori* induces STAMBPL1 degradation

When studying anti-apoptotic proteins in cells infected with *H. pylori*, we observed that the amount of Survivin decreased during infection. A recent report showing that the amount of Survivin is regulated by STAMBPL1 [Woo et al., 2019] prompted us to investigate this mechanism in detail.

Studying the regulation of STAMBPL1, we observed for the first time that STAMBPL1, but not AMSH, is degraded by *H. pylori* in AGS gastric epithelial cells. Further, *H. pylori* also caused STAMBPL1 degradation in NCI-N87 and Hela cells (Figure 10).
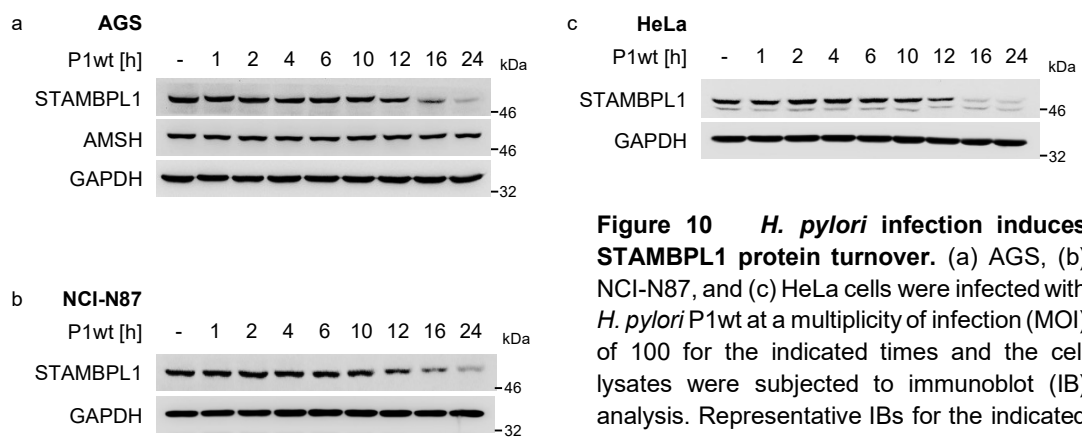
Figure 10 *H. pylori* **infection induces STAMBPL1 protein turnover.** (a) AGS, (b) NCI-N87, and (c) HeLa cells were infected with *H. pylori* P1wt at a multiplicity of infection (MOI) of 100 for the indicated times and the cell lysates were subjected to immunoblot (IB) analysis. Representative IBs for the indicated proteins from at least two independent experiments with similar results are shown.

Next, we investigated whether the *H. pylori* T4SS or the virulence factor CagA are involved in *H. pylori*-induced STAMBPL1 degradation and observed that all tested strains decreased the level of STAMBPL1 protein in a time-dependent manner (Figure 11a). In addition, an increasing MOI decreased the STAMBPL1 protein level congruently (Figure 11b). Similar data were received when we studied AGS cells infected with the *H. pylori* strain P12 (Figure 11c).
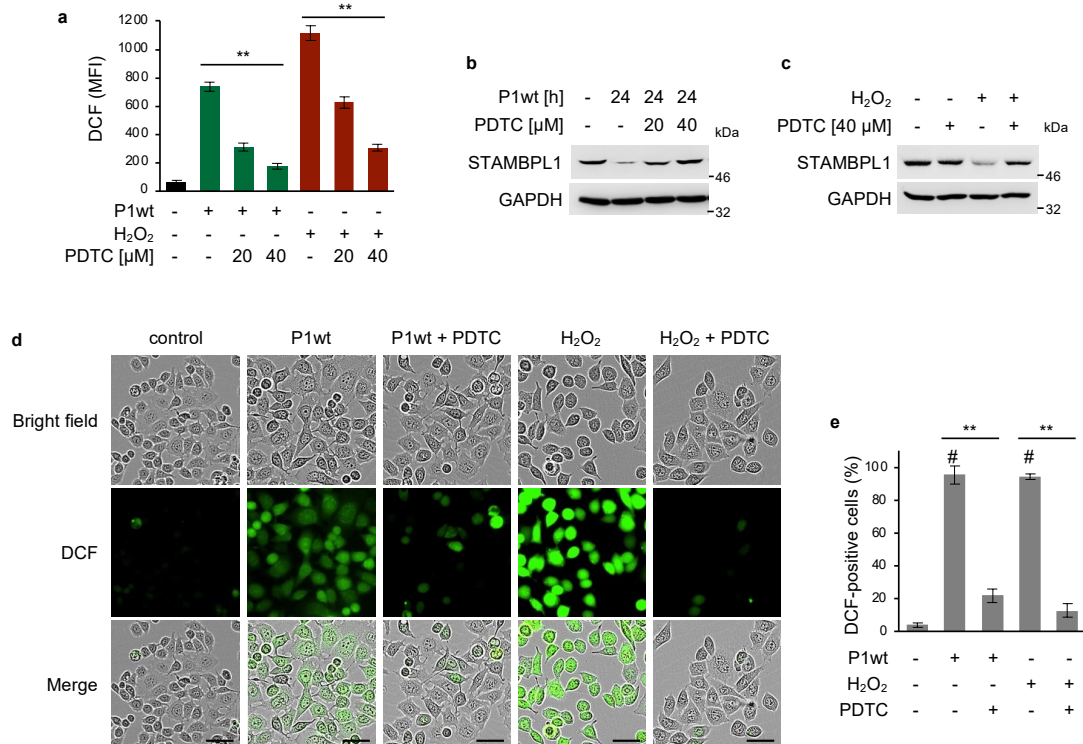
Figure 11 *H. pylori*-induced STAMBPL1 degradation is T4SS- and CagA-independent. (a) AGS cells were infected with different isogenic *H. pylori* strains (wt, virB7 or cagA) and (b) different MOI and then subjected to IB analysis. (c) AGS cells were infected with *H. pylori* P12wt at an MOI of 100 for 24 h. (a-c) Representative IBs for the indicated proteins from at least two independent experiments with similar results are shown.

3.2 Genotoxic stress-induced STAMBPL1 degradation is ROS-dependent

We investigated whether genotoxic stress induced by *H. pylori* or chemotherapeutic agents (CPT, DOX, STS) could regulate the STAMBPL1 abundance. Interestingly, in cells treated with the aforementioned chemotherapeutics, the effect on STAMBPL1 degradation was similar to that observed in the presence of *H. pylori*, whereas the treatment with cytokines had no impact. In contrast, AMSH showed no turnover (Figure 12).

Figure 12   Genotoxic stress-induced STAMBPL1 degradation is ROS-dependent. AGS cells were infected with P1wt at an MOI of 100 or treated with chemotherapeutic agents (CPT, DOX, STS) or cytokines (TNF or IL-1β) for the times indicated. The STAMBPL1 and AMSH protein was analysed by IB. Representative IBs for the indicated proteins from at least two independent experiments with similar results are shown.

H. pylori is known to induce ROS in human gastric epithelial cells [Ding et al., 2007] and most genotoxic drugs generate ROS in cancer cells [Yang et al., 2018]. Thus, prompting us to examine if ROS could be involved in the *H. pylori*-induced loss of STAMBPL1. Here, a redox-sensitive fluorescent dye H2-DCFDA was used to measure ROS production. H2-DCFDA is cleaved by intracellular esterases, resulting in a charged H2-DCF molecule, which is then oxidized by ROS to produce the fluorescent molecule, DCF. *H. pylori* and chemotherapeutic agents dramatically enhanced DCF fluorescence levels, whereas no significant increase in DCF fluorescence was detected in IL-1β or TNF-treated cells (Figure 13).
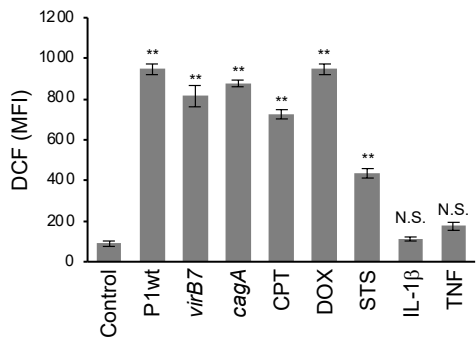
Figure 13   ROS measurement upon *H. pylori* infection and chemotherapeutics treatment. Cells were treated with different stimuli for 4 h and then analysed with a cell-based 2', 7'-dichlorodihydrofluorescein (H2DCF-DA) assay assessed by flow cytometry (**, p≤0.01; N.S., not statistically significant; n = 3).

Further, we pre-treated *H. pylori*-infected AGS cells with pyrrolidine dithiocarbamate (PDTC), a potent ROS scavenger, and determined the fluorescent intensity of DCF assessed by flow cytometry. We observed that increasing amounts of PDTC significantly resulted in a dose-dependent decrease in DCF fluorescence in *H. pylori* infected- or hydrogen peroxide-treated cells (Figure 14a). In concordance with these data, pre-treatment of *H. pylori*-infected AGS cells with PDTC inhibited the degradation of STAMBPL1 (Figure 14b), indicating that *H. pylori*-directed ROS causes STAMBPL1 degradation. Consistently, treatment of cells with hydrogen peroxide also induced a loss of STAMBPL1 while PDTC markedly suppressed hydrogen peroxide-induced STAMBPL1 degradation (Figure 14c). To further corroborate our findings, we assessed by Incucyte® Live-Cell Analysis the generation of ROS in AGS cells. We observed an increased ROS generation in AGS cells following *H. pylori* infection or hydrogen peroxide stimulation, which was diminished by PDTC treatment (Figure 14d, e). Collectively, we have shown that ROS generation by *H. pylori* infection or treatment with chemotherapeutics led to the degradation of STAMBPL1 in gastric epithelial cells.

Figure 14   *H. pylori*-induced ROS causes STAMBPL1 degradation. (a) AGS cells were treated with pyrrolidine dithiocarbamate (PDTC) 1 h before infection. Subsequently, cells were infected with *H. pylori* at MOI 100 or treated with 500 µM of hydrogen peroxide (H_2O_2) for 4 h. ROS production was analysed by flow cytometry (**, p≤0.01; n=2). (b, c) STAMBPL1 protein levels were analysed by IB. (d) Representative images of ROS generation in AGS cells after *H. pylori* infection or H_2O_2 stimulation for 4 h were acquired using IncuCyte® S3 Live Cell Analysis System. Scale bars, 20 µm. PDTC was used at a final concentration of 40 µM. (e) The percentage of DFC-positive cells is shown (# significantly different from the control group, ** Significantly different from the treatment group (p≤0.01; n=2)). (b, c) Representative IBs for the indicated proteins from at least two independent experiments with similar results are shown. Abbreviation: DCF, Dichlorofluorescein; H_2O_2, hydrogen peroxide; MFI, mean fluorescence intensity; PDTC, pyrrolidine dithiocarbamate.

3.3 CRL1-, and 26S proteasome-dependent degradation of STAMBPL1

To assess whether the *H. pylori*-induced down-regulation of STAMBPL1 was due to a transcriptional mechanism, we initially analysed the mRNA expression and observed that *H. pylori* did not inhibit STAMBPL1 mRNA expression (Figure 15a). Next, we investigated STAMBPL1 protein stability in the presence of CHX and found that *H. pylori* infection accelerated the protein turnover of STAMBPL1 (Figure 15b). In contrast, AMSH showed no turnover during CHX treatment (Figure 15b). Since the UPS is involved in the degradation of the majority of proteins, we therefore examined the 26S proteasome participation in the turnover of STAMBPL1 using lactacystin, a proteasome inhibitor, in *H. pylori* infected cells. Here, we observed that the STAMBPL1 protein was stabilised. Consistently, we found an accumulation of K48-ubiquitinylated STAMBPL1

protein in the samples which were treated with lactacystin (Figure 15c). Although, STAMBPL1 is localised also in the nucleus, we found that *H. pylori* promoted STAMBPL1 K48-ubiquitinylation exclusively in the cytoplasm. These findings demonstrate that the downregulation of STAMBPL1 by *H. pylori* was accomplished via the ubiquitin-proteasome degradation pathway.
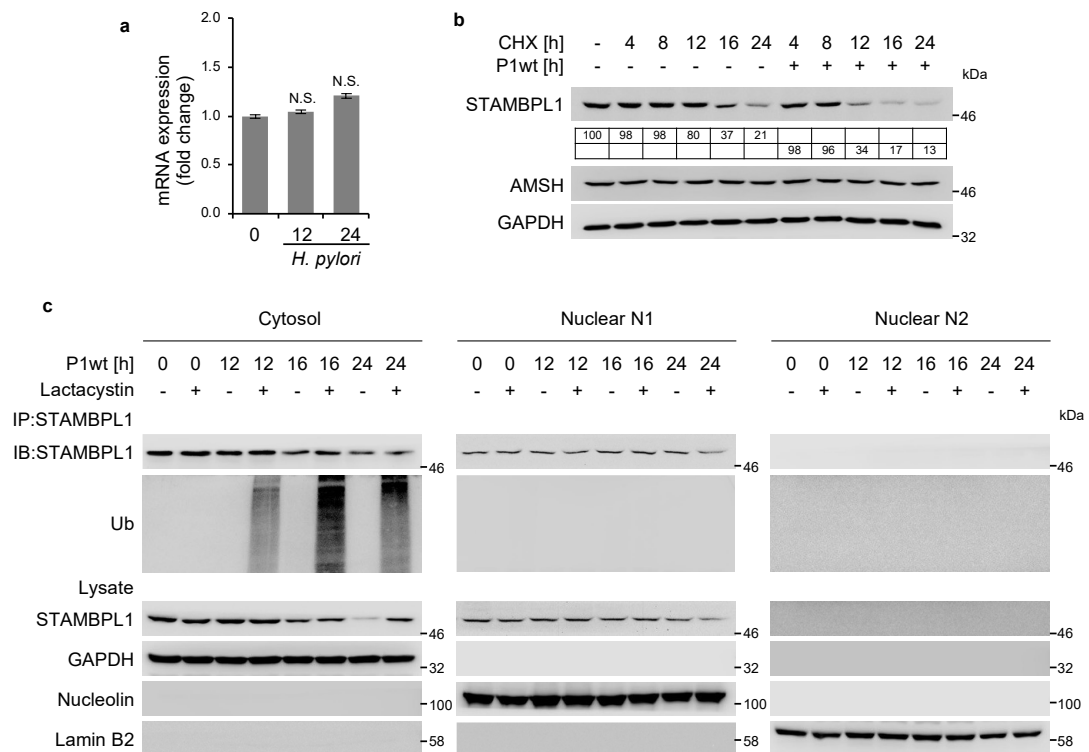

Figure 15   26S proteasome-dependent degradation of STAMBPL1. (a) Total RNA was isolated after *H. pylori* infection at the indicated time points and changes in STAMBPL1 transcript expression were examined by quantitative PCR (N.S., not statistically significant; n = 3). (b) AGS cells were treated with CHX at the indicated time points, or 30 min prior to *H. pylori* infection as times indicated. Quantification of band intensities was performed using ImageJ software. The shown blot strips for STAMBPL1 and GAPDH were selected from the same gel. (c) Cells were infected with *H. pylori* at the indicated time points and subjected to subcellular fractionation. GAPDH, nucleolin and lamin B2 served as controls for purity of subcellular fractions and equal amount of protein loading. STAMBPL1 was immunoprecipitated (IP) from each fraction and the IP subjected to IB analysis. Lactacystin at a final concentration of 10 µM was added 4 h before harvesting. (b, c) Representative IBs for the indicated proteins from at least two independent experiments with similar results are shown.

E3 ubiquitin ligase complexes catalyse ubiquitinylation of particular proteins, targeting them for proteasomal degradation. Within the largest family of E3 ubiquitin ligases, the CRL1 and CRL3 have been shown to be involved in the regulation of the oxidative stress response [Loignon et al.,2009, Bramasole et al., 2019]. To identify the CRLs involved in STAMBPL1 regulation, we knocked down CRL1 and CRL3. We observed that loss of CUL1 stabilised STAMBPL1 protein within *H. pylori* infection. This suggests that CRL1 is involved in *H. pylori*-induced ubiquitinylation of STAMBPL1, but CRL3 is not (Figure 16).
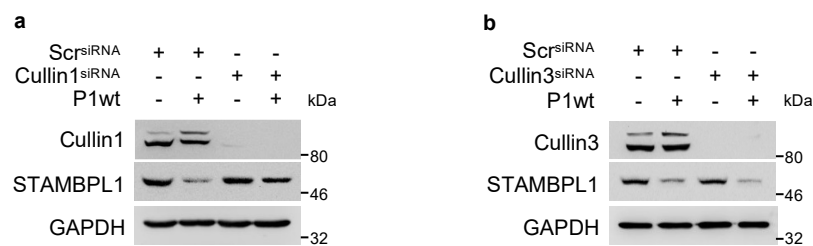
Figure 16 *H. pylori* **induces CRL1-dependent degradation of STAMBPL1.** AGS cells were transfected with (a) cullin 1 or (b) cullin 3 siRNA for 48 h, followed by infection with *H. pylori* for a further 24 h. STAMBPL1 protein level was analysed by IB. (a, b) Representative IBs for the indicated proteins from at least two independent experiments with similar results are shown.

The activity of CRLs is regulated by covalent modification with the ubiquitin-like protein NEDD8, which requires the activity of the NEDD8-activating enzyme, whose activity can be blocked by the small molecule MLN4924. Consequentially, we observed that the treatment with MLN4924 protected against *H. pylori*-induced STAMBPL1 loss in both P1wt (Figure 17a) and the *virB7* mutant (Figure 17b).
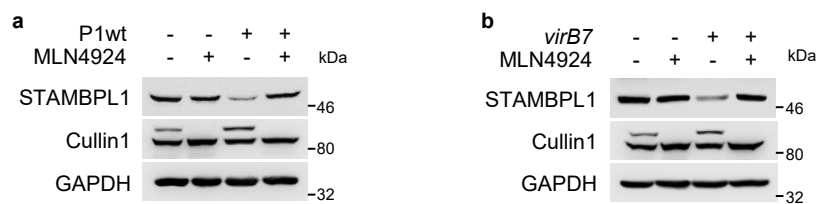
Figure 17   CUL1 activity is requested for STAMBPL1 degradation. (a) Cells were treated with MLN4924 at a final concentration of 1 μM and infected with *H. pylori* P1wt or (b) *virB7*, followed by IB analysis of STAMBPL1. (a, b) Representative IBs for the indicated proteins from at least two independent experiments with similar results are shown.

3.4 STAMBPL1 is a novel CSN-associated DUB

The multifunctional protein CSN complex is composed of eight subunits (CSN1-8) and exerts deneddylase activity directed by the catalytic subunit CSN5 [Cope et al., 2002; Schwehheimer 2004]. In addition, the CSN2 subunit is requested for the integrity of the CSN complex and depletion of one of the CSN subunits affect the protein stability of other CSN subunits [Naumann et al., 1999; Leppert et al., 2011]. Since the CSN regulates CRLs by removing NEDD8, we investigated whether CSN participates in STAMBPL1 stability. The knockdown of CSN2 by siRNA led to a loss of the STAMBPL1 protein (Figure 18a). In addition, we observed in CSN2 knockdown cells treated with the proteasome inhibitor MG132, a significant accumulation of ubiquitinylated STAMBPL1 (Figure 18b), suggesting that a disruption of CSN function enhanced the degradation of STAMBPL1 by CRL1.
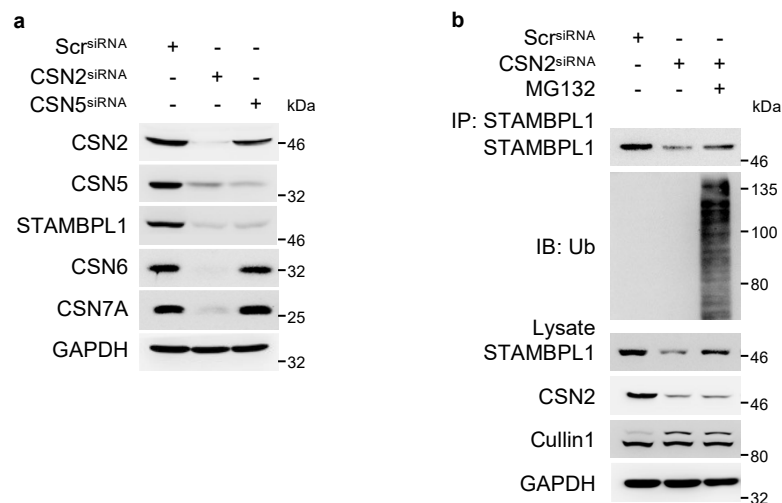
Figure 18   Abrogation of deneddylation activity of CSN by silencing CSN2 or CSN5 subunits promotes STAMBPL1 degradation. (a) AGS cells were transfected with siRNA against CSN2 or CSN5 for 48 h, followed by IB analysis. (b) AGS cells depleted of CSN2 were treated with MG132 at a final concentration of 20 µM 4 h prior to harvest and subjected to IP with an anti-STAMBPL1 antibody. Ubiquitinylation of STAMBPL1 was analysed by IB. Representative IBs for the indicated proteins from at least two independent experiments with similar results are shown.

It is well established that the CSN represents a signalling platform and collaborates with a number of other proteins including DUBs (Dubiel et al., 2020). Interestingly, we found that STAMBPL1, but not AMSH was co-immunoprecipitated with the CSN complex and *vice versa* (Figure 19a-c).
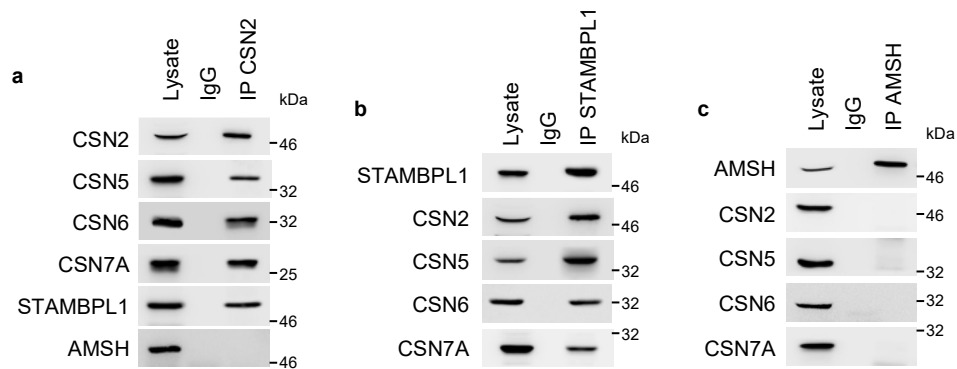
Figure 19   STAMBPL1 interacts with the CSN. IPs of (a) CSN2, (b) STAMBPL1, and (c) AMSH from AGS cell lysates were analysed by IB. (a-c) Representative IBs for the indicated proteins from at least two independent experiments with similar results are shown.

To elucidate the direct binding of STAMBPL1 to the CSN, single CSN subunits were *in vitro* translated, incubated with recombinant GST-STAMBPL1 and subjected to an IP using an anti-GST antibody. We detected direct physical interaction between STAMBPL1 and the CSN subunits CSN5 and CSN6 (Figure 20a). No interaction between recombinant GST and the CSNs was observed (Figure 20b). In addition, CSN-associated USP15 interacts with CSN subunit 7A (Figure 20c), but no interaction was observed between CSN and USP7 (Figure 20d).
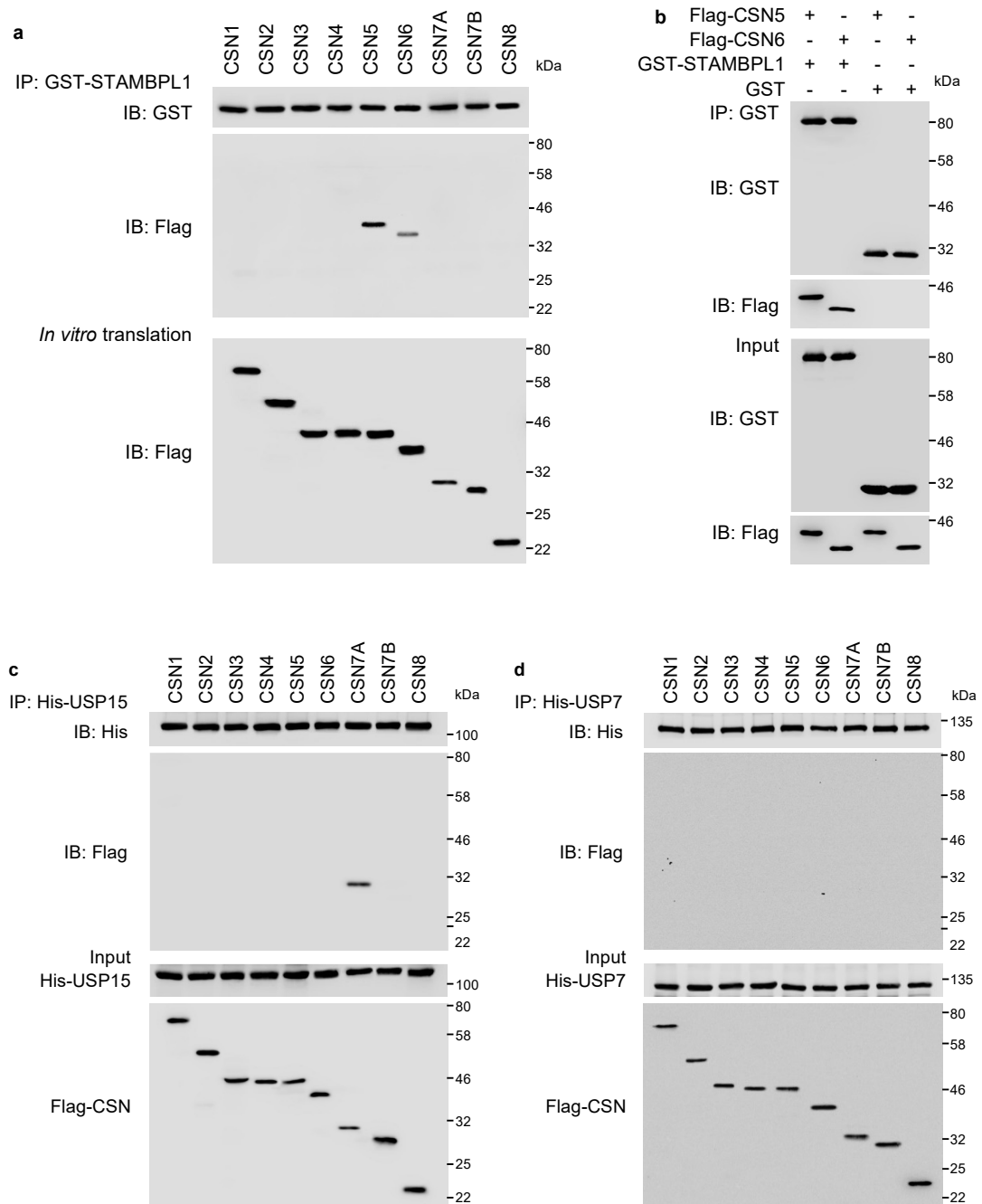
Figure 20 *In vitro* **translation and binding assay of Flag-CSN subunits and recombinant GST-STAMBPL1.** (a) Equimolar amounts of *in vitro*-translated Flag-CSN and the recombinant GST-STAMBPL1 were incubated at 37 °C for 1 h followed by IP of STAMBPL1 using an anti-GST antibody. (b) In addition to Flag-CSN 5 and 6 subunits and recombinant GST-STAMBPL1, recombinant GST-protein was used as a negative control. *In vitro*-translated Flag-CSN and (c) recombinant His-USP15 or (d) recombinant His-USP7 were incubated at 37 °C for 1 h followed by IP with an anti-His antibody. (a-d) Representative IBs for the indicated proteins from at least two independent experiments with similar results are shown.

3.5 STAMBPL1 stabilises the anti-apoptotic protein Survivin by deubiquitinylation

It has been described that STAMBPL1 stabilises the anti-apoptotic regulator Survivin in renal cancer cells [Woo et al., 2019]. We also observed that Survivin protein abundance was found to be significantly decreased in STAMBPL1-depleted gastric epithelial cells, whereas AMSH had no impact on Survivin (Figure 21a). Further, STAMBPL1 co-precipitated with Survivin in an IP (Figure 21b). The STAMBPL1-dependent Survivin degradation is proteasome-dependent (Figure 21c), and we observed an accumulation of ubiquitinylated Survivin in STAMBPL1-depleted and MG132 treated cells (Figure 21d). In order to test the hypothesis that STAMBPL1 deubiquitinylates Survivin, we performed an *in vitro* DUB assay. STAMBPL1 effectively hydrolysed polyubiquitin chains on Survivin *in vitro* while Phenanthroline, a metalloprotease inhibitor, completely inhibited the cleavage of ubiquitin on Survivin (Figure 21e). This data provide evidence that the DUB activity of STAMBPL1 regulates the stability of Survivin.
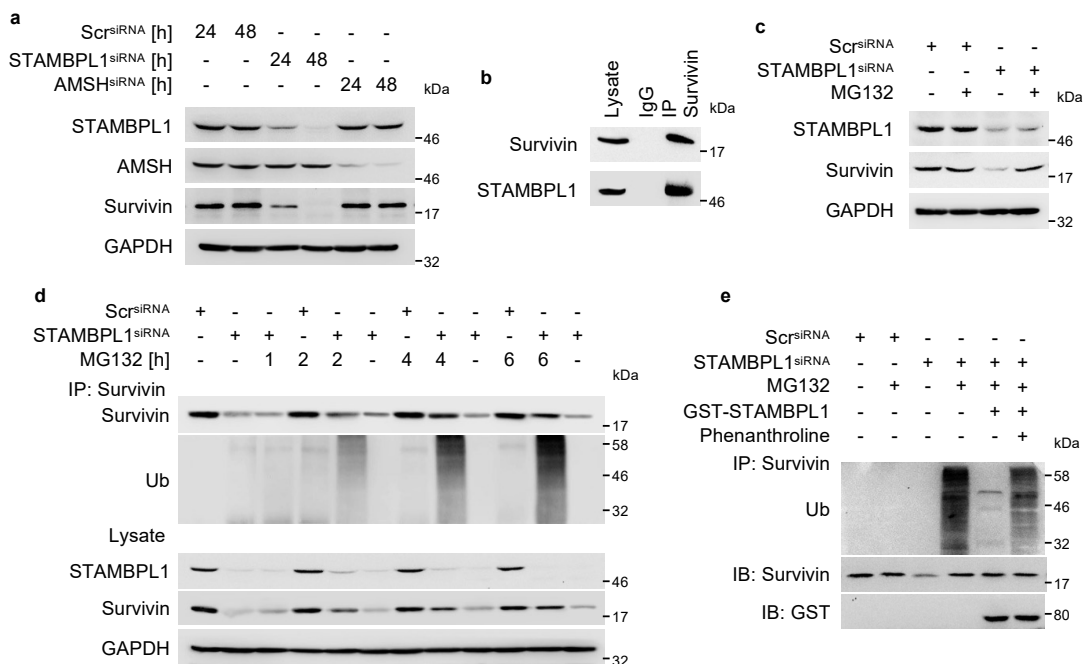
Figure 21   STAMBPL1 stabilises the anti-apoptotic protein Survivin by deubiquitinylation. (a) AGS cells were transfected with siRNAs against STAMBPL1 or AMSH at the indicated time points, followed by IB analysis. (b) IP of Survivin from AGS cell lysates. (c) Cells were transfected with STAMBPL1 siRNA for 24 h and treated with MG132 for a further 4 h before harvesting. (d) IP of Survivin after transient knockdown of STAMBPL1 followed by IB analysis of Survivin ubiquitinylation. (e) *In vitro* DUB assay of a Survivin IP from STAMBPL1 depleted cells incubated for 2 h with recombinant GST-STAMBPL1 in the presence or absence of phenanthroline. (a-e) Representative IBs for the indicated proteins from at least two independent experiments with similar results are shown.

Along these lines, it is conceivable that STAMBPL1 down-regulation by *H. pylori* infection causes the degradation of Survivin. We observed in agreement with the *H. pylori*-induced degradation of STAMBPL1 a decrease in the Survivin protein level in *H. pylori* wt and *virB7* mutant (Figure 22a). Moreover, we detected an enhanced polyubiquitinylation of Survivin upon *H. pylori* infected and MG132 treated cells (Figure 22b) suggesting that STAMBPL1 deubiquitinylates Survivin and sustains Survivin stability in AGS cells.
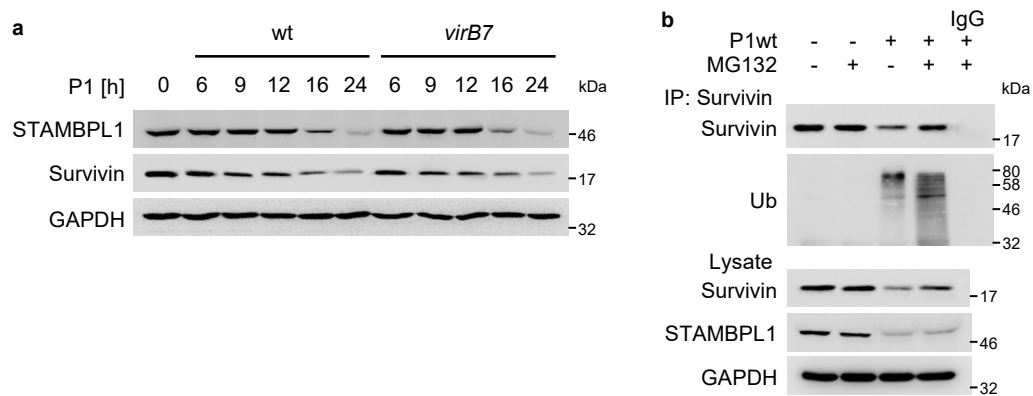
Figure 22   Loss of STAMBPL1 is accompanied by loss of Survivin in *H. pylori*-infected cells. (a) Cells were infected with either P1wt or *virB7* at the indicated time points, followed by IB analysis of Survivin. (b) IP of Survivin from *H. pylori*-infected cells. MG132 was added to the culture media 4 h before harvest. (a, b) Representative IBs for the indicated proteins from at least two independent experiments with similar results are shown.

3.6 *H. pylori*-induced degradation of STAMBPL1 promotes apoptotic cell death

Given that the STAMBPL1 deubiquitinylase activity stabilises Survivin, a crucial regulator of apoptosis at the level of effector caspases, we hypothesised that STAMBPL1 affects apoptotic cell death. We observed that a knockdown of STAMBPL1 in non-stimulated cells led to caspase-3 cleavage, which was raised in *H. pylori*-infected cells and even more pronounced in cells which were additionally transfected with siRNA against STAMBPL1 (Figure 23).
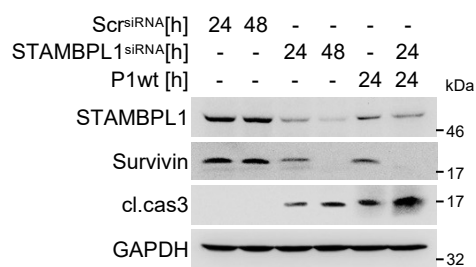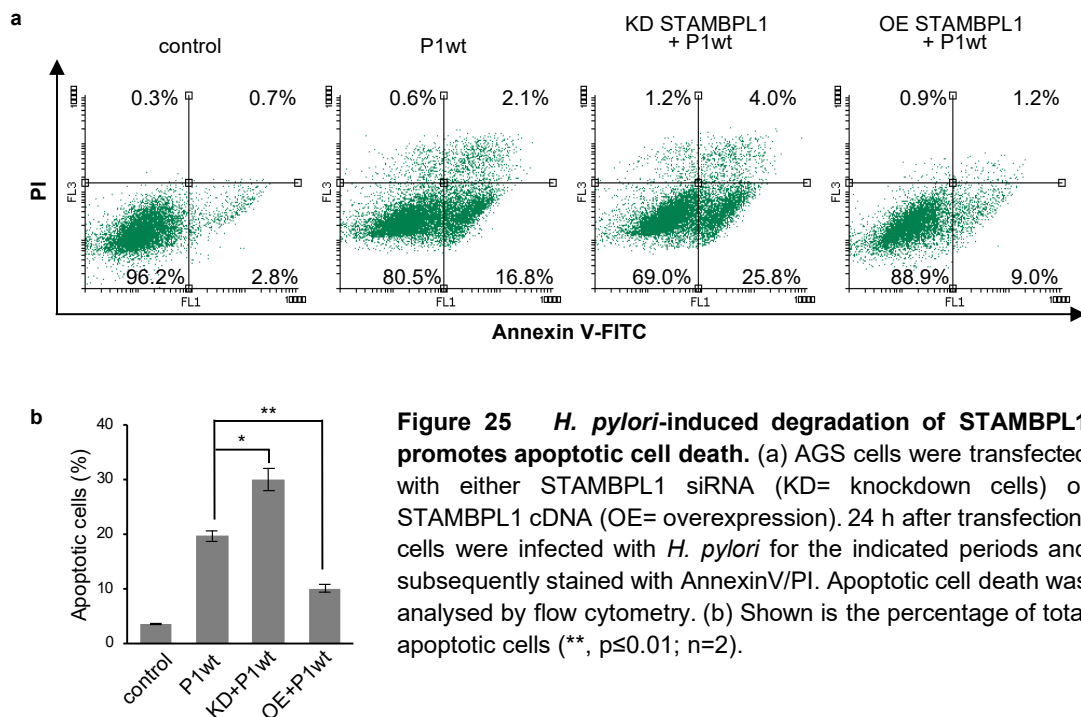

Figure 23   *H. pylori*-induced degradation of STAMBPL1 promotes caspase-3 cleavage. AGS cells were transfected with siRNA against STAMBPL1 for 24 h and then infected with *H. pylori* for 24 h. Survivin and caspase-3 cleavage were analysed by IB. Representative IBs for the indicated proteins from at least two independent experiments with similar results are shown.

The impact of STAMBPL1 on apoptotic cell death in *H. pylori*-infected cells was further analysed by overexpression of Myc-tagged STAMBPL1. Overexpression of STAMBPL1 in *H. pylori*-infected cells notably promoted the stability of Survivin and diminished the caspase-3 cleavage (Figure 24).
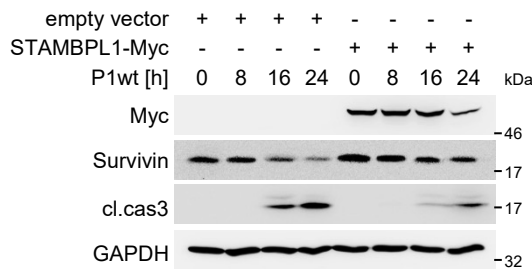

Figure 24   Overexpression of STAMBPL1 suppresses caspase-3 cleavage in *H. pylori*-infected cells. AGS cells were transfected with either empty vector control (pCMV) or STAMBPL1 cDNA for 24 h prior to *H. pylori* infection for the indicated time points. Representative IBs for the indicated proteins from at least two independent experiments with similar results are shown.

AnnexinV-FITC/Propidium Iodide staining assessed by flow cytometry corroborated the previous data and showed that apoptotic cell death in *H. pylori* infection was even more pronounced when cells were transfected with STAMBPL1 siRNA, whereas overexpression of STAMBPL1 markedly reduced apoptotic cell death (Figure 25).

Figure 25   *H. pylori*-induced degradation of STAMBPL1 promotes apoptotic cell death. (a) AGS cells were transfected with either STAMBPL1 siRNA (KD= knockdown cells) or STAMBPL1 cDNA (OE= overexpression). 24 h after transfection, cells were infected with *H. pylori* for the indicated periods and subsequently stained with AnnexinV/PI. Apoptotic cell death was analysed by flow cytometry. (b) Shown is the percentage of total apoptotic cells (**, p≤0.01; n=2).

The suppressive effect of STAMBPL1 on apoptotic cell death in *H. pylori* infection was also observed when we studied apoptotic cell death by Incucyte® Live-Cell Analysis. Using caspase-3/7 Incucyte® reagent, a non-fluorescent membrane-permeable substrate containing a cleavage sequence (DEVD), we monitored the cleavage by activated caspase-3/7 and the release of the green DNA-binding fluorescent dye. Caspases-3/7 cleavage increased continuously in a time-dependent manner in *H. pylori* infection (Figure 26a). Representative images of *H. pylori* infected AGS cells after 24 h are shown (Figure 26b). Furthermore, the caspase-3/7 activation was significantly increased when STAMBPL1 was depleted, whereas it was considerably lowered in STAMBPL1 overexpressing cells (Figure 26b, c).
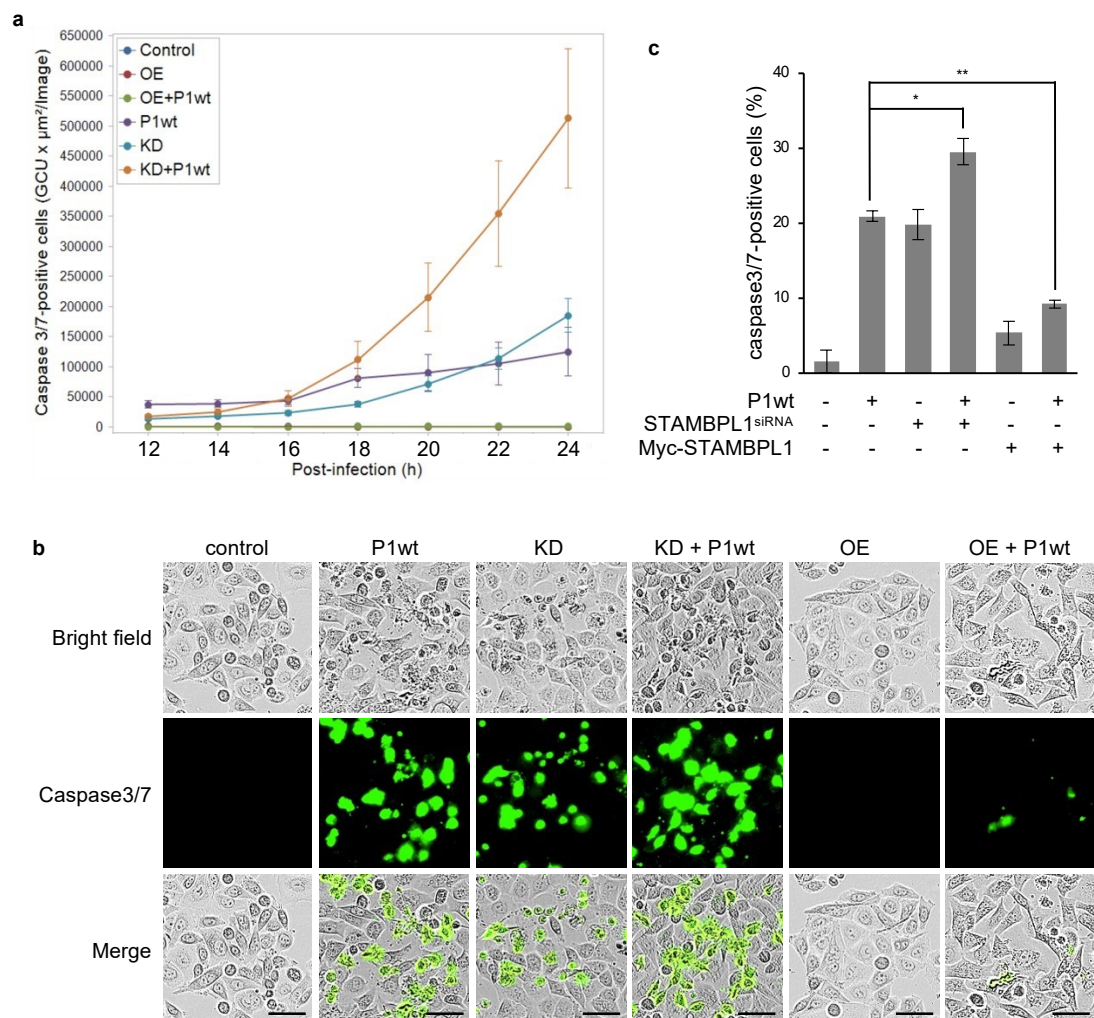
Figure 26   Caspase-3/7 activation in *H. pylori*-infected cells. (a) Caspase-3/7 activation in AGS cells infected with *H. pylori* was analysed in real time using the IncuCyte® S3 Live Cell Analysis System. (b) Representative images after 24 h and (c) the percentage of caspase-3/7-positive cells are shown. Scale bars, 20 µm. Abbreviation: GCU, green mean intensity.

4. Discussion

Although previous studies have enriched our understanding of the role of STAMBPL1 in regulating signalling pathways [Ibarrola et al., 2004; Lavorgna et al., 2011; Li, 2016], apoptotic cell death [Shahriyar et al., 2018; Chen et al., 2019; Woo et al., 2019; Yu et al., 2019], and tumour development [Lee, 2017; Chen et al., 2019; Ambroise et al., 2020; Liu et al., 2022], it is still poorly understood how STAMBPL1 regulates cell survival. In this study, we elucidated the regulation of STAMBPL1 in cells infected by the human microbial pathogen *H. pylori* and highlighted a critical role of STAMBPL1 in apoptotic cell death in gastric epithelial cells.

4.1 Turnover of STAMBPL1 in *H. pylori*-infected gastric epithelial cells

Within an infection of *H. pylori*, deubiquitinylases are frequently dysregulated. For instance, ubiquitin-specific protease 7 (USP7 or HAUSP) expression is decreased in response to *H. pylori* infection in AGS cells [Coombs et al., 2011]. In addition, our group has shown that *H. pylori* regulates the deubiquitinylase gene of A20 (tumor necrosis factor alpha (TNF-α)-induced protein 3 (*TNFAIP3*)) in AGS cells. A20 controls NF-κB activity within a feedback mechanism and in addition counteracts cullin3-mediated K63-linked ubiquitinylation of procaspase 8, therefore restricting the activity of caspase 8 [Lim et al., 2017].

In the present study, we observed a turnover of STAMBPL1, but not AMSH in *H. pylori* infection in AGS gastric epithelial cells as evidenced by a time-dependent decrease in STAMBPL1 protein levels (Figure 10). *H. pylori* regulates in a T4SS-dependent manner a variety of signalling molecules such as inhibitor of IκB kinases (IKKs), c-Jun N-terminal kinase (JNK), mitogen-activated protein (MAP) kinases (p38), transcription factors (activator protein 1 (AP-1) and NF-κB) and cellular processes (proliferation, apoptosis, angiogenesis) [Naumann et al., 2017]. However, STAMBPL1 is regulated by *H. pylori* in a T4SS-independent manner (Figure 11a), similar to epithelial growth factor receptor (EGFR) [Saha et al., 2010], ERK, and the S6 ribosomal protein [Sokolova et al., 2014]. Of note, different *H. pylori* strains (P1 and P12) behave similar (Figure 11c) and mediate the turnover of STAMBPL1. Further, *H. pylori* also caused STAMBPL1 degradation in NCI-N87 gastric epithelial cells and HeLa cervical cancer cells (Figure 10b, c), which suggests that *H. pylori*-induced STAMBPL1 degradation is not only restricted to AGS gastric epithelial cells and may possibly occur via a common pathway across different cell types.

4.2 Regulation of STAMBPL1 protein turnover by ROS

ROS define a group of short-lived, highly reactive, oxygen-containing molecules that are produced at low concentrations endogenously by cellular respiration, protein folding, and end products of multiple metabolic reactions [Reczek et al., 2015]; or upon exposure to exogenous stress such as ionizing radiation, chemotherapeutic drugs, and infections [Kawamura et al., 2018; Kleih et al., 2019; Pecoraro et al., 2020; Han et al., 2022]. ROS act as signalling molecules to regulate biological processes [Ray et al., 2012] and play a role in pathogen elimination [Dickinson et al., 2011]. However, excessive amounts of ROS cause oxidative stress that impairs proteins and essentially all classes of biomolecules, ultimately leading to cell death [Sies et al., 2020]. The mechanisms by which ROS cause, for instance, apoptotic cell death typically include receptor activation, caspase activation, Bcl-2 family proteins, and mitochondrial dysfunction [Ryter et al., 2007]. Therefore, cells activate their low-molecular-mass scavengers (e.g., thiols, carotenoids) or antioxidant enzymes (e.g., superoxide dismutases, glutathione peroxidases) to overcome intracellular oxidative stress. For example, superoxide dismutase catalyses the formation of superoxide ($O_2^{\bullet-}$) into hydrogen peroxide (H_2O_2), which is then converted into H_2O and O_2 by catalase [Franco et al., 2008; Sena et al., 2012].

Various agents such as chemotherapeutic drugs induce genotoxic stress and ROS production. ROS-inducing chemotherapeutic agents are used for the therapeutic treatment of cancer patients with the aim of causing DNA damage and apoptotic cell death of cancer cells [Srinivas et al., 2019]. In addition, microbial pathogens such as *H. pylori*, which colonises the gastric mucosa, initiate ROS production in the cells of the gastric mucosa [Ma et al., 2013] and induce cell line-dependent apoptotic cell death [Moss et al., 1996; Peek et al., 1997; Bhattacharyya et al., 2009; Liu et al., 2021]. Accordingly, we and others [Ren et al., 2019; Shi et al., 2019] showed ROS accumulation after treatment with chemotherapeutic agents or *H. pylori* infection (Figure 13). Interestingly, we observed a ROS-dependent decline of the STAMBPL1 protein amount (Figure 14b, c). Previous studies have shown that hydrogen peroxide-inducing ROS induces the turnover of several cellular proteins such as a serine/threonine-specific protein kinase (Akt) [Kim et al., 2011], histone variant H2AX [Gruosso et al., 2016], and peroxiredoxins (Prxs) [Song et al., 2011]. These findings are in line with other studies showing ROS-dependent turnover of proteins [Wang et al., 2016; Liang et al., 2017; Liu et al., 2020]. Consistent with this observation, cytokines (IL-1β or TNF) do not induce ROS (Figure 13), and therefore we observed no cytokine-

dependent effect on the turnover of STAMBPL1 protein (Figure 12). Although, it has been demonstrated that cytokines increased ROS production [Yang et al., 2007; Sandoval et al., 2018]; however, these experiments were performed in different cell lines, suggesting that cytokine-induced ROS might be cell-type specific.

Infection with *H. pylori* causes a chronic inflammatory response in the host. The persistent ROS exposure during infection is a host defense in an attempt to eradicate *H. pylori*, but at the same time, ROS causes processes implicated in the pathogenesis of cancer [Bhattacharyya et al., 2014]. It has been described that CagA-positive strains are capable of inducing ROS production in gastric epithelial cells, which eventually leads to DNA damage and apoptosis [Chaturvedi et al., 2011; Hanada et al., 2014], whereas in our study infection by all tested strains had no significant effect on ROS production (Figure 13). In addition, *H. pylori* GGT has been shown to contribute to the production of H_2O_2 from the gastric epithelium by glutathione (GSH) hydrolysis [Gong et al., 2010]. Since GGT is highly conserved among different *H. pylori* strains and it has been reported in elevating the level of H_2O_2 [Gong et al., 2010], it is likely that GGT may direct ROS production. In agreement with these findings, we and others [Ding et al., 2007; den Hartog et al., 2016] have demonstrated that *H. pylori* strains, which possess GGT, stimulate the accumulation of intracellular ROS in cultured gastric epithelial cells.

To address whether *H. pylori* modulated STAMBPL1 turnover at the posttranslational level, we checked the mRNA level of STAMBPL1 in *H. pylori*-infected cells and observed no significant change in STAMBPL1 mRNA expression (Figure 15a). Subsequently, we speculated that *H. pylori* could regulate STAMBPL1 at the protein level. Consistently, we found in the administration of protein synthesis inhibitor CHX that *H. pylori* accelerated STAMBPL1 protein degradation (Figure 15b). While a previous study of USP7 showed that *H. pylori* infection resulted in the reduction of USP7 at the transcript and protein levels [Coombs et al., 2011], STAMBPL1 was regulated by *H. pylori* only at the protein level.

Proteins are among the main targets for radicals or oxidative modifications due to their abundance and the fact that some amino acids (arginine, methionine, lysine, proline, and tyrosine) are susceptible to non-enzymatic modifications [Cai & Yan, 2013]. Several proteins have been reported to be unstable in response to oxidative stress, for instance, transcription factor Nrf2 [Kobayashi et al., 2004] and gasdermin-D (Gsdmd) [Wang et al., 2019]. In the present study, we found that STAMBPL1 is instable in

response to oxidative stress-induced by *H. pylori*. ROS can affect proteins by directly attacking the protein backbone, amino acid side chains or causing protein carbonylation [Augustyniak et al., 2015]. As oxidatively modified proteins are mostly irreversible and irreparable, they must be eliminated [Jung et al., 2014; Davies, 2016]. Consequently, ROS-induced ubiquitinylation and degradation can be a quality control mechanism of oxidized redox-sensitive proteins including STAMBPL1.

4.3 CRLs modify STAMBPL1 for degradation during *H. pylori* infection

CRLs represent the largest family of E3 ubiquitin ligases, containing as core structure cullin proteins [Lydeard et al., 2013]. In this study, we identified STAMBPL1 as a novel substrate of CRL1 ubiquitin ligase. We found that CRL1 knockdown resulted in the accumulation of STAMBPL1 upon *H. pylori* infection (Figure 16a). Although CRL3 has also been shown to be activated by cellular ROS [Loignon et al., 2009], we provided evidence showing that CRL3 was not responsible for STAMBPL1 degradation (Figure 16b). In response to a drastic increase in cellular ROS production, many proteins become K48-ubiquitinylated and readily degraded by the 26S proteasome [Loignon et al., 2009; Liang et al., 2017]. Therefore, it is likely that ROS leads very fast to CRL1-dependent ubiquitinylation of STAMBPL1 and marks it for degradation. Interestingly, only STAMBPL1 localised in the cytosol was ubiquitinylated and degraded, whereas the nuclear population of the protein was unaffected (Figure 15c). This is consistent with other studies showing ROS-dependent turnover of cytosolic proteins [Liang et al., 2017].

Cullins act as scaffolding proteins in the CRL complex that binds to an adaptor protein and a substrate recognition protein at the N-terminus and a RING protein at the C-terminus. The specificity to target proteins for ubiquitinylation is defined by substrate binding of proteins including F-box proteins. There are a number of substrate-binding proteins described (beta-transducin repeats-containing protein (β-TrCP), cell division control protein 4 (CDC4), S-phase kinase-associated protein 2 (SKP2), Cyclin F) which could be assembled in the CRL1 complex [Harper & Schulman, 2021]. However, the identification of the substrate-binding protein, which recognises STAMBPL1 demands further investigations.

The activity of CRLs is dynamically regulated and requires cullin modifications by covalent attachment with the ubiquitin-like protein NEDD8 by NAE, whose activity can be blocked by a small molecule MLN4924 (also known as pevonedistat) [Brownell et al., 2010]. Thus, blocking NAE activity results in the inhibition of CRL activity and the

stabilisation of CRL substrates. Several studies have reported that substrates of CRLs were accumulated upon MLN4924 treatment [Milhollen et al., 2012]. This is in agreement with our results, which showed that STAMBPL1 protein is stabilised in MLN4924-treated cells during *H. pylori* infection (Figure 17). Therefore, we further demonstrated mechanistically that CRL1 promotes STAMBPL1 ubiquitinylation and turnover, which completely depends on CUL1 neddylation.

The CSN removes NEDD8 from the cullin subunit of CRLs [Lyapina et al., 2001], thus inhibiting the CRL activity. Hence, it comes as no surprise that the CSN involves the protein half-life control of STAMBPL1. Knockdown of the CSN2 subunit that abrogated the CSN holocomplex also destabilised the STAMBPL1 protein (Figure 18a), suggesting the possibility that the CSN stabilises STAMBPL1 by direct interaction or deneddylation. This is in agreement with several studies showing that disruption of CSN impairs the degradation of CRL substrates [Peth et al., 2007; Pan et al., 2012; Schweitzer & Naumann 2015; Ba et al., 2017; Zarich et al., 2019]. Based on these data, the CSN might control the stability of STAMBPL1 and regulates the assembly of the CRL1 leading to STAMBPL1 ubiquitinylation by deneddylation [Mosadeghi et al., 2016].

4.4 STAMBPL1 as associated molecule of the multiprotein complex CSN

Previous studies revealed that DUBs are frequently associated with multiprotein complexes [Sowa et al., 2009; Ventii & Wilkinson, 2008]. For instance, USP14, UCH37 and metalloprotease Rpn11 are associated with the 26S proteasome [Sowa et al., 2009; Yao et al., 2006; Pathare et al., 2014; de Poot et al., 2017]. Furthermore, USP3 and USP39 interact with the eukaryotic initiation factor 3 (eIF3) complex [Sowa et al., 2009]. In addition to remove NEDD8, CSN also functions as a signalling platform and integrates the activity of several proteins, including DUBs [Dubiel et al., 2020]. CSN-associated DUBs USP15 and USP48 contribute to NF-κB regulation [Schweitzer et al., 2007; Schweitzer & Naumann, 2015] and cylindromatosis (CYLD) is involved in hepatic steatosis [Huang et al., 2021]. Here, we identified STAMBPL1 as a novel CSN-associated DUB in AGS gastric epithelial cells (Figure 19). Direct physical interaction was observed with CSN subunits CSN5 and CSN6 (Figure 20). The MPN domain of CSN5 has been previously demonstrated to mediate the binding of the CSN complex to several proteins e.g., cell cycle inhibitor p27 [Tomoda et al., 2002], DNA topoisomerase IIα [Yun et al., 2004], macrophage migration inhibitory factor (MIF) [Park et al., 2017], and LIM as well as SH3 protein 1 (LASP1) [Zhou et al., 2018]. In their

studies, the MPN domain of CSN5, but not the JAMM motif, is required for the interaction of CSN5 with binding partner proteins. In our study, we observed the interaction of STAMBPL1 with both MPN domain proteins, CSN5 and CSN6. Accordingly, although STAMBPL1 contains a JAMM motif, it is likely that instead of the JAMM motif, the MPN domain may facilitate the interaction between CSN proteins CSN5 and CSN6 with STAMBPL1. Significantly, this association is requested to maintain the stability and function of STAMBPL1 protein (Figure 18b). Thus, protein modifications that regulate the interaction between STAMBPL1 and the CSN might be involved in the regulation of STAMBPL1 protein abundance, in addition to ROS-dependent turnover of STAMBPL1.

### 4.5 STAMBPL1 and regulation of the anti-apoptotic protein Survivin

By investigating anti-apoptotic proteins in cells infected with *H. pylori*, we observed that the amount of Survivin decreases during infection. Survivin is a member of the IAP family that has been implicated in the regulation of cell division as well as the suppression of apoptosis [van der Waal, 2012]. E3 ubiquitin ligases SCF complex subunit F-box/leucine rich repeat protein 7 (FBXL7) [Liu et al., 2015; Kamran et al., 2017] and XIAP [Arora et al., 2007] ubiquitinylate Survivin for proteasomal degradation.

It has been described that Survivin is deubiquitinylated by STAMBPL1 in renal cancer cells [Woo et al., 2019]. Similarly, we show that the depletion of STAMBPL1 led to the reduction of the Survivin protein level (Figure 21a) and promoting the accumulation of polyubiquitinylated Survivin in MG132-treated gastric epithelial cells (Figure 21d). The molecular basis behind our observations could be explained by STAMBPL1 dependent deubiquitinylation of Survivin (Figure 21e). Mechanistically, STAMBPL1 disassembled K48-linked polyubiquitin chains from Survivin. Consequently, the knockdown of STAMBPL1 resulted in accelerated degradation of Survivin. However, in prostate cancer, STAMBPL1 did not affect the stability of Survivin protein [Chen et al., 2019], which might differ because of genetic alterations in this cancer cells. Accordingly, our findings confirmed and extended the earlier report, according to which Survivin loss upon *H. pylori* infection is due to the lack of its DUB, STAMBPL1. Thus, a corresponding accumulation of K48-ubiquitinylated Survivin was observed in MG132-treated cells during *H. pylori* infection (Figure 22b). These findings strongly suggest that STAMBPL1 interacts with and deubiquitinylates Survivin, as a result, stabilises the Survivin protein level.

Due to the known role of Survivin as a negative regulator of caspases in apoptosis [Pavlyukov et al., 2011; Zhou et al., 2020], we hypothesised that STAMBPL1-dependent Survivin degradation is crucial for the apoptotic cell death during *H. pylori* infection. Survivin forms a complex with HBXIP to prevent the activation of caspase cascades [Marusawa et al., 2003]. Survivin also blocks the release of Apaf1 from the mitochondria or prevents the Smac/DIABLO from interacting with other IAPs [Song et al., 2004], thus, inhibiting the apoptotic pathway. STAMBPL1 knockdown in non-stimulated cells caused moderate caspase-3 cleavage (Figure 23). This observation is due to the destabilisation of Survivin because STAMBPL1 overexpression successfully prevented Survivin degradation and caspase-3 cleavage (Figure 24), thus supporting the idea of a significant role of STAMBPL1 in preventing caspase-3 cleavage in *H. pylori* infection. Interestingly, caspase-3 cleavage was considerably elevated in STAMBPL1 depleted- and *H. pylori*-infected cells. This effect is due to the fact, that *H. pylori* infection induces a number of factors that might contribute to the regulation of apoptotic cell death [Liu et al., 2021]. Further, evidence for an anti-apoptotic effect of STAMBPL1 was provided by decreased numbers of apoptotic cells (Figure 25) and detection of less caspase-3 cleavage (Figure 26) in cells that overexpress STAMBPL1. This is consistent with previous studies showing that *H. pylori* induces caspase-3-dependent apoptosis in gastric epithelium [Kim et al., 2007; Pierzchalski et al., 2009; Gong et al., 2010]. STAMBPL1 is degraded upon *H. pylori* infection, resulting in the loss of Survivin and the activation of the apoptotic pathway, hence providing the link between STAMBPL1 and its ability to induce apoptotic cell death. Our findings strongly suggest that STAMBPL1 degradation is a prerequisite for apoptotic cell death observed in *H. pylori* infection. In addition, with increasing stages of gastric cancer (stage I-IV), STAMBPL1 protein expression was considerably upregulated [Yu et al., 2019], which could explain the emergence of apoptotic resistance and gastric carcinogenesis.

5. Conclusion

In this study, we demonstrated that *H. pylori* infection induces ROS-dependent degradation of STAMBPL1 by E3 ligase CRL1 (Figure 27). Further, *H. pylori*-mediated down-regulation of STAMBPL1 is very likely to contribute to the apoptotic cell death in *H. pylori*-infected cells. Herein, we elucidated for the first time that STAMBPL1 interacts physically with the CSN complex and that this association is crucial to prevent apoptotic cell death in non-stimulated cells. Thus, our data contribute to a better understanding of the *H. pylori*-induced regulation of STAMBPL1 and Survivin and the apoptotic cell death, which could provide novel insights into the pathophysiology of *H. pylori* associated gastric diseases.
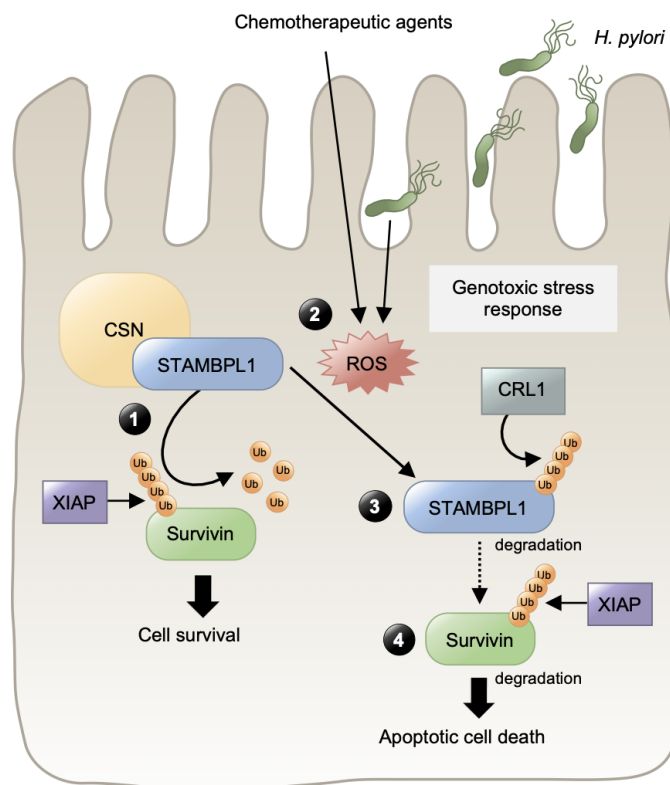
Figure 27   Schematic diagram summarising the major findings of this study. (1) STAMBPL1 physically interacts with the CSN complex to enhance cell survival by stabilising the anti-apoptotic protein Survivin by counteracting XIAP-dependent degradation of Survivin. (2) The ROS-dependent turnover of the STAMBPL1 protein during genotoxic stress (chemotherapeutic agents or *H. pylori*) (3) is mediated by E3 ligase CRL1. (4) Degradation of STAMBPL1 also leads to degradation of Survivin (in the absence of STAMBPL1 protective function) and apoptotic cell death.

6. List of abbreviations

%	Percent
∞	Infinity
Abl	ABL proto-oncogene 1
AEBSF	4-(2-aminoethyl) benzenesulfonyl fluoride hydrochloride
Akt	Serine/threonine-specific protein kinase
Ala	Alanine
AMPK	Adenosine monophosphate-activated protein kinase
AMSH	SRC Homology 3 (SH3) domain of STAM
AP-1	Activator protein 1
Apaf-1	Apoptosis-activating factor 1
Asn	Asparagine
Asp	Aspartate
ATCC	American type culture collection
Atg8	Autophagy-related protein 8
ATP	Adenosine 5′-triphosphate
Bak	Bcl2 antagonist/killer 1
Bax	Bcl-2-associated X protein
BCA	Bicinchoninic acid
Bcl-2	B-cell lymphoma 2
BID	BH3-interacting domain death agonist
BIR	Baculovirus IAP repeat
BIRC5	Baculoviral IAP repeat containing 5
BRCC36	BRCA1-BRCA2-containing complex subunit 36
BSA	Bovine serum albumin
C	Carboxyl-terminus, COOH-terminus
c-FLIP	Cellular FLICE-inhibitory protein
c-Myc	Cellular Myc
CagA	Cytotoxin-associated gene A
cagPAI	Cag pathogenicity island
CAND1	Cullin-associated Nedd8-dissociated protein 1
CARD	Caspase recruitment domain
CBS	Clathrin binding site
CD95	Cluster of differentiation 95
CDC4	Cell division control protein 4

Cdc42	Cell division cycle 42
cDNA	Complementary DNA
CHX	Cycloheximide
cIAP1	Cellular inhibitor of apoptosis protein 1
cIAP2	Cellular inhibitor of apoptosis protein 2
Cl⁻	Chloride ion
Co-IP	Co-immunoprecipitation
CO_2	Carbon dioxide
COP9	Constitutive photomorphogenesis 9
COX-2	Cyclooxygenase 2
CPT	Camptothecin
Crk	Chicken tumor virus 10 regulator of kinase
CRL	Cullin-RING ubiquitin ligase
CRL1	Cullin 1-RING ubiquitin ligase
CRL3	Cullin 3-RING ubiquitin ligase
CRLs	Cullin-RING ligases
CSN	COP9 signalosome
CSN2	COP9 signalosome subunit 2
CSN5	COP9 signalosome subunit 5
CSN6	COP9 signalosome subunit 6
CSN7A	COP9 signalosome subunit 7A
CT	Cycle threshold
Cul	Cullin
Cul1	Cullin 1
Cul3	Cullin 3
CYLD	Cylindromatosis
Cys	Cysteine
DCF	Dichlorofluorescein
DEVD	Cleavage sequence (Asp-Glu-Val-Asp)
DISC	Death-inducing signalling complex
DNA	Deoxyribonucleic acid
DOX	Doxorubicin
DTT	Dithiothreitol
DUBs	Deubiquitinylases
E1	Ubiquitin-activating enzyme

E2	Ubiquitin-conjugating enzyme
E3	Ubiquitin-ligating enzyme
EDTA	Ethylenediaminetetraacetic acid
EGFR	Epithelial growth factor receptor
EMT	Epithelial-mesenchymal transition
EPIYA	Glu-Pro-Ile-Tyr-Ala
ER	Endoplasmic reticulum
ERAD	Endoplasmatic reticulum-associated protein degradation
ERK	Extracellular-signal regulated kinase
ERK1/2	Extracellular signal-regulated kinase 1/2
ESCRT	Endosomal sorting complexes required for transport
et al	et alia
FADD	Fas-associated death domain
FBS	Fetal bovine serum
FBXL7	F-box/leucine rich repeat protein 7
Fe^{3+}	Ferric ion
FITC	Fluorescein isothiocyanate
FLICE	FADD-like IL-1β-converting enzyme
g	Gram
g	Relative centrifuge force
G1	Growth 1
GCU	Green mean intensity
GGT	Gamma-glutamyl transferase
Glu	Glutamate
Gly	Glycine
Gsdmd	Gasdermin-D
GSH	Glutathione
GST	Glutathione S-transferase
h	Hour(s)
H. pylori	*Helicobacter pylori*
H2AX	Gamma-histone 2A variant X
H2DCF-DA	Dichlorodihydrofluorescein diacetate
H_2O	Water
H_2O_2	Hydrogen peroxide
HBXIP	Hepatitis B virus X-interacting protein

HCl	Hydrochloric acid
HECT	Homologous to E6AP C-terminus
HEPES	N-2-hydroxyethylpiperazine-N'-2-ethanesulfonic acid
His	Histidine
HRP	Horseradish peroxidase
I-SMAD	Inhibitory SMAD
IAP	Inhibitor of apoptosis protein
IB	Immunoblot
IgG	Immunoglobulin G
IKK	Inhibitor of IκB kinase
IL-1β	Interleukin-1 beta
IL-8	Interleukin-8
Ile	Isoleucine
ILP-2	Inhibitor of apoptosis protein-like protein-2
Ins-1	Insertion 1
Ins-2	Insertion 2
IP	Immunoprecipitation
ISG15	Interferon-stimulated gene product 15
IκB	Inhibitor of kB
JAMM	Jab1/MPN/Mov34 domain
JAMMs	Jab1/Pad1/MPN domain-associated metallopeptidases
JNK	c-Jun N-terminal kinase
K	Lysine
Kb	Kilobase
KD	Knockdown
kDa	Kilodalton
L	Liter
LASP1	LIM as well as SH3 protein 1
LPS	Lipopolysaccharide
LRP1	Low-density lipoprotein receptor-related protein 1
Lys	Lysine
M	Methionine
M	Molar
MALT	Mucosa-associated lymphoid tissue
MAP	Mitogen-activated protein

Mcl-1	Induced myeloid leukemia cell differentiation protein
MDa	Million Dalton
MEK	Mitogen-activated protein kinase
MFI	Mean fluorescence intensity
mg	Milligram
MIF	Macrophage migration inhibitory factor
min	Minute(s)
MINDY	Motif interacting with ubiquitin containing novel DUB family
MIT	Microtubule-interacting and transport
MKP-1	Mitogen-activated protein kinase phosphatase-1
ml	Milliliter
ML-IAP	Melanoma inhibitor of apoptosis protein
mm	Millimeter
mM	Millimolar
MOI	Multiplicity of infection
MPN	Mpr1-Pad1-N-terminal
mRNA	Messenger RNA
MYSM1	Myb-like, Swirm and MPN domain-containing protein-1
N	Amino-terminus, NH_2-terminus
n	Number of trials
N.S.	Not statistically significant
NaCl	Sodium Chloride
NADPH	Nicotinamide adenine dinucleotide phosphate
NAE	NEDD8-activating enzyme
NAIP	Neuronal apoptosis inhibitory protein
NEDD8	Neural precursor cell expressed, developmentally down-regulated 8
NEM	N-ethylmaleimide
NF-κB	Nuclear factor kappa-light-chain-enhancer of activated B cells
ng	Nanogram
NH_2	Amino group
NLS	Nuclear localisation sequence
nM	Nanomolar
Nox1	NADPH oxidase 1
Nrf2	Nuclear factor-erythroid factor 2-related factor 2

O_2	Oxygen
O^{2-}	Superoxide anions
OE	Overexpression
OPT	Phenanthroline
OTUs	Ovarian tumor proteases
p38	MAP kinase
PBS	Phosphate-buffered saline
PCI	Proteasome, COP9 signalosome, initiation factor 3
pCMV	Porcine cytomegalovirus
PCR	Polymerase chain reaction
PDTC	Pyrrolidine dithiocarbamate
PERK	Protein kinase R-like endoplasmic reticulum kinase
PI	Propidium iodide
PI3K	Phosphoinositide 3-kinase
PMs	Protein modifications
Pro	Proline
Prxs	Peroxiredoxins
PVDF	Polyvinylidene difluoride
QM/MM	Quantum mechanical/molecular mechanical
qPCR	Quantitative PCR
Rac1	Ras-related C3 botulinum toxin substrate 1
RAS	Rat sarcoma virus
RBR	RING-between-RING
RBX1	RING-box protein 1
RBX2	RING-box protein 2
RING	Really interesting new gene
RIPA	Radioimmunoprecipitation assay
RNA	Ribonucleic acid
RNF167	Ring finger protein 167
RNS	Reactive nitrogen species
ROS	Reactive oxygen species
Rpm	Revolutions per minute
RPMI1640	Roswell Park Memorial Institute 1640 medium
RPN11	Regulatory particle non-ATPase 11
RPTPα	Receptor protein-tyrosine phosphatase α

RPTPβ	Receptor protein-tyrosine phosphatase β
RT	Reverse transcription
RT-qPCR	Reverse transcription-quantitative polymerase chain reaction
s	Second(s)
S.D.	Standard deviation
SBM	SH3-binding motif
SCF	S-phase kinase-associated protein 1-cullin-1/F-box
Scr	Proto-oncogene tyrosine-protein kinase
Scr	Scramble
SDS	Sodium dodecyl sulfate
SDS-PAGE	Sodium dodecyl sulfate-polyacrylamide gel electrophoresis
Ser	Serine
SH3	SRC Homology 3
SHP-2	Src homology region 2 (SH2)-containing protein tyrosine phosphatase 2
siRNA	Small interfering RNA
Skp1	S-phase kinase-associated protein 1
Skp2	S-phase kinase-associated protein 2
Smac	Second mitochondrial-derived activator of caspases
SMAD	Acronym from the fusion of Caenorhabditis elegans Sma genes and the Drosophila Mad, Mothers against decapentaplegic
Snail-1	Signal transducer and activator of transcription 3 down-regulates SNAI-1
SOC	Super optimal broth with catabolite repression
STAMBPL1	STAM-binding protein like 1
STS	Staurosporine
SUMO	Small ubiquitin-like modifier
T-cell	T lymphocytes
T4SS	Type IV secretion system
Tax	Transactivator from the X-gene region
tBID	Truncated Bid
TBS	Tris-buffered saline
TBST	Tris-buffered saline-Tween-20
TEMED	Tetramethylethylenediamine
TGF-β	Transforming growth factor beta
Thr	Threonine

TNF	Tumor necrosis factor
TRAF1	TNF receptor-associated factor 1
TRAF2	TNF receptor-associated factor 2
Tyr	Tyrosine
Ub	Ubiquitin
UBA	Ubiquitin-associated domain
UBC	Ubiquitin conjugating domain
UBLs	Ubiquitin-like proteins
UBPs	Ubiquitin-specific proteases
UCH37	Ubiquitin carboxy-terminal hydrolases 37
UCHs	Ubiquitin carboxy-terminal hydrolases
UPS	Ubiquitin-proteasome system
USP14	Ubiquitin carboxyl-terminal hydrolase 14
USP15	Ubiquitin-specific protease 15
USP48	Ubiquitin-specific protease 48
USP7	Ubiquitin-specific protease 7
USPs	Ubiquitin-specific proteases
V	Volt
VacA	Vacuolating cytotoxin A
Val	Valine
Wnt/β	Wingless-related integration site/β-catenin
wt	Wild-type
XAF1	XIAP-associated factor 1
XIAP	X-linked inhibitor of apoptosis protein
Zn^{2+}	Zinc ion
Δ	Delta
ϵ	Epsilon
μg	Microgram
μl	Microliter
μm	Micrometer
β-TrCP	Beta-transducin repeats-containing protein
°C	Degree Celsius

7. List of figures

8. References

Al-Hakim, A. K., Zagorska, A., Chapman, L., Deak, M., Peggie, M., & Alessi, D. R. (2008). Control of AMPK-related kinases by USP9X and atypical Lys(29)/Lys(33)-linked polyubiquitin chains. *The Biochemical journal*, 411(2), 249–260.

Alipour M. (2021). Molecular Mechanism of *Helicobacter pylori*-Induced Gastric Cancer. *Journal of gastrointestinal cancer*, 52(1), 23–30.

Ambroise, G., Yu, T. T., Zhang, B., Kacal, M., Hao, Y., Queiroz, A. L., Ouchida, A. T., Lindskog, C., Norberg, E., & Vakifahmetoglu-Norberg, H. (2020). Systematic analysis reveals a functional role for STAMBPL1 in the epithelial-mesenchymal transition process across multiple carcinomas. *British journal of cancer*, 123(7), 1164–1177.

Ansari, S., & Yamaoka, Y. (2019). *Helicobacter pylori* Virulence Factors Exploiting Gastric Colonization and its Pathogenicity. *Toxins*, 11(11), 677.

Arora, V., Cheung, H. H., Plenchette, S., Micali, O. C., Liston, P., & Korneluk, R. G. (2007). Degradation of survivin by the X-linked inhibitor of apoptosis (XIAP)-XAF1 complex. *The Journal of biological chemistry*, 282(36), 26202–26209.

Ashktorab, H., Frank, S., Khaled, A. R., Durum, S. K., Kifle, B., & Smoot, D. T. (2004). Bax translocation and mitochondrial fragmentation induced by *Helicobacter pylori*. *Gut*, 53(6), 805–813.

Augustyniak, E., Adam, A., Wojdyla, K., Rogowska-Wrzesinska, A., Willetts, R., Korkmaz, A., Atalay, M., Weber, D., Grune, T., Borsa, C., Gradinaru, D., Chand Bollineni, R., Fedorova, M., & Griffiths, H. R. (2015). Validation of protein carbonyl measurement: a multi-centre study. *Redox biology*, 4, 149–157.

Ba, M. A., Surina, J., Singer, C. A., & Valencik, M. L. (2017). Knockdown of subunit 3 of the COP9 signalosome inhibits C2C12 myoblast differentiation via NF-KappaB signaling pathway. *BMC pharmacology & toxicology*, 18(1), 47.

Backert, S., Tegtmeyer, N., & Fischer, W. (2015). Composition, structure and function of the Helicobacter pylori cag pathogenicity island encoded type IV secretion system. *Future microbiology*, 10(6), 955–965.

Backert, S., Tegtmeyer, N., & Selbach, M. (2010). The versatility of Helicobacter pylori CagA effector protein functions: The master key hypothesis. *Helicobacter*, 15(3), 163–176.

Backert, S., Ziska, E., Brinkmann, V., Zimny-Arndt, U., Fauconnier, A., Jungblut, P. R., Naumann, M., & Meyer, T. F. (2000). Translocation of the *Helicobacter pylori* CagA protein in gastric epithelial cells by a type IV secretion apparatus. *Cellular microbiology*, 2(2), 155–164.

Bhattacharyya, A., Chattopadhyay, R., Burnette, B. R., Cross, J. V., Mitra, S., Ernst, P. B., Bhakat, K. K., & Crowe, S. E. (2009). Acetylation of apurinic/apyrimidinic endonuclease-1 regulates *Helicobacter pylori*-mediated gastric epithelial cell apoptosis. *Gastroenterology*, 136(7), 2258–2269.

Bhattacharyya, A., Chattopadhyay, R., Mitra, S., & Crowe, S. E. (2014). Oxidative stress: an essential factor in the pathogenesis of gastrointestinal mucosal diseases. *Physiological reviews*, 94(2), 329–354.

Bramasole, L., Sinha, A., Gurevich, S., Radzinski, M., Klein, Y., Panat, N., Gefen, E., Rinaldi, T., Jimenez-Morales, D., Johnson, J., Krogan, N. J., Reis, N., Reichmann, D., Glickman, M. H., & Pick, E. (2019). Proteasome lid bridges mitochondrial stress with Cdc53/Cullin1 NEDDylation status. *Redox biology*, 20, 533–543.

Bremm, A., & Komander, D. (2011). Emerging roles for Lys11-linked polyubiquitin in cellular regulation. *Trends in biochemical sciences*, 36(7), 355–363.

Brownell, J. E., Sintchak, M. D., Gavin, J. M., Liao, H., Bruzzese, F. J., Bump, N. J., Soucy, T. A., Milhollen, M. A., Yang, X., Burkhardt, A. L., Ma, J., Loke, H. K., Lingaraj, T., Wu, D., Hamman, K. B., Spelman, J. J., Cullis, C. A., Langston, S. P., Vyskocil, S., Sells, T. B., Dick, L. R. (2010). Substrate-assisted inhibition of ubiquitin-like protein-activating enzymes: the NEDD8 E1 inhibitor MLN4924 forms a NEDD8-AMP mimetic in situ. *Molecular cell*, 37(1), 102–111.

Burkitt, M. D., Duckworth, C. A., Williams, J. M., & Pritchard, D. M. (2017). *Helicobacter pylori*-induced gastric pathology: insights from *in vivo* and *ex vivo* models. Disease models & mechanisms, 10(2), 89–104.

Busiello, I., Acquaviva, R., Di Popolo, A., Blanchard, T. G., Ricci, V., Romano, M., & Zarrilli, R. (2004). *Helicobacter pylori* gamma-glutamyltranspeptidase upregulates COX-2 and EGF-related peptide expression in human gastric cells. *Cellular microbiology*, 6(3), 255–267.

Cai, Z., & Yan, L. J. (2013). Protein Oxidative Modifications: Beneficial Roles in Disease and Health. *Journal of biochemical and pharmacological research*, 1(1), 15–26.

Calore, F., Genisset, C., Casellato, A., Rossato, M., Codolo, G., Esposti, M. D., Scorrano, L., & de Bernard, M. (2010). Endosome-mitochondria juxtaposition during apoptosis induced by *H. pylori* VacA. *Cell death and differentiation*, 17(11), 1707–1716.

Cappadocia, L., & Lima, C. D. (2018). Ubiquitin-like Protein Conjugation: Structures, Chemistry, and Mechanism. *Chemical reviews*, 118(3), 889–918.

Chaturvedi, R., Asim, M., Romero-Gallo, J., Barry, D. P., Hoge, S., de Sablet, T., Delgado, A. G., Wroblewski, L. E., Piazuelo, M. B., Yan, F., Israel, D. A., Casero, R. A., Jr, Correa, P., Gobert, A. P., Polk, D. B., Peek, R. M., Jr, & Wilson, K. T. (2011). Spermine oxidase mediates the gastric cancer risk associated with *Helicobacter pylori* CagA. *Gastroenterology*, 141(5), 1696–708.e7082.

Chen, L., & Kashina, A. (2021). Post-translational Modifications of the Protein Termini. *Frontiers in cell and developmental biology*, 9, 719590.

Chen, X., Shi, H., Bi, X., Li, Y., & Huang, Z. (2019). Targeting the deubiquitinase STAMBPL1 triggers apoptosis in prostate cancer cells by promoting XIAP degradation. *Cancer letters*, 456, 49–58.

Cheng, G., Diebold, B. A., Hughes, Y., & Lambeth, J. D. (2006). Nox1-dependent reactive oxygen generation is regulated by Rac1. *The Journal of biological chemistry*, 281(26), 17718–17726.

Clague, M. J., Urbé, S., & Komander, D. (2019). Breaking the chains: deubiquitylating enzyme specificity begets function. Nature reviews. *Molecular cell biology*, 20(6), 338–352.

Cohen, P., & Strickson, S. (2017). The role of hybrid ubiquitin chains in the MyD88 and other innate immune signalling pathways. *Cell death and differentiation*, 24(7), 1153–1159.

Collins, G. A., & Goldberg, A. L. (2017). The Logic of the 26S Proteasome. *Cell*, 169(5), 792–806.

Connell, C. M., Colnaghi, R., & Wheatley, S. P. (2008). Nuclear survivin has reduced stability and is not cytoprotective. *The Journal of biological chemistry*, 283(6), 3289–3296.

Coombs, N., Sompallae, R., Olbermann, P., Gastaldello, S., Göppel, D., Masucci, M. G., & Josenhans, C. (2011). *Helicobacter pylori* affects the cellular deubiquitinase USP7 and ubiquitin-regulated components TRAF6 and the tumour suppressor p53. *International journal of medical microbiology*, 301(3), 213–224.

Cope, G. A., Suh, G. S., Aravind, L., Schwarz, S. E., Zipursky, S. L., Koonin, E. V., & Deshaies, R. J. (2002). Role of predicted metalloprotease motif of Jab1/Csn5 in cleavage of Nedd8 from Cul1. *Science*, 298(5593), 608–611.

Cover, T. L., & Blanke, S. R. (2005). *Helicobacter pylori* VacA, a paradigm for toxin multifunctionality. Nature reviews. Microbiology, 3(4), 320–332.

Davies M. J. (2016). Protein oxidation and peroxidation. *The Biochemical journal*, 473(7), 805–825.

Davies, C. W., Paul, L. N., Kim, M. I., & Das, C. (2011). Structural and thermodynamic comparison of the catalytic domain of AMSH and AMSH-LP: nearly identical fold but different stability. *Journal of molecular biology*, 413(2), 416–429.

de Brito, B. B., da Silva, F., Soares, A. S., Pereira, V. A., Santos, M., Sampaio, M. M., Neves, P., & de Melo, F. F. (2019). Pathogenesis and clinical management of Helicobacter pylori gastric infection. *World journal of gastroenterology*, 25(37), 5578–5589.

De Cesare, V., Carbajo Lopez, D., Mabbitt, P. D., Fletcher, A. J., Soetens, M., Antico, O., Wood, N. T., & Virdee, S. (2021). Deubiquitinating enzyme amino acid profiling reveals a class of ubiquitin esterases. *Proceedings of the National Academy of Sciences of the United States of America*, 118(4), e2006947118.

De Falco, M., Lucariello, A., Iaquinto, S., Esposito, V., Guerra, G., & De Luca, A. (2015). Molecular mechanisms of *Helicobacter pylori* pathogenesis. *Journal of cellular physiology*, 230(8), 1702–1707.

De Guzman, B. B., Hisatsune, J., Nakayama, M., Yahiro, K., Wada, A., Yamasaki, E., Nishi, Y., Yamazaki, S., Azuma, T., Ito, Y., Ohtani, M., van der Wijk, T., den Hertog, J., Moss, J., & Hirayama, T. (2005). Cytotoxicity and recognition of receptor-like protein tyrosine phosphatases, RPTPalpha and RPTPbeta, by *Helicobacter pylori* m2VacA. *Cellular microbiology*, 7(9), 1285–1293.

de Poot, S., Tian, G., & Finley, D. (2017). Meddling with Fate: The Proteasomal Deubiquitinating Enzymes. *Journal of molecular biology*, 429(22), 3525–3545.

den Hartog, G., Chattopadhyay, R., Ablack, A., Hall, E. H., Butcher, L. D., Bhattacharyya, A., Eckmann, L., Harris, P. R., Das, S., Ernst, P. B., & Crowe, S. E. (2016). Regulation of Rac1 and Reactive Oxygen Species Production in Response to Infection of Gastrointestinal Epithelia. *PLoS pathogens*, 12(1), e1005382.

Deol, K. K., Lorenz, S., & Strieter, E. R. (2019). Enzymatic Logic of Ubiquitin Chain Assembly. *Frontiers in physiology*, 10, 835.

Díaz, P., Román, A., Carrasco-Aviño, G., Rodríguez, A., H Corvalán, A., Lavandero, S., & FG Quest, A. (2021). *Helicobacter pylori* infection triggers PERK-associated Survivin loss in gastric tissue samples and cell lines. *Journal of Cancer Science and Clinical Therapeutics*, 5, 063–082.

Dickinson, B. C., & Chang, C. J. (2011). Chemistry and biology of reactive oxygen species in signaling or stress responses. *Nature chemical biology*, 7(8), 504–511.

Ding, S. Z., Minohara, Y., Fan, X. J., Wang, J., Reyes, V. E., Patel, J., Dirden-Kramer, B., Boldogh, I., Ernst, P. B., & Crowe, S. E. (2007). *Helicobacter pylori* infection induces oxidative stress and programmed cell death in human gastric epithelial cells. *Infection and immunity*, 75(8), 4030–4039.

Domańska, G., Motz, C., Meinecke, M., Harsman, A., Papatheodorou, P., Reljic, B., Dian-Lothrop, E. A., Galmiche, A., Kepp, O., Becker, L., Günnewig, K., Wagner, R., & Rassow, J. (2010). *Helicobacter pylori* VacA toxin/subunit p34: targeting of an anion channel to the inner mitochondrial membrane. *PLoS pathogens*, 6(4), e1000878.

Domhan, S., Stremmel, W., & Rudi, J. (2004). Role of apoptosis and CD95-receptor/ligand system in aspirin- and *Helicobacter pylori*-induced cell death. *European journal of clinical investigation*, 34(6), 422–428.

Dubiel, W., Chaithongyot, S., Dubiel, D., & Naumann, M. (2020). The COP9 Signalosome: A Multi-DUB Complex. *Biomolecules*, 10(7), 1082.

Duda, D. M., Borg, L. A., Scott, D. C., Hunt, H. W., Hammel, M., & Schulman, B. A. (2008). Structural insights into NEDD8 activation of cullin-RING ligases: conformational control of conjugation. *Cell*, 134(6), 995–1006.

Enchev, R. I., Schulman, B. A., & Peter, M. (2015). Protein neddylation: beyond cullin-RING ligases. Nature reviews. *Molecular cell biology*, 16(1), 30–44.

Finley, D., Ulrich, H. D., Sommer, T., & Kaiser, P. (2012). The ubiquitin-proteasome system of Saccharomyces cerevisiae. *Genetics*, 192(2), 319–360.

Flahou, B., Haesebrouck, F., Chiers, K., Van Deun, K., De Smet, L., Devreese, B., Vandenberghe, I., Favoreel, H., Smet, A., Pasmans, F., D'Herde, K., & Ducatelle, R. (2011). Gastric epithelial cell death caused by *Helicobacter suis* and *Helicobacter pylori* γ-glutamyl transpeptidase is mainly glutathione degradation-dependent. *Cellular microbiology*, 13(12), 1933–1955.

Franco, R., Schoneveld, O., Georgakilas, A. G., & Panayiotidis, M. I. (2008). Oxidative stress, DNA methylation and carcinogenesis. *Cancer letters*, 266(1), 6–11.

Gatti, M., Pinato, S., Maiolica, A., Rocchio, F., Prato, M. G., Aebersold, R., & Penengo, L. (2015). RNF168 promotes noncanonical K27 ubiquitination to signal DNA damage. *Cell reports*, 10(2), 226–238.

Gauthier, N. C., Monzo, P., Kaddai, V., Doye, A., Ricci, V., & Boquet, P. (2005). *Helicobacter pylori* VacA cytotoxin: a probe for a clathrin-independent and Cdc42-dependent pinocytic pathway routed to late endosomes. *Molecular biology of the cell*, 16(10), 4852–4866.

Ghavami, S., Kerkhoff, C., Los, M., Hashemi, M., Sorg, C., & Karami-Tehrani, F. (2004). Mechanism of apoptosis induced by S100A8/A9 in colon cancer cell lines: the role of ROS and the effect of metal ions. *Journal of leukocyte biology*, 76(1), 169–175.

Gierisch, M. E., Giovannucci, T. A., & Dantuma, N. P. (2020). Reporter-Based Screens for the Ubiquitin/Proteasome System. *Frontiers in chemistry*, 8, 64.

Gong, M., & Ho, B. (2004). Prominent role of gamma-glutamyl-transpeptidase on the growth of *Helicobacter pylori*. *World journal of gastroenterology*, 10(20), 2994–2996.

Gong, M., Ling, S. S., Lui, S. Y., Yeoh, K. G., & Ho, B. (2010). *Helicobacter pylori* gamma-glutamyl transpeptidase is a pathogenic factor in the development of peptic ulcer disease. *Gastroenterology*, 139(2), 564–573.

Gravina, A. G., Zagari, R. M., De Musis, C., Romano, L., Loguercio, C., & Romano, M. (2018). *Helicobacter pylori* and extragastric diseases: A review. *World journal of gastroenterology*, 24(29), 3204–3221.

Gruosso, T., Mieulet, V., Cardon, M., Bourachot, B., Kieffer, Y., Devun, F., Dubois, T., Dutreix, M., Vincent-Salomon, A., Miller, K. M., & Mechta-Grigoriou, F. (2016). Chronic oxidative stress promotes H2AX protein degradation and enhances chemosensitivity in breast cancer patients. *EMBO molecular medicine*, 8(5), 527–549.

Gupta, V. R., Patel, H. K., Kostolansky, S. S., Ballivian, R. A., Eichberg, J., & Blanke, S. R. (2008). Sphingomyelin functions as a novel receptor for *Helicobacter pylori* VacA. *PLoS pathogens*, 4(5), e1000073.

Han, L., Shu, X., & Wang, J. (2022). *Helicobacter pylori*-Mediated Oxidative Stress and Gastric Diseases: A Review. *Frontiers in microbiology*, 13, 811258.

Hanada, K., Uchida, T., Tsukamoto, Y., Watada, M., Yamaguchi, N., Yamamoto, K., Shiota, S., Moriyama, M., Graham, D. Y., & Yamaoka, Y. (2014). *Helicobacter pylori* infection introduces DNA double-strand breaks in host cells. *Infection and immunity*, 82(10), 4182–4189.

Handa, O., Naito, Y., & Yoshikawa, T. (2010). *Helicobacter pylori*: a ROS-inducing bacterial species in the stomach. *Inflammation research*, 59(12), 997–1003.

Harper, J. W., & Schulman, B. A. (2021). Cullin-RING Ubiquitin Ligase Regulatory Circuits: A Quarter Century Beyond the F-Box Hypothesis. *Annual review of biochemistry*, 90, 403–429.

Hatakeyama M. (2014). Helicobacter pylori CagA and gastric cancer: a paradigm for hit-and-run carcinogenesis. *Cell host & microbe*, 15(3), 306–316.

Hay-Koren, A., Caspi, M., Zilberberg, A., & Rosin-Arbesfeld, R. (2011). The EDD E3 ubiquitin ligase ubiquitinates and up-regulates beta-catenin. *Molecular biology of the cell*, 22(3), 399–411.

Hayes, J. D., Chowdhry, S., Dinkova-Kostova, A. T., & Sutherland, C. (2015). Dual regulation of transcription factor Nrf2 by Keap1 and by the combined actions of β-TrCP and GSK-3. *Biochemical Society transactions*, 43(4), 611–620.

He, Y., Wang, C., Zhang, X., Lu, X., Xing, J., Lv, J., Guo, M., Huo, X., Liu, X., Lu, J., Du, X., Li, C., & Chen, Z. (2020). Sustained Exposure to Helicobacter pylori Lysate Inhibits Apoptosis and Autophagy of Gastric Epithelial Cells. *Frontiers in oncology*, 10, 581364.

Helmstaedt, K., Schwier, E. U., Christmann, M., Nahlik, K., Westermann, M., Harting, R., Grond, S., Busch, S., & Braus, G. H. (2011). Recruitment of the inhibitor Cand1 to the cullin substrate adaptor site mediates interaction to the neddylation site. *Molecular biology of the cell*, 22(1), 153–164.

Hennig, E. E., Godlewski, M. M., Butruk, E., & Ostrowski, J. (2005). Helicobacter pylori VacA cytotoxin interacts with fibronectin and alters HeLa cell adhesion and cytoskeletal organization in vitro. *FEMS immunology and medical microbiology*, 44(2), 143–150.

Higashi, H., Tsutsumi, R., Muto, S., Sugiyama, T., Azuma, T., Asaka, M., & Hatakeyama, M. (2002). SHP-2 tyrosine phosphatase as an intracellular target of *Helicobacter pylori* CagA protein. *Science*, 295(5555), 683–686.

Hoffman, W. H., Biade, S., Zilfou, J. T., Chen, J., & Murphy, M. (2002). Transcriptional repression of the anti-apoptotic survivin gene by wild type p53. *The Journal of biological chemistry*, 277(5), 3247–3257.

Hooi, J., Lai, W. Y., Ng, W. K., Suen, M., Underwood, F. E., Tanyingoh, D., Malfertheiner, P., Graham, D. Y., Wong, V., Wu, J., Chan, F., Sung, J., Kaplan, G. G., & Ng, S. C. (2017). Global prevalence of *Helicobacter pylori* infection: systematic review and meta-analysis. *Gastroenterology*, 153(2), 420–429.

Huang, X., Dubiel, D., & Dubiel, W. (2021). The COP9 Signalosome Variant CSNCSN7A Stabilizes the Deubiquitylating Enzyme CYLD Impeding Hepatic Steatosis. *Livers*, 1(3), 116–131.

Ibarrola, N., Kratchmarova, I., Nakajima, D., Schiemann, W. P., Moustakas, A., Pandey, A., & Mann, M. (2004). Cloning of a novel signaling molecule, AMSH-2, that potentiates transforming growth factor beta signaling. *BMC cell biology*, 5, 2.

Isomoto, H., Moss, J., & Hirayama, T. (2010). Pleiotropic actions of *Helicobacter pylori* vacuolating cytotoxin, VacA. *The Tohoku journal of experimental medicine*, 220(1), 3–14.

Jain, U., Saxena, K., & Chauhan, N. (2021). *Helicobacter pylori* induced reactive oxygen Species: A new and developing platform for detection. *Helicobacter*, 26(3), e12796.

Jeong, J. C., Kim, M. S., Kim, T. H., & Kim, Y. K. (2009). Kaempferol induces cell death through ERK and Akt-dependent down-regulation of XIAP and survivin in human glioma cells. *Neurochemical research*, 34(5), 991–1001.

Jones, K. R., Joo, Y. M., Jang, S., Yoo, Y. J., Lee, H. S., Chung, I. S., Olsen, C. H., Whitmire, J. M., Merrell, D. S., & Cha, J. H. (2009). Polymorphism in the CagA EPIYA motif impacts development of gastric cancer. *Journal of clinical microbiology*, 47(4), 959–968.

Jung, T., Höhn, A., & Grune, T. (2014). The proteasome and the degradation of oxidized proteins: Part II - protein oxidation and proteasomal degradation. *Redox biology*, 2, 99–104.

Kamran, M., Long, Z. J., Xu, D., Lv, S. S., Liu, B., Wang, C. L., Xu, J., Lam, E. W., & Liu, Q. (2017). Aurora kinase A regulates Survivin stability through targeting FBXL7 in gastric cancer drug resistance and prognosis. *Oncogenesis*, 6(2), e298.

Kawahara, T., Kohjima, M., Kuwano, Y., Mino, H., Teshima-Kondo, S., Takeya, R., Tsunawaki, S., Wada, A., Sumimoto, H., & Rokutan, K. (2005). *Helicobacter pylori* lipopolysaccharide activates Rac1 and transcription of NADPH oxidase Nox1 and its organizer NOXO1 in guinea pig gastric mucosal cells. *Cell physiology*, 288(2), C450–C457.

Kawamura, K., Qi, F., & Kobayashi, J. (2018). Potential relationship between the biological effects of low-dose irradiation and mitochondrial ROS production. *Journal of radiation research*, 59, ii91–ii97.

Khago, D., Fucci, I. J., & Byrd, R. A. (2020). The role of conformational dynamics in the recognition and regulation of ubiquitination. *Molecules*, 25(24), 5933.

Kikuchi, K., Ishii, N., Asao, H., & Sugamura, K. (2003). Identification of AMSH-LP containing a Jab1/MPN domain metalloenzyme motif. *Biochemical and biophysical research communications*, 306(3), 637–643.

Kim, K. M., Lee, S. G., Kim, J. M., Kim, D. S., Song, J. Y., Kang, H. L., Lee, W. K., Cho, M. J., Rhee, K. H., Youn, H. S., & Baik, S. C. (2010). *Helicobacter pylori* gamma-glutamyltranspeptidase induces cell cycle arrest at the G1-S phase transition. *Journal of microbiology*, 48(3), 372–377.

Kim, K. M., Lee, S. G., Park, M. G., Song, J. Y., Kang, H. L., Lee, W. K., Cho, M. J., Rhee, K. H., Youn, H. S., & Baik, S. C. (2007). Gamma-glutamyltranspeptidase of *Helicobacter pylori* induces mitochondria-mediated apoptosis in AGS cells. *Biochemical and biophysical research communications*, 355(2), 562–567.

Kim, S. Y., Bae, S., Choi, K. H., & An, S. (2011). Hydrogen peroxide controls Akt activity via ubiquitination/degradation pathways. *Oncology reports*, 26(6), 1561–1566.

Kleiger, G., & Mayor, T. (2014). Perilous journey: a tour of the ubiquitin-proteasome system. *Trends in cell biology*, 24(6), 352–359.

Kleih, M., Böpple, K., Dong, M., Gaißler, A., Heine, S., Olayioye, M. A., Aulitzky, W. E., & Essmann, F. (2019). Direct impact of cisplatin on mitochondria induces ROS production that dictates cell fate of ovarian cancer cells. *Cell death & disease*, 10(11), 851.

Knauer, S. K., Krämer, O. H., Knösel, T., Engels, K., Rödel, F., Kovács, A. F., Dietmaier, W., Klein-Hitpass, L., Habtemichael, N., Schweitzer, A., Brieger, J., Rödel, C., Mann, W., Petersen, I., Heinzel, T., & Stauber, R. H. (2007). Nuclear export is essential for the tumor-promoting activity of survivin. *FASEB journal*, 21(1), 207–216.

Kobayashi, A., Kang, M. I., Okawa, H., Ohtsuji, M., Zenke, Y., Chiba, T., Igarashi, K., & Yamamoto, M. (2004). Oxidative stress sensor Keap1 functions as an adaptor for Cul3-based E3 ligase to regulate proteasomal degradation of Nrf2. *Molecular and cellular biology*, 24(16), 7130–7139.

Komander D. (2009). The emerging complexity of protein ubiquitination. *Biochemical Society transactions*, 37, 937–953.

Komander D. (2010). Mechanism, specificity and structure of the deubiquitinases. *Sub-cellular biochemistry*, 54, 69–87.

Königer, V., Holsten, L., Harrison, U., Busch, B., Loell, E., Zhao, Q., Bonsor, D. A., Roth, A., Kengmo-Tchoupa, A., Smith, S. I., Mueller, S., Sundberg, E. J., Zimmermann, W., Fischer, W., Hauck, C. R., & Haas, R. (2016). *Helicobacter pylori* exploits human CEACAMs via HopQ for adherence and translocation of CagA. *Nature microbiology*, 2, 16188.

Laemmli U. K. (1970). Cleavage of structural proteins during the assembly of the head of bacteriophage T4. *Nature*, 227(5259), 680–685.

Lalaoui, N., & Vaux, D. L. (2018). Recent advances in understanding inhibitor of apoptosis proteins. *F1000Research*, 7, 1889–1889.

Lambeth J. D. (2004). NOX enzymes and the biology of reactive oxygen. Nature reviews. *Immunology*, 4(3), 181–189.

Lavorgna, A., & Harhaj, E. W. (2012). An RNA interference screen identifies the Deubiquitinase STAMBPL1 as a critical regulator of human T-cell leukemia virus type 1 tax nuclear export and NF-κB activation. *Journal of virology*, 86(6), 3357–3369.

Lee, J. H., Yi, L., Li, J., Schweitzer, K., Borgmann, M., Naumann, M., & Wu, H. (2013). Crystal structure and versatile functional roles of the COP9 signalosome subunit 1. *Proceedings of the National Academy of Sciences of the United States of America*, 110(29), 11845–11850.

Lee, N. H., Kim, M., Oh, S. Y., Kim, S. G., Kwon, H. C., & Hwang, T. H. (2017). Gene expression profiling of hematologic malignant cell lines resistant to oncolytic virus treatment. *Oncotarget*, 8(1), 1213–1225.

Lei, H., Ma, Y., Tan, J., & Liu, Q. (2021). Helicobacter pylori Regulates the Apoptosis of Human Megakaryocyte Cells via NF-κB/IL-17 Signaling. *OncoTargets and therapy*, 14, 2065–2074.

Leppert, U., Henke, W., Huang, X., Müller, J. M., & Dubiel, W. (2011). Post-transcriptional fine-tuning of COP9 signalosome subunit biosynthesis is regulated by the c-Myc/Lin28B/let-7 pathway. *Journal of molecular biology*, 409(5), 710–721.

Li, C. W., & Chen, B. S. (2016). Investigating core genetic-and-epigenetic cell cycle networks for stemness and carcinogenic mechanisms, and cancer drug design using big database mining and genome-wide next-generation sequencing data. *Cell cycle*, 15(19), 2593–2607.

Li, Y., & Reverter, D. (2021). Molecular Mechanisms of DUBs Regulation in Signaling and Disease. *International journal of molecular sciences*, 22(3), 986.

Li, Y., Lan, Q., Gao, Y., Xu, C., Xu, Z., Wang, Y., Chang, L., Wu, J., Deng, Z., He, F., Finley, D., & Xu, P. (2020). Ubiquitin Linkage Specificity of Deubiquitinases Determines Cyclophilin Nuclear Localization and Degradation. *iScience*, 23(4), 100984.

Li, Z., Chen, J., Chan, K. W., Qiao, L., & Wong, B. C. (2011). A possible role of cIAP2 in Helicobacter pylori-associated gastric cancer. *Cancer letters*, 313(2), 192–200.

Liang, J., Cao, R., Wang, X., Zhang, Y., Wang, P., Gao, H., Li, C., Yang, F., Zeng, R., Wei, P., Li, D., Li, W., & Yang, W. (2017). Mitochondrial PKM2 regulates oxidative stress-induced apoptosis by stabilizing Bcl2. *Cell research*, 27(3), 329–351.

Lim, M., Maubach, G., Sokolova, O., Feige, M. H., Diezko, R., Buchbinder, J., Backert, S., Schlüter, D., Lavrik, I. N., & Naumann, M. (2017). Pathogen-induced ubiquitin-editing enzyme A20 bifunctionally shuts off NF-κB and caspase-8-dependent apoptotic cell death. *Cell death and differentiation*, 24(9), 1621–1631.

Lin, W. C., Tsai, H. F., Liao, H. J., Tang, C. H., Wu, Y. Y., Hsu, P. I., Cheng, A. L., & Hsu, P. N. (2014). Helicobacter pylori sensitizes TNF-related apoptosis-inducing ligand (TRAIL)-mediated apoptosis in human gastric epithelial cells through regulation of FLIP. *Cell death & disease*, 5(3), e1109.

Liu, J. F., Guo, D., Kang, E. M., Wang, Y. S., Gao, X. Z., Cong, H. Y., Liu, P., Zhang, N. Q., & Wang, M. Y. (2021). Acute and chronic infection of H. pylori caused the difference in apoptosis of gastric epithelial cells. *Microbial pathogenesis*, 150, 104717.

Liu, R., Yang, G., Bao, M., Zhou, Z., Mao, X., Liu, W., Jiang, X., Zhu, D., Ren, X., Huang, J., & Chen, C. (2022). STAMBPL1 promotes breast cancer cell resistance to cisplatin partially by stabilizing MKP-1 expression. *Oncogene*, 10.1038/s41388-022-02252-7. Advance online publication.

Liu, X., Irfan, M., Xu, X., Tay, C.-Y., & Marshall, B. J. (2020). Helicobacter pylori infection induced genome instability and gastric cancer. *Genome Instability & Disease*, 1, 129–142.

Liu, Y., Lear, T., Iannone, O., Shiva, S., Corey, C., Rajbhandari, S., Jerome, J., Chen, B. B., & Mallampalli, R. K. (2015). The Proapoptotic F-box Protein Fbxl7 Regulates Mitochondrial Function by Mediating the Ubiquitylation and Proteasomal Degradation of Survivin. *The Journal of biological chemistry*, 290(19), 11843–11852.

Loignon, M., Miao, W., Hu, L., Bier, A., Bismar, T. A., Scrivens, P. J., Mann, K., Basik, M., Bouchard, A., Fiset, P. O., Batist, Z., & Batist, G. (2009). Cul3 overexpression depletes Nrf2 in breast cancer and is associated with sensitivity to carcinogens, to oxidative stress, and to chemotherapy. *Molecular cancer therapeutics*, 8(8), 2432–2440.

Lyapina, S., Cope, G., Shevchenko, A., Serino, G., Tsuge, T., Zhou, C., Wolf, D. A., Wei, N., Shevchenko, A., & Deshaies, R. J. (2001). Promotion of NEDD-CUL1 conjugate cleavage by COP9 signalosome. *Science*, 292(5520), 1382–1385.

Lydeard, J. R., Schulman, B. A., & Harper, J. W. (2013). Building and remodelling Cullin-RING E3 ubiquitin ligases. *EMBO reports*, 14(12), 1050–1061.

Ma, Y., Zhang, L., Rong, S., Qu, H., Zhang, Y., Chang, D., Pan, H., & Wang, W. (2013). Relation between gastric cancer and protein oxidation, DNA damage, and lipid peroxidation. *Oxidative medicine and cellular longevity*, 2013, 543760.

Marusawa, H., Matsuzawa, S., Welsh, K., Zou, H., Armstrong, R., Tamm, I., & Reed, J. C. (2003). HBXIP functions as a cofactor of survivin in apoptosis suppression. *The EMBO journal*, 22(11), 2729–2740.

Maubach, G., Lim, M., Sokolova, O., Backert, S., Meyer, T. F., & Naumann, M. (2021). TIFA has dual functions in *Helicobacter pylori*-induced classical and alternative NF-κB pathways. *EMBO reports*, 22(9), e52878.

Metzger, M. B., Pruneda, J. N., Klevit, R. E., & Weissman, A. M. (2014). RING-type E3 ligases: master manipulators of E2 ubiquitin-conjugating enzymes and ubiquitination. *Biochimica et biophysica acta*, 1843(1), 47–60.

Mevissen, T. E. T., & Komander, D. (2017). Mechanisms of Deubiquitinase Specificity and Regulation. *Annual review of biochemistry*, 86, 159–192.

Milhollen, M. A., Thomas, M. P., Narayanan, U., Traore, T., Riceberg, J., Amidon, B. S., Bence, N. F., Bolen, J. B., Brownell, J., Dick, L. R., Loke, H. K., McDonald, A. A., Ma, J., Manfredi, M. G., Sells, T. B., Sintchak, M. D., Yang, X., Xu, Q., Koenig, E. M., Gavin, J. M., Smith, P. G. (2012). Treatment-emergent mutations in NAEβ confer resistance to the NEDD8-activating enzyme inhibitor MLN4924. *Cancer cell*, 21(3), 388–401.

Miller, E. F., & Maier, R. J. (2014). Ammonium metabolism enzymes aid Helicobacter pylori acid resistance. *Journal of bacteriology*, 196(17), 3074–3081.

Mimuro, H., Suzuki, T., Nagai, S., Rieder, G., Suzuki, M., Nagai, T., Fujita, Y., Nagamatsu, K., Ishijima, N., Koyasu, S., Haas, R., & Sasakawa, C. (2007). Helicobacter pylori dampens gut epithelial self-renewal by inhibiting apoptosis, a bacterial strategy to enhance colonization of the stomach. *Cell host & microbe*, 2(4), 250–263.

Morris, J. R., & Solomon, E. (2004). BRCA1: BARD1 induces the formation of conjugated ubiquitin structures, dependent on K6 of ubiquitin, in cells during DNA replication and repair. *Human molecular genetics*, 13(8), 807–817.

Mosadeghi, R., Reichermeier, K. M., Winkler, M., Schreiber, A., Reitsma, J. M., Zhang, Y., Stengel, F., Cao, J., Kim, M., Sweredoski, M. J., Hess, S., Leitner, A., Aebersold, R., Peter, M., Deshaies, R. J., & Enchev, R. I. (2016). Structural and kinetic analysis of the COP9-Signalosome activation and the cullin-RING ubiquitin ligase deneddylation cycle. *eLife*, 5, e12102.

Moss, S. F., Calam, J., Agarwal, B., Wang, S., & Holt, P. R. (1996). Induction of gastric epithelial apoptosis by *Helicobacter pylori*. *Gut*, 38(4), 498–501.

Naito, Y., & Yoshikawa, T. (2002). Molecular and cellular mechanisms involved in *Helicobacter pylori*-induced inflammation and oxidative stress. *Free radical biology & medicine*, 33(3), 323–336.

Naumann, M., Bech-Otschir, D., Huang, X., Ferrell, K., & Dubiel, W. (1999). COP9 signalosome-directed c-Jun activation/stabilization is independent of JNK. *The Journal of biological chemistry*, 274(50), 35297–35300.

Naumann, M., Sokolova, O., Tegtmeyer, N., & Backert, S. (2017). *Helicobacter pylori*: A Paradigm Pathogen for Subverting Host Cell Signal Transmission. *Trends in microbiology*, 25(4), 316–328.

Nijman, S. M., Luna-Vargas, M. P., Velds, A., Brummelkamp, T. R., Dirac, A. M., Sixma, T. K., & Bernards, R. (2005). A genomic and functional inventory of deubiquitinating enzymes. *Cell*, 123(5), 773–786.

Oh, E., Akopian, D., & Rape, M. (2018). Principles of Ubiquitin-Dependent Signaling. *Annual review of cell and developmental biology*, 34, 137–162.

Ordureau, A., Sarraf, S. A., Duda, D. M., Heo, J. M., Jedrychowski, M. P., Sviderskiy, V. O., Olszewski, J. L., Koerber, J. T., Xie, T., Beausoleil, S. A., Wells, J. A., Gygi, S. P., Schulman, B. A., & Harper, J. W. (2014). Quantitative proteomics reveal a feedforward mechanism for mitochondrial PARKIN translocation and ubiquitin chain synthesis. *Molecular cell*, 56(3), 360–375.

Palframan, S. L., Kwok, T., & Gabriel, K. (2012). Vacuolating cytotoxin A (VacA), a key toxin for Helicobacter pylori pathogenesis. *Frontiers in cellular and infection microbiology*, 2, 92.

Pan, Y., Zhang, Q., Tian, L., Wang, X., Fan, X., Zhang, H., Claret, F. X., & Yang, H. (2012). Jab1/CSN5 negatively regulates p27 and plays a role in the pathogenesis of nasopharyngeal carcinoma. *Cancer research*, 72(7), 1890–1900.

Park, Y. H., Jeong, M. S., Ha, K. T., Yu, H. S., & Jang, S. B. (2017). Structural characterization of As-MIF and hJAB1 during the inhibition of cell-cycle regulation. *BMB reports*, 50(5), 269–274.

Pathare, G. R., Nagy, I., Śledź, P., Anderson, D. J., Zhou, H. J., Pardon, E., Steyaert, J., Förster, F., Bracher, A., & Baumeister, W. (2014). Crystal structure of the proteasomal deubiquitylation module Rpn8-Rpn11. *Proceedings of the National Academy of Sciences of the United States of America*, 111(8), 2984–2989.

Pavlyukov, M. S., Antipova, N. V., Balashova, M. V., Vinogradova, T. V., Kopantzev, E. P., & Shakhparonov, M. I. (2011). Survivin monomer plays an essential role in apoptosis regulation. *The Journal of biological chemistry*, 286(26), 23296–23307.

Pecoraro, M., Pala, B., Di Marcantonio, M. C., Muraro, R., Marzocco, S., Pinto, A., Mincione, G., & Popolo, A. (2020). Doxorubicin-induced oxidative and nitrosative stress: Mitochondrial connexin 43 is at the crossroads. *International journal of molecular medicine*, 46(3), 1197–1209.

Peek, R. M., Jr, Moss, S. F., Tham, K. T., Pérez-Pérez, G. I., Wang, S., Miller, G. G., Atherton, J. C., Holt, P. R., & Blaser, M. J. (1997). *Helicobacter pylori* cagA+ strains and dissociation of gastric epithelial cell proliferation from apoptosis. *Journal of the National Cancer Institute*, 89(12), 863–868.

Peng, D. J., Zeng, M., Muromoto, R., Matsuda, T., Shimoda, K., Subramaniam, M., Spelsberg, T. C., Wei, W. Z., & Venuprasad, K. (2011). Noncanonical K27-linked polyubiquitination of TIEG1 regulates Foxp3 expression and tumor growth. *Journal of immunology*, 186(10), 5638–5647.

Pérez Berrocal, D. A., Witting, K. F., Ovaa, H., & Mulder, M. (2020). Hybrid Chains: A Collaboration of Ubiquitin and Ubiquitin-Like Modifiers Introducing Cross-Functionality to the Ubiquitin Code. *Frontiers in chemistry*, 7, 931.

Perry, J. J., Tainer, J. A., & Boddy, M. N. (2008). A SIM-ultaneous role for SUMO and ubiquitin. *Trends in biochemical sciences*, 33(5), 201–208.

Peth, A., Berndt, C., Henke, W., & Dubiel, W. (2007). Downregulation of COP9 signalosome subunits differentially affects the CSN complex and target protein stability. *BMC biochemistry*, 8, 27.

Pierzchalski, P., Pytko-Polonczyk, J., Jaworek, J., Konturek, S. J., & Gonciarz, M. (2009). Only live Helicobacter pylori is capable of caspase-3 dependent apoptosis induction in gastric mucosa epithelial cells. *Journal of physiology and pharmacology*, 60(4), 119–128.

Popovic, D., Vucic, D., & Dikic, I. (2014). Ubiquitination in disease pathogenesis and treatment. *Nature medicine*, 20(11), 1242–1253.

Pyburn, T. M., Foegeding, N. J., González-Rivera, C., McDonald, N. A., Gould, K. L., Cover, T. L., & Ohi, M. D. (2016). Structural organization of membrane-inserted hexamers formed by *Helicobacter pylori* VacA toxin. *Molecular microbiology*, 102(1), 22–36.

Radin, J. N., González-Rivera, C., Ivie, S. E., McClain, M. S., & Cover, T. L. (2011). Helicobacter pylori VacA induces programmed necrosis in gastric epithelial cells. *Infection and immunity*, 79(7), 2535–2543.

Rassow, J., & Meinecke, M. (2012). Helicobacter pylori VacA: a new perspective on an invasive chloride channel. *Microbes and infection*, 14(12), 1026–1033.

Ravid, T., & Hochstrasser, M. (2008). Diversity of degradation signals in the ubiquitin-proteasome system. Nature reviews. *Molecular cell biology*, 9(9), 679–690.

Ray, P. D., Huang, B. W., & Tsuji, Y. (2012). Reactive oxygen species (ROS) homeostasis and redox regulation in cellular signaling. *Cellular signalling*, 24(5), 981–990.

Reczek, C. R., & Chandel, N. S. (2015). ROS-dependent signal transduction. *Current opinion in cell biology*, 33, 8–13.

Reiter, K. H., & Klevit, R. E. (2018). Characterization of RING-Between-RING E3 Ubiquitin Transfer Mechanisms. *Methods in molecular biology*, 1844, 3–17.

Reitsma, J. M., Liu, X., Reichermeier, K. M., Moradian, A., Sweredoski, M. J., Hess, S., & Deshaies, R. J. (2017). Composition and Regulation of the Cellular Repertoire of SCF Ubiquitin Ligases. *Cell*, 171(6), 1326–1339.e14.

Ren, X., Zhang, L., Zhang, Y., Mao, L., & Jiang, H. (2019). Oxidative stress induced by camptothecin and hydroxyl-camptothecin in IOZCAS-Spex-II cells of Spodoptera exigua Hübner. Comparative biochemistry and physiology. *Toxicology & pharmacology*, 216, 52–59.

Ribeiro-Rodrigues, T. M., Catarino, S., Marques, C., Ferreira, J. V., Martins-Marques, T., Pereira, P., & Girão, H. (2014). AMSH-mediated deubiquitination of Cx43 regulates internalization and degradation of gap junctions. *FASEB journal*, 28(11), 4629–4641.

Rosser, M. F., Washburn, E., Muchowski, P. J., Patterson, C., & Cyr, D. M. (2007). Chaperone functions of the E3 ubiquitin ligase CHIP. *The Journal of biological chemistry*, 282(31), 22267–22277.

Rotin, D., & Kumar, S. (2009). Physiological functions of the HECT family of ubiquitin ligases. Nature reviews. *Molecular cell biology*, 10(6), 398–409.

Ryter, S. W., Kim, H. P., Hoetzel, A., Park, J. W., Nakahira, K., Wang, X., & Choi, A. M. (2007). Mechanisms of cell death in oxidative stress. *Antioxidants & redox signaling*, 9(1), 49–89.

Saha, A., Backert, S., Hammond, C. E., Gooz, M., & Smolka, A. J. (2010). *Helicobacter pylori* CagL activates ADAM17 to induce repression of the gastric H, K-ATPase alpha subunit. *Gastroenterology*, 139(1), 239–248.

Salama, N. R., Hartung, M. L., & Müller, A. (2013). Life in the human stomach: persistence strategies of the bacterial pathogen Helicobacter pylori. Nature reviews. *Microbiology*, 11(6), 385–399.

Sandoval, R., Lazcano, P., Ferrari, F., Pinto-Pardo, N., González-Billault, C., & Utreras, E. (2018). TNF-α Increases Production of Reactive Oxygen Species through Cdk5 Activation in Nociceptive Neurons. *Frontiers in physiology*, 9, 65.

Sato, Y., Yoshikawa, A., Yamagata, A., Mimura, H., Yamashita, M., Ookata, K., Nureki, O., Iwai, K., Komada, M., & Fukai, S. (2008). Structural basis for specific cleavage of Lys 63-linked polyubiquitin chains. *Nature*, 455(7211), 358–362.

Schmees, C., Prinz, C., Treptau, T., Rad, R., Hengst, L., Voland, P., Bauer, S., Brenner, L., Schmid, R. M., & Gerhard, M. (2007). Inhibition of T-cell proliferation by Helicobacter pylori gamma-glutamyl transpeptidase. *Gastroenterology*, 132(5), 1820–1833.

Schwechheimer C. (2004). The COP9 signalosome (CSN): an evolutionary conserved proteolysis regulator in eukaryotic development. *Biochimica et biophysica acta*, 1695(1-3), 45–54.

Schweitzer, K., & Naumann, M. (2015). CSN-associated USP48 confers stability to nuclear NF-κB/RelA by trimming K48-linked Ub-chains. *Biochimica et biophysica acta*, 1853(2), 453–469.

Schweitzer, K., Bozko, P. M., Dubiel, W., & Naumann, M. (2007). CSN controls NF-kappaB by deubiquitinylation of IkappaBalpha. *The EMBO journal*, 26(6), 1532–1541.

Sena, L. A., & Chandel, N. S. (2012). Physiological roles of mitochondrial reactive oxygen species. *Molecular cell*, 48(2), 158–167.

Shahriyar, S. A., Woo, S. M., Seo, S. U., Min, K. J., & Kwon, T. K. (2018). Cepharanthine Enhances TRAIL-Mediated Apoptosis Through STAMBPL1-Mediated Downregulation of Survivin Expression in Renal Carcinoma Cells. *International journal of molecular sciences*, 19(10), 3280.

Shalini, S., Dorstyn, L., Dawar, S., & Kumar, S. (2015). Old, new and emerging functions of caspases. *Cell death and differentiation*, 22(4), 526–539.

Shi, Y., Wang, P., Guo, Y., Liang, X., Li, Y., & Ding, S. (2019). *Helicobacter pylori*-Induced DNA Damage Is a Potential Driver for Human Gastric Cancer AGS Cells. *DNA and cell biology*, 38(3), 272–280.

Shibayama, K., Wachino, J., Arakawa, Y., Saidijam, M., Rutherford, N. G., & Henderson, P. J. (2007). Metabolism of glutamine and glutathione via gamma-glutamyltransferase and glutamate transport in *Helicobacter pylori*: possible significance in the pathophysiology of the organism. *Molecular microbiology*, 64(2), 396–406.

Shrestha, R., & Das, C. (2021). Crystal structure of the Thr316Ala mutant of a yeast JAMM deubiquitinase: implication of active-site loop dynamics in catalysis. *Structural biology communications*, 77(6), 163–170.

Sies, H., & Jones, D. P. (2020). Reactive oxygen species (ROS) as pleiotropic physiological signalling agents. Nature reviews. *Molecular cell biology*, 21(7), 363–383.

Sokolova, O., Maubach, G., & Naumann, M. (2014). MEKK3 and TAK1 synergize to activate IKK complex in *Helicobacter pylori* infection. *Biochimica et biophysica acta*, 1843(4), 715–724.

Song, I. S., Kim, H. K., Jeong, S. H., Lee, S. R., Kim, N., Rhee, B. D., Ko, K. S., & Han, J. (2011). Mitochondrial peroxiredoxin III is a potential target for cancer therapy. *International journal of molecular sciences*, 12(10), 7163–7185.

Song, Z., Liu, S., He, H., Hoti, N., Wang, Y., Feng, S., & Wu, M. (2004). A single amino acid change (Asp 53 --> Ala53) converts Survivin from anti-apoptotic to pro-apoptotic. *Molecular biology of the cell*, 15(3), 1287–1296.

Sowa, M. E., Bennett, E. J., Gygi, S. P., & Harper, J. W. (2009). Defining the human deubiquitinating enzyme interaction landscape. *Cell*, 138(2), 389–403.

Srinivas, U. S., Tan, B., Vellayappan, B. A., & Jeyasekharan, A. D. (2019). ROS and the DNA damage response in cancer. *Redox biology*, 25, 101084.

Swatek, K. N., & Komander, D. (2016). Ubiquitin modifications. *Cell research*, 26(4), 399–422.

Takahashi-Kanemitsu, A., Knight, C. T., & Hatakeyama, M. (2020). Molecular anatomy and pathogenic actions of *Helicobacter pylori* CagA that underpin gastric carcinogenesis. *Cellular & molecular immunology*, 17(1), 50–63.

Tasaki, T., Sriram, S. M., Park, K. S., & Kwon, Y. T. (2012). The N-end rule pathway. *Annual review of biochemistry*, 81, 261–289.

Thrower, J. S., Hoffman, L., Rechsteiner, M., & Pickart, C. M. (2000). Recognition of the polyubiquitin proteolytic signal. *The EMBO journal*, 19(1), 94–102.

Tomoda, K., Kubota, Y., Arata, Y., Mori, S., Maeda, M., Tanaka, T., Yoshida, M., Yoneda-Kato, N., & Kato, J. Y. (2002). The cytoplasmic shuttling and subsequent degradation of p27Kip1 mediated by Jab1/CSN5 and the COP9 signalosome complex. *The Journal of biological chemistry*, 277(3), 2302–2310.

Torres, V. A., Tapia, J. C., Rodríguez, D. A., Párraga, M., Lisboa, P., Montoya, M., Leyton, L., & Quest, A. F. (2006). Caveolin-1 controls cell proliferation and cell death by suppressing expression of the inhibitor of apoptosis protein survivin. *Journal of cell science*, 119(9), 1812–1823.

Tracz, M., & Bialek, W. (2021). Beyond K48 and K63: non-canonical protein ubiquitination. *Cellular & molecular biology letters*, 26(1), 1.

Valenzuela, M., Bravo, D., Canales, J., Sanhueza, C., Díaz, N., Almarza, O., Toledo, H., & Quest, A. F. (2013). *Helicobacter pylori*-induced loss of survivin and gastric cell viability is attributable to secreted bacterial gamma-glutamyl transpeptidase activity. *The Journal of infectious diseases*, 208(7), 1131–1141.

Valenzuela, M., Pérez-Pérez, G., Corvalán, A. H., Carrasco, G., Urra, H., Bravo, D., Toledo, H., & Quest, A. F. (2010). *Helicobacter pylori*-induced loss of the inhibitor-of-apoptosis protein survivin is linked to gastritis and death of human gastric cells. *The Journal of infectious diseases*, 202(7), 1021–1030.

van der Waal, M. S., Hengeveld, R. C., van der Horst, A., & Lens, S. M. (2012). Cell division control by the Chromosomal Passenger Complex. *Experimental cell research*, 318(12), 1407–1420.

Varshavsky A. (2019). N-degron and C-degron pathways of protein degradation. *Proceedings of the National Academy of Sciences of the United States of America*, 116(2), 358–366.

Venne, A. S., Kollipara, L., & Zahedi, R. P. (2014). The next level of complexity: crosstalk of posttranslational modifications. *Proteomics*, 14(4-5), 513–524.

Ventii, K. H., & Wilkinson, K. D. (2008). Protein partners of deubiquitinating enzymes. *The Biochemical journal*, 414(2), 161–175.

Walden, H., & Rittinger, K. (2018). RBR ligase-mediated ubiquitin transfer: a tale with many twists and turns. *Nature structural & molecular biology*, 25(6), 440–445.

Wan, X. K., Yuan, S. L., Tao, H. X., Diao, L. P., Wang, Y. C., Cao, C., & Liu, C. J. (2016). The Upregulation of TRAF1 Induced by Helicobacter pylori Plays an Antiapoptotic Effect on the Infected Cells. *Helicobacter*, 21(6), 554–564.

Wang, D., Xu, C., Yang, W., Chen, J., Ou, Y., Guan, Y., Guan, J., & Liu, Y. (2022). E3 ligase RNF167 and deubiquitinase STAMBPL1 modulate mTOR and cancer progression. *Molecular cell*, 82(4), 770–784.e9.

Wang, N., Kang, H. S., Ahmmed, G., Khan, S. A., Makarenko, V. V., Prabhakar, N. R., & Nanduri, J. (2016). Calpain activation by ROS mediates human ether-a-go-go-related gene protein degradation by intermittent hypoxia. *Cell physiology*, 310(5), C329–C336.

Wang, Y., Shi, P., Chen, Q., Huang, Z., Zou, D., Zhang, J., Gao, X., & Lin, Z. (2019). Mitochondrial ROS promote macrophage pyroptosis by inducing GSDMD oxidation. *Journal of molecular cell biology*, 11(12), 1069–1082.

Willhite, D. C., & Blanke, S. R. (2004). *Helicobacter pylori* vacuolating cytotoxin enters cells, localizes to the mitochondria, and induces mitochondrial membrane permeability changes correlated to toxin channel activity. *Cellular microbiology*, 6(2), 143–154.

Woo, S. M., Seo, S. U., Kubatka, P., Min, K. J., & Kwon, T. K. (2019). Honokiol Enhances TRAIL-Mediated Apoptosis through STAMBPL1-Induced Survivin and c-FLIP Degradation. *Biomolecules*, 9(12), 838.

Worden, E. J., Dong, K. C., & Martin, A. (2017). An AAA motor-driven mechanical switch in Rpn11 controls deubiquitination at the 26S proteasome. *Molecular cell*, 67(5), 799–811.e8.

Wüstner, S., Anderl, F., Wanisch, A., Sachs, C., Steiger, K., Nerlich, A., Vieth, M., Mejías-Luque, R., & Gerhard, M. (2017). *Helicobacter pylori* γ-glutamyl transferase contributes to colonization and differential recruitment of T cells during persistence. *Scientific reports*, 7(1), 13636.

Xu, P., Duong, D. M., Seyfried, N. T., Cheng, D., Xie, Y., Robert, J., Rush, J., Hochstrasser, M., Finley, D., & Peng, J. (2009). Quantitative proteomics reveals the

function of unconventional ubiquitin chains in proteasomal degradation. *Cell*, 137(1), 133–145.

Yahiro, K., Satoh, M., Nakano, M., Hisatsune, J., Isomoto, H., Sap, J., Suzuki, H., Nomura, F., Noda, M., Moss, J., & Hirayama, T. (2012). Low-density lipoprotein receptor-related protein-1 (LRP1) mediates autophagy and apoptosis caused by Helicobacter pylori VacA. *The Journal of biological chemistry*, 287(37), 31104–31115.

Yahiro, K., Wada, A., Nakayama, M., Kimura, T., Ogushi, K., Niidome, T., Aoyagi, H., Yoshino, K., Yonezawa, K., Moss, J., & Hirayama, T. (2003). Protein-tyrosine phosphatase alpha, RPTP alpha, is a *Helicobacter pylori* VacA receptor. *The Journal of biological chemistry*, 278(21), 19183–19189.

Yamasaki, E., Wada, A., Kumatori, A., Nakagawa, I., Funao, J., Nakayama, M., Hisatsune, J., Kimura, M., Moss, J., & Hirayama, T. (2006). *Helicobacter pylori* vacuolating cytotoxin induces activation of the proapoptotic proteins Bax and Bak, leading to cytochrome c release and cell death, independent of vacuolation. *The Journal of biological chemistry*, 281(16), 11250–11259.

Yang, D., Elner, S. G., Bian, Z. M., Till, G. O., Petty, H. R., & Elner, V. M. (2007). Pro-inflammatory cytokines increase reactive oxygen species through mitochondria and NADPH oxidase in cultured RPE cells. *Experimental eye research*, 85(4), 462–472.

Yang, H., Villani, R. M., Wang, H., Simpson, M. J., Roberts, M. S., Tang, M., & Liang, X. (2018). The role of cellular reactive oxygen species in cancer chemotherapy. *Journal of experimental & clinical cancer research*, 37(1), 266.

Yang, Q., Zhao, J., Chen, D., & Wang, Y. (2021). E3 ubiquitin ligases: styles, structures and functions. *Molecular biomedicine*, 2(1), 23.

Yao, T., Song, L., Xu, W., DeMartino, G. N., Florens, L., Swanson, S. K., Washburn, M. P., Conaway, R. C., Conaway, J. W., & Cohen, R. E. (2006). Proteasome recruitment and activation of the Uch37 deubiquitinating enzyme by Adrm1. *Nature cell biology*, 8(9), 994–1002.

Ye, Y., & Rape, M. (2009). Building ubiquitin chains: E2 enzymes at work. Nature reviews. *Molecular cell biology*, 10(11), 755–764.

Yu, D. J., Qian, J., Jin, X., Li, J., Guo, C. X., & Yue, X. C. (2019). STAMBPL1 knockdown has antitumour effects on gastric cancer biological activities. *Oncology letters*, 18(5), 4421–4428.

Yuan, W. C., Lee, Y. R., Lin, S. Y., Chang, L. Y., Tan, Y. P., Hung, C. C., Kuo, J. C., Liu, C. H., Lin, M. Y., Xu, M., Chen, Z. J., & Chen, R. H. (2014). K33-Linked Polyubiquitination of Coronin 7 by Cul3-KLHL20 Ubiquitin E3 Ligase Regulates Protein Trafficking. *Molecular cell*, 54(4), 586–600.

Yun, J., Tomida, A., Andoh, T., & Tsuruo, T. (2004). Interaction between glucose-regulated destruction domain of DNA topoisomerase IIalpha and MPN domain of Jab1/CSN5. *The Journal of biological chemistry*, 279(30), 31296–31303.

Zamani, M., Ebrahimtabar, F., Zamani, V., Miller, W. H., Alizadeh-Navaei, R., Shokri-Shirvani, J., & Derakhshan, M. H. (2018). Systematic review with meta-analysis: the worldwide prevalence of Helicobacter pylori infection. *Alimentary pharmacology & therapeutics*, 47(7), 868–876.

Zarich, N., Anta, B., Fernández-Medarde, A., Ballester, A., de Lucas, M. P., Cámara, A. B., Anta, B., Oliva, J. L., Rojas-Cabañeros, J. M., & Santos, E. (2019). The CSN3 subunit of the COP9 signalosome interacts with the HD region of Sos1 regulating stability of this GEF protein. *Oncogenesis*, 8(1), 2.

Zhou, J., Guo, X., Chen, W., Wang, L., & Jin, Y. (2020). Targeting survivin sensitizes cervical cancer cells to radiation treatment. *Bioengineered*, 11(1), 130–140.

Zhou, R., Shao, Z., Liu, J., Zhan, W., Gao, Q., Pan, Z., Wu, L., Xu, L., Ding, Y., & Zhao, L. (2018). COPS5 and LASP1 synergistically interact to downregulate 14-3-3σ expression and promote colorectal cancer progression via activating PI3K/AKT pathway. *International journal of cancer*, 142(9), 1853–1864.

Zhu, W., Liu, Y., & Ling, B. (2015). Quantum mechanics and molecular mechanics study of the catalytic mechanism of human AMSH-LP domain deubiquitinating enzymes. *Biochemistry*, 54(33), 5225–5234.

9. Declaration of Honour

"I hereby declare that I prepared this thesis without the impermissible help of third parties and that none other that the aids indicated have been used; all sources of information are clearly marked, including my own publications.

In particular I have not consciously:
- fabricated data or rejected undesirable results,
- misused statistical methods with the aim of drawing other conclusions than those warranted by the available data,
- plagiarized external data or publications,
- presented the results of other researchers in a distorted way.

I am aware that violations of copyright may lead to injunction and damage claims by the author and also to prosecution by law enforcement authorities.
I hereby agree that the thesis may be electronically reviewed with the aim of identifying plagiarism.

This work has not been submitted as a doctoral thesis in the same or a similar form in Germany, nor in any other country. It has not yet been published as a whole."

Bangkok, 19.10.2022

(Place, date)   (Signature)